ESTI 2008

May 30 – June 1, 2008

16th Annual Meeting
of the European Society of Thoracic Imaging

Nice, France

FINAL PROGRAMME

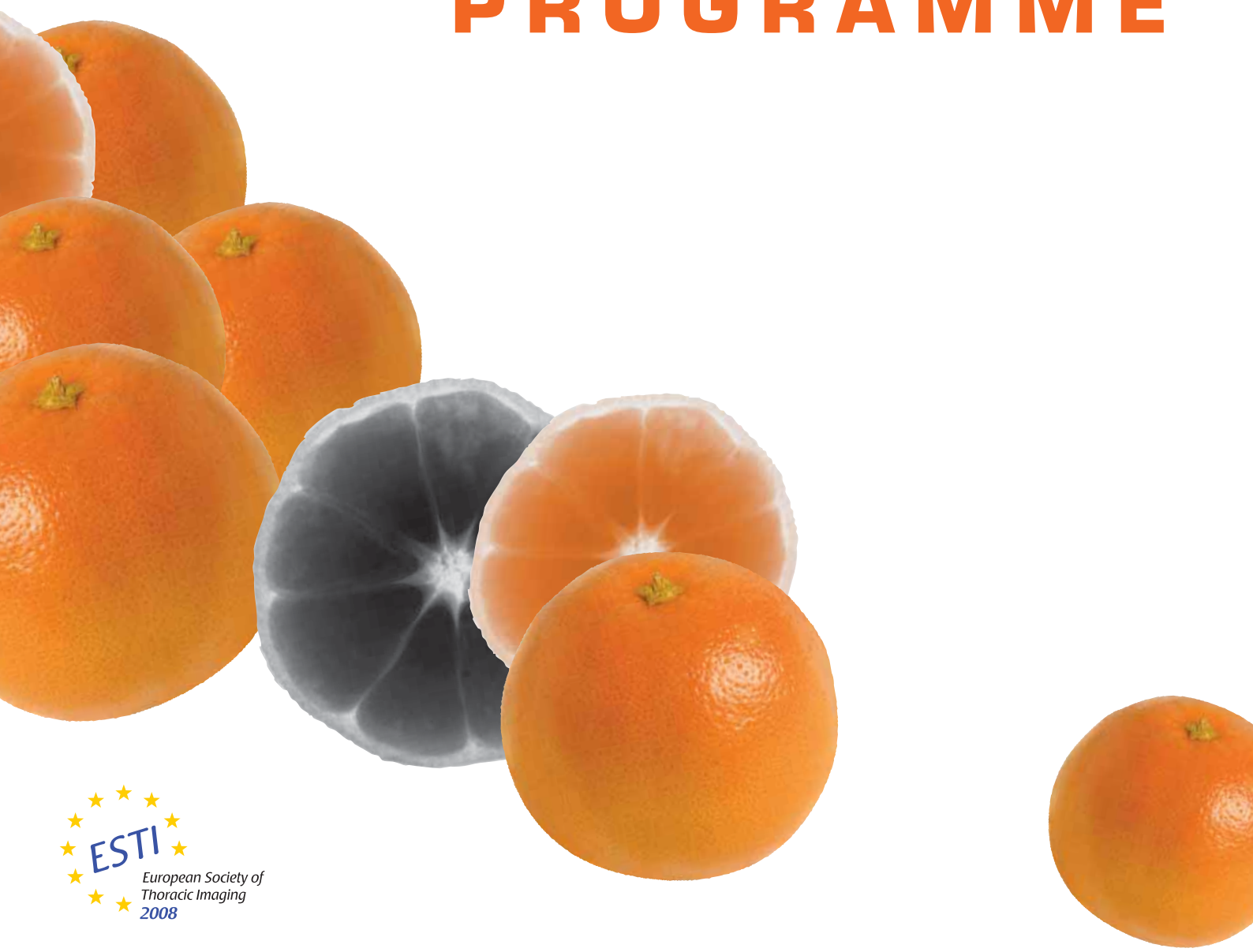

ESTI
European Society of Thoracic Imaging
2008

DOTAREM®

Acide gadotérique

Le plus stable des complexes de gadolinium

Risque limité de libération de gadolinium

Constante de stabilité thermodynamique

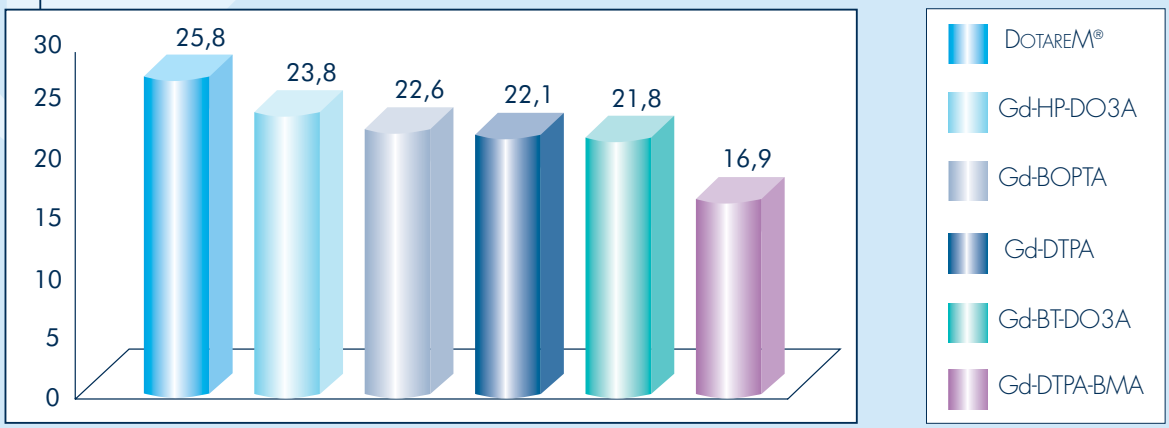

Estimée en log K à pH 11.

TWEEDLE M. Physicochemical properties of gadoteridol and other magnetic resonance contrast agents. Invest. Radiol.; 1992 vol.27 suppl.1 p.2-6
WEDEKING P, et al. Dissociation of gadolinium chelates in mice: relationship to chemical characteristics. Magn. Reson. Imaging; 1992 vol.10 p.641-648
KIRCHIN MA, et al. Contrast agents for magnetic resonance imaging - safety update. Top. Magn. Reson. Imaging; 2003 vol.14 p.426-435
BELLIN MF, et al. Currently used non specific extracellular MR contrast media. Eur. Radiol.; 2003 vol.13 p.2688-2698

DOTAREM 0,5 mmol/ML, solution injectable en flacons et seringues préremplies - COMPOSITION QUALITATIVE ET QUANTITATIVE POUR 100 mL : Acide gadotérique* (27,932 g) correspondant à DOTA (20,246 g) - Oxyde de gadolinium (9,062 g) - Excipients : Méglumine - Eau pour préparations injectables (* Acide gadotérique:complexe de gadolinium de l'acide 1, 4, 7, 10 tétr-aazacyclododécane N, N', N'', N''' tétra-acétique). **DONNEES CLINIQUES : Indications thérapeutiques :** Imagerie par résonance magnétique pour : pathologies cérébrales et médullaires, pathologies du rachis et autres pathologies du corps entier (dont angiographie). **Posologie et mode d'administration :** La dose recommandée est de 0,1 mmol/kg soit 0,2 mL/kg chez l'adulte comme chez l'enfant et le nourrisson. En angiographie, lorsque les résultats de l'examen en cours le rendent nécessaire, une deuxième injection au cours de la même session est possible. Dans quelques cas exceptionnels comme la confirmation du caractère unique d'une métastase ou la détection de tumeurs leptoméningées, une deuxième injection de 0.2 mmol/kg peut être administrée. Le produit doit être administré en injection intraveineuse stricte. **Contre-indications :** Antécédents d'hypersensibilité aux sels de gadolinium. Contre-indications liées à l'IRM : sujet porteur de pace-maker, sujet porteur de clip vasculaire. **Mises en garde et précautions particulières d'emploi (cf. Vidal) :** A administrer uniquement par voie intraveineuse stricte. Ne jamais injecter par voie subarachnoïdienne (ou épidurale). La prudence est conseillée par rapport aux réactions de type anaphyllactique, à l'insuffisance rénale et aux troubles du système nerveux central. Des cas de FNS ont été rapportés après injection de certains produits de contraste contenant du gadolinium chez des patients ayant une insuffisance rénale sévère. Etant donné qu'il est possible que des cas de FNS surviennent avec Dotarem, ce produit doit être utilisé avec précaution chez ces patients. **Interactions avec d'autres médicaments et autres formes d'interactions (cf Vidal). Grossesse et allaitement (cf.Vidal) :** L'utilisation de Dotarem ne doit être envisagée au cours de la grossesse que si nécessaire. Il est prudent d'interrompre transitoirement l'allaitement pendant les jours qui suivent l'examen pratiqué avec Dotarem. **Effets indésirables :** Comme pour toute injection de complexes paramagnétiques, de rares réactions de type anaphylactique pouvant aller jusqu'au choc peuvent survenir, nécessitant un traitement d'urgence. Des troubles généraux (très rares) et des accidents liés au site d'administration (extravasation), de très rares troubles cutanés et des tissus sous-cutanés, de très rares troubles du système nerveux central, de très rares troubles musculaires. **PROPRIETES PHARMACOLOGIQUES (cf. Vidal) - DONNEES PHARMACEUTIQUES (cf Vidal) - PRESENTATION ET NUMERO D'IDENTIFICATION ADMINISTRATIVE - CONDITIONS DE DELIVRANCE :** 358 954.2 : 5 ml en flacon (verre) Prix : 27,46 € - 331 713.4 : 10 ml en flacon (verre) Prix : 47,56 € - 3589536 : 10 ml en seringue pré-remplie (verre) Agréée Collectivités - 331 714.0 : 15 ml en flacon (verre) Prix : 67,06 € - 338 403.0 : 15 ml en seringue pré-remplie (verre) Prix : 68,90 € - 331 715.7 : 20 ml en flacon (verre) Prix : 85,75 € - 338 404.7 : 20 ml en seringue pré-remplie (verre) Prix : 88,17 € - Liste I - Remb Séc. Soc. à 65 % - Collect. **GUERBET - BP 57400 - 95943 Roissy CdG Cedex -Tel : 01.45.91.50.00** (ref.06/07). **Pour une information complète, consulter le dictionnaire VIDAL.**

PF0743 - Octobre 2007

Guerbet

Contrast for Life

ESTI 2008

May 30 – June 1, 2008

FINAL PROGRAMME

CONTENT

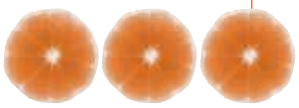

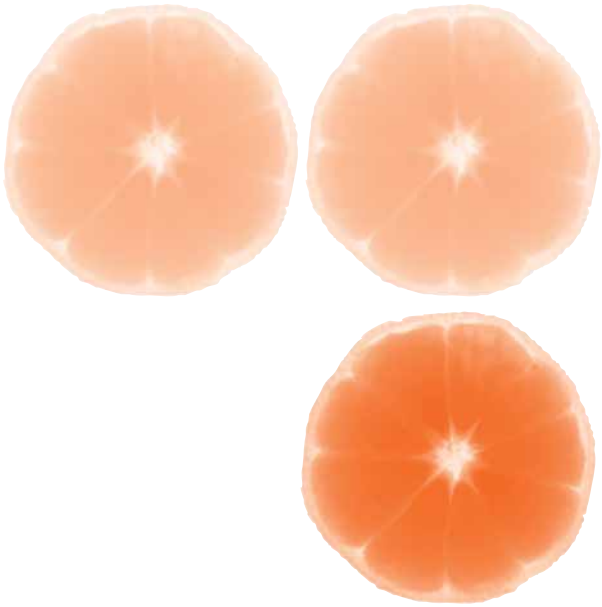

ESTI EXECUTIVE COMMITTEE 2007 – 2008

President
Philippe A. Grenier, Paris/FR

Past-President
Katerina Malagari, Athens/FR

President-Elect
José Vilar, Valencia/ES

Vice President
Peter Vock, Berne/CH

Treasurer
Nigel Howarth, Chêne-Bougeries/CH

Secretary General
Denis Tack, Brussels/BE

Councillors
Cornelia Schaefer-Prokop, Amsterdam/NL
Alexander Bankier, Boston, MA/US
Fergus Gleeson, Oxford/UK

Electronic Media Committee
Jiri Neuwirth, Prague/CZ

Industry Relationship Committee
Hans-Ulrich Kauczor, Heidelberg/DE

Programme Committee
Tomas Franquet, Barcelona/ES

By Law Committee
Mathias Prokop, Utrecht/NL

Jury Committee
Maria Luisa Storto, Chieti/IT

Training and Educational Committee
Johny A. Verschakelen, Leuven/BE

Strategic Committee
Lorenzo Bonomo, Rome/IT

ORGANISING SECRETARIAT

ESTI Office
Neutorgasse 9/2
AT – 1010 Vienna, Austria
Phone: +43-1-533 40 64-0
Fax: +43-1-535 70 37
E-Mail: office@esti2008.org

WEBSITE

www.esti2008.org

HOTEL ACCOMMODATION/TRAVEL AGENT

Voyages C. Mathez
4, Av Georges Clemenceau
FR – 06 000 Nice, France
Phone: +33-4-93 82 68 82
Fax: +33-4-93 87 93 60
E-Mail: esti2008@matheztravel.com

CONFERENCE VENUE

Hotel "Le Méridien"
1, Promenade des Anglais
FR – 06046 Nice, France

graphic & layout: www.mulina.at, 2008

This congress is organised within the framework of an A-level school project and school leaving examination of the Commercial College, "International Business", Steyr, Austria. The participating students are: Sabrina Adami, Alexandra Haller, Marlene Hollnbuchner, Sandra Königstorfer, Eva Lindlbauer. Grade 4 - 5 (2007/2008)

Vital Images is a leading provider of enterprise-wide advanced visualization and analysis software solutions. The company's technology gives radiologists, cardiologists, oncologists and other medical specialists time-saving productivity and communications tools that can be accessed throughout the enterprise and via the Web for easy use in the day-to-day practice of medicine. Vital Images maintains offices in the U.S., Europe and Asia.


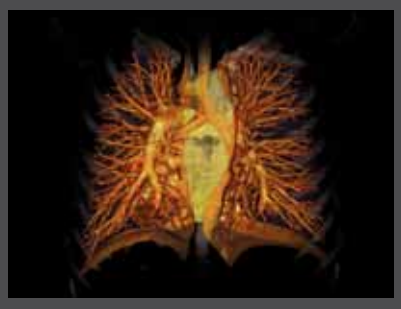

Advanced visualization software for the life of your enterprise.
www.vitalimages.com

VITAL

INVITATION

Dear Members, Dear Participants,

On behalf of the ESTI Executive Committee, I would like to warmly welcome you to the 16th ESTI Annual Meeting in Nice.

The scientific programme of this meeting is well structured and balanced. It was designed to guarantee that attendees will maximise their learning experience, providing both knowledge refreshment as well as cutting-edge developments in chest imaging. An international faculty, formed by the leading experts in their fields, has gathered. All the relevant topics, from technological developments to molecular and functional imaging will be covered by them throughout the meeting.

I would like to acknowledge the efforts of the members of the Programme Committee, perfectly driven by Tomas Franquet and thank them for their outstanding work that resulted in an exciting scientific and educational programme.

Let me thank all authors who submitted abstracts to be presented as oral presentations during 4 scientific sessions, or scientific or education exhibits shown in the EPOS™ format.
I also thank the reviewing panel and the EPOS™ jury for reviewing the submissions and for guaranteeing the high quality content of our meeting.

I am also pleased to thank our partners from the industry who have accepted to support the meeting, and to contribute to its success in presenting the technical innovations in chest imaging.
Furthermore, I am very grateful for all the organisational efforts provided by the ESR Office staff, which led this final programme to reality.

Nice is the pearl of the French Riviera, located in the middle of superb and attractive surroundings. I hope that the social events fulfil your expectations and turn out to be unforgettable and entertaining moments of friendship in this beautiful seaside city.

Philippe A. Grenier

President of ESTI

MEETING PRESIDENT
Prof. Philippe A. Grenier
Hôpital Pitié-Salpêtrière
Service Central de Radiologie
47-83, Boulevard de l'Hôpital
FR – 75013 Paris, France
Phone: +33-1-4217 8215 (8225)
Fax: +33-1-4217 8224
E-Mail: philippe.grenier@psl.aphp.fr

HONORARY MEMBERSHIP

Pierre Schnyder

was born in Switzerland in 1943. He is married and is the father of 2 children.
From 1964 to 1971, he studied medicine at the University of Lausanne, Switzerland, where he obtained his Federal Medical Degree in 1971. After one year of residency in pathology and one year in surgery, he started a 4-year-term of training in radiology at the University of Lausanne. Then, he completed his training by a 1-year fellowship in the Department of Radiology at the Moffit Hospital, University of California, San Francisco. In 1978, he received his board certification in radiology. He was appointed Director of the CT unit at the University Hospital of Lausanne, a place where he was successively appointed Privat-Docent and Agrégé in 1985, Professor and Chairman of the Department of Radiology in 1988, and Professor and Chairman, Director of the Department of Radiology, Radio oncology and Nuclear Medicine in 1993, a post he is still holding.

Pierre Schnyder has demonstrated several fields of interest in radiology, including chest, abdomen, and emergency radiology. He is the author or co-author of more than 300 articles, 45 books or book chapters. He presented more than 500 lectures, scientific presentations or posters at national or international meetings.
His commitment to radiology is also manifested in several memberships of radiological societies, such as the Swiss Society of Radiology of which he was awarded by the Schinz Medal, the Sociétés Française and Belge de Radiologie, both of which he received honorary membership, the American Ray Society, the Radiological Society of North America, the European Society of Gastrointestinal and Abdominal Radiology. He is a member of the Advisory Board of Radiology Outreach Foundation, and Advisor of the International Diagnostic Course in Davos. He was a member of the Executive Bureau and Chair of the Education Committee of the European Association of Radiology, between 1995 and 1999.
Pierre Schnyder is a founder member of the European Society of Thoracic Imaging (ESTI). He entered the Executive Committee of the Society in 1994, he served as treasurer between 1995 and 1999, became President in 2002 and organised the annual meeting in Lausanne in 2003, a meeting regarded as one of the most successful of the Society.

Beside his intensive work, Pierre Schnyder is keen of speed sports (sportive cars, motorbike, motorboat) and he is a passionate skier.

In recognition of his remarkable achievements in chest radiology, and his contribution and commitment to ESTI, Pierre Schnyder is awarded Honorary Membership of the European Society of Thoracic Imaging.

Philippe A. Grenier
President of ESTI

HONORARY MEMBERSHIP WILL BE AWARDED DURING THE OPENING CEREMONY ON FRIDAY, MAY 30.

GENERAL INFORMATION

BEACH PARTY

Friday, May 30, 2008
19:30 – 21:30

The welcome reception will be a stylish beach party, located on Le Méridien´s private beach, facing one of the most beautiful bays in the world.
ESTI 2008 participants who have registered for the welcome reception are heartly welcome to join the party.

CME

The European Society of Thoracic Imaging, ESTI, is accredited by the European Accreditation Council for Continuing Medical Education (EACCME). The EACCME is an institution of the European Union of Medical Specialists (UEMS), www.uems.be.

Accreditation for ESTI 2008 has been requested from the UEMS and the number of credit hours of European external CME credits will be announced on the confirmation of attendance, which will be handed out at the congress.

COFFEE BREAKS

Coffee, during the official coffee break times, is included in the registration fee.

May 30 – June 1: 10:00 – 10:30
May 30 – May 31: 15:30 – 16:00

EDUCATIONAL AND SCIENTIFIC PROGRAMME FEATURES

Abbreviations in the programme as follows

SS	Scientific Session
SY	Lunch Symposia
ES	Educational Session
CD	Case of the day
FP	Film Panel Interpretation

THE ACTIVE STUDY

iomeron®
imeron®
Iomeprol

Go Higher See Better

A multicenter, randomized, double-blind, parallel-group study has shown that the rate of post-dose increases in serum creatinine ≥ 0.5 mg/dL, as well as mean changes in serum creatinine from baseline, were significantly ($p<0.05$) greater following the IV injection of iodixanol-320 compared to iomeprol-400 in patients with moderate-to-severe chronic kidney disease.[1]

Incidence of Contrast-induced Nephropathy (CIN): All Patients (n=148)

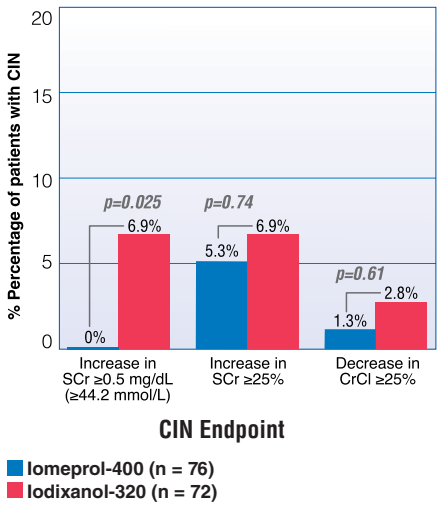

Incidence of CIN: Patients with creatinine clearance <40mL/min and/or SCr ≥2.0 mg/dL (n=73)

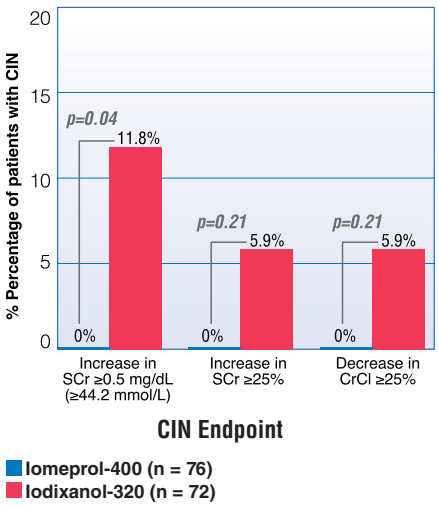

The **A**bdominal **C**omputed **T**omography: **I**omeron®-400 vs **V**isipaque™-320 **E**nhancement (**ACTIVE**) study was a prospective, multicenter study performed to compare the effects on renal function and incidence of CIN after the intravenous injection of equi-iodine doses of iomeprol-400 and iodixanol-320 in patients at risk for CIN undergoing MDCT imaging of the liver.

REFERENCE: 1)Henrik S. Thomsen, Sameh K. Morcos, Christiane M. Erley, Luigi Grazioli, Lorenzo Bonomo, Zhaohui Ni, Luigia Romano, and the Investigators in the Abdominal Computed Tomography: IOMERON®-400 Versus VISIPAQUE™-320 Enhancement (ACTIVE) Study The ACTIVE Trial: Comparison of the Effects on Renal Function of Iomeprol-400 and Iodixanol-320 in Patients With Chronic Kidney Disease Undergoing Abdominal Computed Tomography; Invest Radiol 2008;43(3):170–178

BRACCO
IT'S FROM INSIDE

IOMERON® - CORE SUMMARY OF PRODUCT CHARACTERISTICS

1. NAME OF THE MEDICINAL PRODUCT. IOMERON 150 mg/ml Solution for Injection. IOMERON 200 mg/ml Solution for Injection. IOMERON 250 mg/ml Solution for Injection. IOMERON 300 mg/ml Solution for Injection. IOMERON 350 mg/ml Solution for Injection. IOMERON 400 mg/ml Solution for Injection.

2. QUALITATIVE AND QUANTITATIVE COMPOSITION IOMERON 150 contains (quantity/100 ml): Active ingredient: Iomeprol: 30.62 g. IOMERON 200 contains (quantity/100 ml): Active ingredient: Iomeprol: 40.82 g. IOMERON 250 contains (quantity/100 ml): Active ingredient: Iomeprol: 51.03 g. IOMERON 300 contains (quantity/100 ml): Active ingredient: Iomeprol: 61.24 g. IOMERON 350 contains (quantity/100 ml): Active ingredient: Iomeprol: 71.44 g. IOMERON 400 contains (quantity/100 ml): Active ingredient: Iomeprol: 81.65 g. For excipients see 6.1

3. PHARMACEUTICAL FORM Solution for injection displaying the following physicochemical characteristics by Iodine Strengths as below

Iodine concentration MgI/mL	Osmolality MosmL/kg water (x ± s.t95)*	Viscosity MPa.s (x ± s.t95)	
	37°C	20°C	37°C
150	301 ± 14	2.0 ± 0.2	1.4 ± 0.1
200	362 ± 17	3.1 ± 0.2	2.0 ± 0.2
250	435 ± 20	4.9 ± 0.4	2.9 ± 0.3
300	521 ± 24	8.1 ± 0.7	4.5 ± 0.4
350	618 ± 29	14.5 ± 1.1	7.5 ± 0.6
400	726 ± 34	27.5 ± 2.3	12.6 ± 1.1

*Vapour tension method

4. CLINICAL PARTICULARS

4.1 Therapeutic indications This medicinal product is for diagnostic use only Iomeron 150 Infusion urography, digital substraction phlebography, CT (brain and body) cavernosography, intravenous and intraarterial DSA, ERCP, MCU, MCU in paediatrics. Iomeron 200 Peripheral phlebography, digital subtraction phlebography, CT (brain and body), cavernosography, intravenous and intraarterial DSA, ERCP, arthrography, hysterosalpingography, cholangiography, retrograde urethrography, retrograde pyelo-ureterography, myelography. Iomeron 250 Intravenous urography, peripheral phlebography, CT (brain and body), intravenous and intraarterial DSA, myelography. Iomeron 300 Intravenous urography (in adults and paediatrics), peripheral phlebography, CT (brain and body), cavernosography, intravenous DSA, conventional angiography, intraarterial DSA, angiocardiography (in adults and paediatrics), conventional selective coronary arteriography, interventional coronary arteriography, ERCP, arthrography, hysterosalpingography, fistulography, discography, galactography, cholangiography, dacryocystography, sialography, retrograde urethrography, retrograde pyelo-ureterography, myelography. Iomeron 350 Intravenous urography (in adults and paediatrics), CT (body), intravenous DSA, conventional angiography, intraarterial DSA, angiocardiography (in adults and paediatrics), conventional selective coronary arteriography, interventional coronary arteriography, arthrography, hysterosalpingography, fistulography, galactography, retrograde cholangiography, dacryocystography, sialography. Iomeron 400 Intravenous urography (in adults including those with renal impairment or diabetes), CT (body), conventional angiography, intraarterial DSA, angiocardiography (in adults and paediatrics), conventional selective coronary arteriography, interventional coronary arteriography, fistulography, galactography, dacryocystography, sialography. CT: Computed Tomography, DS: Digital Subtraction, DSA: Digital Subtraction Angiography, ERCP: Endoscopic Retrograde Cholangio-Pancreatography, MCU: Micturating Cisto-Urethrography.

4.2 Posology and method of administration Instructions for use: Dosage and rate of administration may vary depending on the clinical question, the technique to be employed, the body area to be examined, the instrumentation, as well as on the age, body size, cardiac output and patient's clinical conditionsIn the CNS the imaging window has been shown to be up to 60 minutes after the administration. In the liver delayed imaging can be performed between 40 and 120 minutes following the injection, depending on the individual imaging needs.

Indication	Formulation mg (iodine)/ml	Proposed dosages
Intravenous urography	250, 300, 350, 400	Adults: 50 - 150 ml Newborns: 3 - 4.8 ml/kg Infants: 2.5 - 4 ml/kg Paediatric patients: 1 - 2.5 ml/kg[a]
Infusion urography	150	Adults: 250 ml Paediatric patients[a]
Peripheral phlebography	200, 250, 300	Adults: 10 - 100 ml. repeat as necessary[b] (10 - 50 ml upper extremities; 50 - 100 ml lower extremities)
Phlebography in DS	150, 200	Adults: 10 - 100 ml. repeat as necessary[b] (10 - 50 ml upper extremities; 50 - 100 ml lower extremities)
CT brain	150, 200, 250, 300	Adults: 50 - 200 ml Paediatric patients[a]
CT body	150, 200, 250, 300, 350, 400	Adults: 100-200 ml Paediatric patients[a]
Cavernosography	150, 200, 300	Adults: up to 100 ml
Intravenous DSA	250, 300, 350, 400	Adults: 100-250 ml Paediatric patients[a]
Conventional angiography		
Arteriography of upper extremities:	300, 350	Adults[b]
Arteriography of pelvis and lower extremities:	300, 350, 400	Adults[b]
Abdominal arteriography:	300, 350, 400	Adults[b]
Arteriography of descending aorta:	300, 350	Adults[b]
Pulmonary angiography:	300, 350, 400	Adults: up to 170 ml
Cerebral angiography:	300, 350	Adults: up to 100 ml
Paediatric arteriography:	300	Children: up to 130 mla
Interventional:	300, 350, 400	Adults[b] Paediatric patients[a]
Intraarterial DSA		
- Cerebral:	150, 200, 300, 350	Adults: 30 - 60 ml for general view; 5 - 10 ml for selective injections Paediatric Patients[a]
- Thoracic:	200, 300	Adults[b]: 20 - 25 ml (aorta) repeat as necessary 20 ml (bronchial arteries)
- Aortic arch:	150, 200, 300, 350	Adults[c]
- Abdomen:	150, 200, 250, 300	Adults[c]
Aortography	150, 200, 300, 350	Adults[c]
Translumbar aortography	150, 200, 300	Adults[b]
Peripheral arteriography:	150, 200, 250, 300	Adults: 5 - 10 ml for selective injections up to 250 ml Paediatric patients[a]
Interventional:	150, 200, 300	Adults: 10-30 ml for selective injections up to 250 ml Paediatric patients[a]
Angiocardiography	300, 350 ,400	Adults[b] Paediatric patients[a]
Conventional selective coronary arteriography	300, 350, 400	Adults: 4-10 ml artery repeat as necessary
ERCP	150, 200, 300	Adults: up to 100 ml
Arthrography	200, 300, 350	Adults: up to 10 ml per injection
Hysterosalpingography	200, 300, 350	Adults: up to 35 ml
Fistulography	300, 350, 400	Adults: up to 100 ml
Discography	300	Adults: up to 4 ml
Galactography	300, 350, 400	Adults: 0.15 - 1.2 ml per injection
Dacryocystography	300, 350, 400	Adults: 2.5 - 8 ml per injection
Sialography	300, 350, 400	Adults: 1 - 3 ml per injection
MCU	150	Adults: 100 - 250 ml
	150	Paediatric patients: 40 - 210 ml[a]
Retrograde cholangiography	200, 300, 350	Adults: up to 60 ml
Retrograde ureterography	200, 300	Adults: 20 - 100 ml
Retrograde pyelo-ureterography	200, 300	Adults: 10 - 20 ml per injection
Myelography	200, 250, 300	Adults: 200: 13-22 ml, 250: 10-18 ml, 300: 8-15 ml

a = According to body weight and age
b = Do not exceed 250 ml. Single injection volume depends on the vascular area to be examined
c = Do not exceed 350 ml

4.3 Contra-indications Hypersensitivity to the active principle and to any of its ingredients. Intravascular administration There are no precise and absolute contraindications to the use of non-ionic uroangiographic contrast media. Investigations of the female genitalia are contraindicated in suspected or confirmed pregnancy and in cases of acute inflammation. Intrathecal administration Concomitant administration of Iomeprol with corticosteroids is contraindicated (see 4.5 Interactions). Due to overdose considerations, immediate repeat myelography in the event of technical failure is contraindicated.

4.4 Special warnings and special precaution for use Special Warnings **General for all administration routes:** Consideration of possible serious side effects, the use of iodinated contrast media should be limited to cases for which there is a precise need for a contrast examination. The need should be evaluated on the basis of the clinical status of the patient, in particular in relation to history of pathologies of the cardiovascular, renal and/or hepatobiliary systems. The use of contrast media should be avoided in case of Waldenstroem's paraproteinemia, and multiple myeloma and of advanced hepato and/or renal diseases. Cardioangiographic diagnostic procedures that involve the use of any radiopaque contrast media should be carried out in Hospitals where appropriate emergency facilities and personnel trained in life support is readily available. After any other contrast-enhanced X-ray procedures, competent personnel and adequate emergency facilities should be available (AMBU, oxygen, antihistaminics, vasoconstrictors, cortisonics, etc.) in the radiology departments of public or private clinics. After any other contrast-enhanced X-ray procedures, competent personnel and adequate emergency facilities should be available (AMBU, oxygen, antihistaminics, vasoconstrictors, cortisonics, etc.) in the radiology departments of public or private clinics. Special care should be taken in patients with suspected thrombosis, phlebitis, severe ischemia, local infection or artero-venous obstruction. **Use in specific patients: Neonates, infants, children.** Young infants (age < 1 year) especially neonates, are particularly susceptible to electrolyte imbalances and haemodynamic alterations. Care should be taken regarding the dosage to be used, the details of the procedure and the patient's status. **Elderly.** The elderly are at special risk of reactions due to CM high dosage. Myocardial ischemia, major arrhythmias and extrasystoles are more likely to occur in these patients. The frequently encountered combination of neurological disturbances and severe vascular pathologies constitutes a serious complication. The probability of acute renal insufficiency is higher in these subjects. **Women Of Child-Bearing Potential:** Appropriate investigations and measures should be taken when exposing women of child-bearing potential to any X-ray examination, whether with or without contrast medium. **Use in patients with specific pathologic conditions. Hypersensitivity to iodinated contrast media.** Hypersensitivity or a previous history of a reaction to iodinated contrast media also increases the risk of recurrence of a severe reaction with non ionic media. **Allergic disposition.** It is generally agreed that adverse reactions to iodinated contrast media are more common in patients having a history of allergy: hay fever, hives and food allergy. **Asthmatic patients.** The risk of bronchospasm, inducing reactions in asthmatic patients, is higher after contrast. **Hyperthyroidism, nodular goitre.** The small amount of free inorganic iodide that may be present in contrast media, might have some effects on thyroid function: these effects appear more evident in patients with hyperthyroidism or goitre. Thyroid storms have been reported following administration of ionic contrast media. **Intraarterial and intravenous administration. Use in patients with specific pathologic conditions. Renal failure.** Pre-existing renal impairment may predispose to acute renal dysfunction following contrast media administration. Preventive measures include: identification of high risk patients; ensuring adequate hydration before CM administration, preferably by maintaining i.v. infusion before and during the procedure and until the CM has been cleared by the kidneys; avoiding whenever possible, the administration of nephrotoxic drugs or major surgery or procedure such as renal angioplasty, until the CM has been cleared; postponing a new contrast agent examination until renal function returns to pre-examination levels. Patients on dialysis may receive CM, such as iomeprol, before dialysis.**Diabetes mellitus.** The presence of renal damage in diabetic patients is one of the factors predisposing to renal impairment following CM administration. This may precipitate lactic acidosis in patients who are taking biguanides. As a precaution, biguanides should be stopped 48 hours prior to the CM examination and reinstated only after control of renal function has been regained. **Multiple myeloma, paraproteinaemia (Waldestroem's paraproteinemia).** It is necessary to consider that the presence of myelomatosis or paraproteinaemias is a factor predisposing to renal impairment following CM administration. Adequate hydration and monitoring the renal function are recommended. **Phaeochromocytoma.** These patients may develop severe (rarely uncontrollable) hypertensive crises following intravascular CM-usage during radiological procedures. **Sickle Cell Disease.** Contrast media may promote sickling in individuals who are homozigous for sickle cell disease. Adequate hydration is recommended. **Myasthenia Gravis.** The administration of iodinated contrast media may aggravate myasthenia signs and symptoms. Severe liver and renal dysfunctions. It is necessary to consider that a combination of severe hepatic and renal impairment can delay CM excretion, therefore predisposing to untoward reactions. **Severe cardiovascular disease.**There is an increased risk of severe reactions in individuals with severe cardiac disease and particularly in those with heart failure and coronary artery disease. The intravascular CM injection may precipitate pulmonary oedema in patients with manifest or incipient heart failure, whereas CM administration, in pulmonary hypertension and heart valvular diseases, may lead to pronounced haemodynamic changes. Ischaemic ECG changes and major arrhythmias are commonest in elderly patients and in those with preexisting cardiac disease: their frequency and severity appear to be related to the severity of cardiac impairment. Severe and chronic hypertension may increase the risk of renal damage following CM administration and the risks associated with the catheterisation procedure. **CNS disorders.** Particular care should be paid to the intravascular administration of CM in patients with acute cerebral infarction, acute intracranial haemorrhage, and conditions involving blood-brain-barrier (BBB) damage, brain oedema and acute demyelination. The presence of intracranial tumors or metastases and a history of epilepsy may increase the probability of the occurrence of convulsive seizures. Neurological symptoms due to degenerative, inflammatory or neoplastic cerebrovascular pathologies may be exacerbated by CM administration. Vasospasm and consequent cerebral ischaemic phenomena may be caused by intravascular injections of CM, often procedurally related and possibly triggered by the tip of the catheter or excess of catheter pressure. Patients with symptomatic cerebrovascular diseases, recent stroke or frequent TIA (transient ischaemic attack) have an increased risk of transient neurological complications. **Alcoholism.** Acute and chronic alcoholism have been proven both experimentally and clinically to increase BBB permeability. This facilitates the passage of iodinated agents into the cerebral tissue, possibly leading to CNS disorders. Caution must be exercised in alcoholics because of the possibility of a reduced seizure threshold. **Drug addiction.** Caution must be exercised in drug addicts because of the possibility of a reduced seizure threshold. Keep away of reach of children. Special Precautions for use **In relation to the patient. Hydration:** Any severe disorders of water and electrolyte balance should be corrected. Especially in patients with multiple myeloma, diabetes mellitus, polyuria, oliguria, hyperuricemia, as well as in babies, small children and elderly patients adequate hydration must be ensured before examination. **Dietary advice:** Unless otherwise instructed by the doctor, a normal diet may be maintained on the day of the examination. Adequate fluid intake must be ensured. However, it is advised that the patient should refrain from eating for two hours prior to the procedure. **Pre-medication:** In patients with phaeochromocytoma pre-medication with alpha-receptor blockers is recommended because of the risk of blood pressure crises. **Hypersensitivity:** In patients with an allergic disposition, known hypersensitivity to iodinated contrast media and a history of asthma, pre-medication with anti-histamines and/or corticoids is recommended to prevent possibile anaphylactoid reactions. **Anxiety:** Pronounced states of excitement, anxiety and pain can be the cause of side effects or intensify contrast-related reactions. These patients may be given a sedative. **Concomitant Treatments:** Treatment with drugs that lower the seizure threshold such as neuroleptics, analgesics, anti-emetics, and phenotiazine derivatives should be discontinued 48 hours before the examination. Treatment should not be resumed until 24 hours post-procedure. Anticonvulsant therapy must not be discontinued and should be administered in optimal dosage. **In relation to the procedure. Coagulation, flushing of catheters.** A property of non-ionic contrast media is the extremely low interference with normal physiological functions. Non-ionic contrast media have less anti-coagulant activity in-vitro than ionic contrast media. Medical personnel performing vascular catheterisation should be aware of this and pay meticulous attention to the angiographic technique and catheter flushing so as to minimize the risk of procedure-related thrombosis and embolism, including catheter flushing with physiological saline solution (if necessary with heparin added). **Observation of the patient.** Intravascular administration of contrast media should, if possible, be done with the patient lying down. The patient should be kept under close supervision for 15 minutes following the injection as the majority of severe reactions occur at this time. Intrathecal administration. After completion of direct cervical or lumbo-cervical procedures: - raise the head of table steeply (45° angle) for about two minutes to restore CM to lower levels, - raise head of stretcher to at least 30° before moving patient into it; - avoid excessive and particularly active patient movement or straining; - maintain the patient under close observation, quiet and in a "head up" position, especially in the first few hours; - the patient should remain supine and at bed rest during this period; - encourage oral fluids and diet as tolerated. **Pre-testing.** Sensitivity test doses are not recommended since severe or fatal reactions to contrast media are not predictable from a patient's history or a sensitivity test. **Extravasation:** Extreme caution during injection of contrast media is necessary to avoid extravasation. This is especially important in patients with severe arterial or venous disease.

4.5 Interaction with other medicinal products and other forms of interaction Epidural and intrathecal corticosteroids should never be concurrently administered when iodinated contrast media are used, because corticosteroids may promote and affect the signs and symptoms of arachnoiditis. (see 4.3 Contraindications) **Thyroid function tests.** Following administration of iodinated contrast media, the capacity of the thyroid tissue to take up radioisotopes for the diagnosis of thyroid disorders is reduced for up to two weeks, or even longer in individual cases. The results of Protein Binding Iodine and radioactive iodine uptake studies, which depend on iodine estimations, will not accurately reflect thyroid function for up to 16 days following administration of iodinated contrast media. However, thyroid function tests not depending on iodine estimations, e.g., T3 resin uptake and total or free thyroxine (T4) assays are not affected. **Oral Cholecystographic Agents.** Recent literature has revealed no evidence of interactions of renally-excreted contrast media with oral cholecystographic contrast media. **Laboratory tests.** High concentrations of contrast media in serum and urine can interfere with laboratory test results of bilirubin, proteins or inorganic substances (e.g. iron, copper, calcium, phosphate).

4.6 Pregnancy and lactation Animal studies do not indicate any teratogenic or foetotoxic effects. As with other non-ionic contrast media, there are no adequate and well-controlled studies in pregnant women to confirm no harmful effect also in human beings. Whenever possible, radiation exposure, either with or without contrast media use, should be avoided during pregnancy and its benefit accurately weighted against the possible risks. Iodinated contrast media are poorly excreted in human breast milk, and from experience it appears there should be no damage to the breast-fed baby. However, as a cautionary measure, breast-feeding should be discontinued prior to the administration of iomeprol and should not be recommenced until at least 24 hours after the administration of the contrast medium.

4.7 Effects on ability to drive and use machines No data is available. However, given the rare possibility of delayed adverse reactions to contrast media, driving or using machinery should be avoided for 24 hours following the administration.

4.8 Undesirable effects General The use of iodinated contrast media may cause untoward side effects. They are usually mild to moderate. However, more serious reactions up to anaphylactoid shock, with possible fatal outcome, may occur. In most cases reactions occur within minutes of dosing up. However, reactions may manifest also later on up to 24 hours from the injection, depending on the administration route. **Anaphylaxis** (anaphylactoid/hypersensitivity reactions) may manifest with various symptoms, and rarely does any one patient develop all the symptoms. Typically, in 1 to 15 min (but rarely after as long as 2 h), the patient complains of feeling abnormal, agitation, flushing, feeling hot, sweating increased, dizziness, lacrimation increased, rhinitis, palpitations, paraesthesia, pruritus, head throbbing, pharyngolaryngeal pain and throat tightness, dysphagia, cough, sneezing, urticaria, erythema, and mild localised oedema or angioneurotic oedema and dyspnoea owing to tongue and laryngeal oedema and/or laryngospasm manifesting with wheezing and bronchospasm. Nausea, vomiting, abdominal pain, and diarrhoea are less common. These reactions, which can occur independently of the dose administered or the route of administration, may represent the first signs of circulatory collapse. Administration of the contrast medium must be discontinued immediately and, if needed, appropriate specific treatment urgently initiated via venous access. Severe anaphylactic reactions involving the cardiovascular system, such as vasodilatation, with pronounced hypotension, reflex tachycardia, dyspnoea, agitation, cyanosis and loss of consciousness progressing to respiratory and/or cardiac arrest may result in death. These events can occur rapidly and require full and aggressive cardio-pulmonary resuscitation. Primary circulatory collapse, can occur as the only and/or initial presentation without respiratory symptoms or without other signs or symptoms outlined above. **From Clinical Studies** Adverse experiences reported among patients treated with Iomeprol during clinical trials are shown below.

	Common	Uncommon	Rare
Cardiovascular (mainly after cardio-vascular procedures/ interventions)		Bradycardia, tachycardia, hypertension, hypotension	Vasodilatation, cyanosis, circulatory collapse
Nervous System	Asthenia, syncope,headache	Dizziness,paralysis, agitation	Tremor, muscle spasms, confusion, loss of consciousness, visual field defect, aphasia, convulsions, coma
Gastrointestinal system	Nausea	Vomiting	
Respiratory system	Dyspnoea, nasal congestion, laryngeal oedema		
Skin and Subcutaneous Tissue		Wheals, pruritus, rash	
General	Injection site warmth and pain, pallor	Back pain, chest pain, rigors, injection site haemorrhage, pyrexia, sweating increased	Anaphylactoid reaction (characterized by cardiovascular,respiratory and cutaneous symptoms)
Renal and Urinary Disorders			Renal insufficiency, oliguria, proteinuria, blood creatinine increased

Some of these events may occur as a consequence of the procedure. **Post Marketing Surveillance.** The following undesirable effects have been reported during post- marketing in <3/10.000 patients. **Intravascular and intra-thecal administration:** - General: shock, malaise, fatigue, hot flushes, flushing, cold sweat, coldness local, taste abnormality, thirst, injection site reaction. - Nervous system: hyperkinetic syndrome, encephalopathy, paralysis, oculomotor nerve paralysis, paraesthesia, dysarthria, dizziness, dysphonia,faecal incontinence, brain oedema, -Cardiovascular: cardiac arrest, myocardial infarction, angina pectoris, extrasystoles, arrhythmia, ventricular or atrial fibrillation, tachycardia, palpitations, atrioventricular block, electrocardiogram abnormal, ST segment elevation. - Respiratory: respiratory arrest, pulmonary oedema, acute respiratory distress syndrome (ARDS), bronchospasm, asthma, pharyngeal oedema, laryngeal stridor, rhinitis, cough, hyperventilation, hypoxia, pharynx and/or laryngeal discomfort. - Skin and subcutaneous tissue disorders: angioneurotic oedema, eczema, urticaria, wheals - cold sweat., - Vascular (extracardiac): cerebrovascular disorder, transient ischaemic attack.- Gastrointestinal disorders: pancreatitis acute, ileus, diarrhea, abdominal pain, salivary hypersecretion, dysphagia. - Urogenital: urinary incontinence, blood urea increased. - Senses: parosmia - Eye disorders: blindness transient, visual disturbance, conjunctivitis, lacrimation increased, photopsia, photophobia. - Musculoskeletal: arthralgia, muscle stiffness. - Psychiatric disorders: amnesia, anorexia, anxiety, somnolence. - Liver and biliary system: liver function tests abnormal. - Platelets, bleeding and coagulation: thrombocytopenia. **Administration to body cavities** Blood amylase increase is common following ERCP (Endoscopic retrograde cholangiopancreatography). Rare cases of pancreatitis have been described. The reactions reported in cases of arthrography and fistulography usually represent irritative manifestations superimposed on pre-existing conditions of tissue inflammation. Generalised hypersensitivity reactions are rare, generally mild and in the form of skin reactions. However, the possibility of severe anaphylactoid reactions cannot be excluded. (see beginning of chapter "Undesirable effects"). As with other iodinated contrast media, pelvic pain and malaise may occur after hysterosalpingography.

4.9 Overdose Overdose may lead to life-threatening adverse effects mainly through effects on the pulmonary and cardiovascular system. Treatment of overdosage is directed toward the support of all vital functions, and prompt institution of symptomatic therapy. Iomeprol does not bind to plasma or serum proteins and is therefore dialysable. If needed, hemodialysis can be used to eliminate iomeprol from the body. If intracranial entry of the medium occurs, prophylactic anticovulsant treatment with diazepam or barbiturates orally for 24 to 48 hours should be considered.

5. PHARMACOLOGICAL PROPERTIES

5.1 Pharmacodynamic properties Pharmacotherapeutic category: Radiological contrast media: hydrosoluble, nephrotropic, low osmolality. ATC code: V08AB10. The active ingredient of Iomeron formulations is iomeprol, N,N'-bis(2,3-dihydroxypropyl)-5-[(hydroxyacetyl)-methylamino]-2,4,6-tri-iodo-1,3-benzenedicarboxamide, a tri-iodinated, non-ionic contrast agent, and is indicated for use in X-ray examinations.

5.2 Pharmacokinetic properties Intravascular Administration The pharmacokinetic, tolerability and diagnostic efficacy of Iomeprol in solutions containing up to 400 mg iodine/mL have been determined in healthy volunteers and patients requiring urographic, angiographic, computed tomography (CT) and body cavity examinations. There were no clinically significant changes in laboratory test values and vital signs. The pharmacokinetic of Iomeprol, for intravascular administration, when described by a two-compartment model, shows a rapid phase for drug distribution and a slower phase for drug elimination. In healthy volunteers the mean half-lives of the distribution and elimination phases of Iomeprol were 23 14 (s) min and 109 20 (s) min, respectively. Iomeprol is excreted mainly through the kidneys following intravascular administration. In the absence of renal dysfunction, the cumulative urinary excretion of iomeprol, expressed as percentage of administered intravenous dose, is approximately 24 to 34% at 60 minutes, 84% at 8 hours, 87% at 12 hours, and 95% in the 24 to 96 hour period after administration. In patients with impaired renal function, the elimination half-life is prolonged dependent upon the degree of impairment. Iomeprol does not bind to serum or plasma proteins. **Intra-thecal Administration** The pharmacokinetics of iomeprol after intra-thecal administration shows that Iomeprol is completely absorbed from the cerebrospinal fluid about 3 to 6 hours. The half-life of elimination is between 8 to 11 hours and is independent from the dose. Plasma concentrations were quantifiable up to 24 hours in 93% of the patients. It is completely excreted from the body through the kidney as unchanged Iomeprol. The majority of urinary excretion occurs in the first 24 hours post-dose, with smaller percentage excreted during the 24-48 hour period.

5.3 Preclinical safety data Pre-clinical data reveal no special hazard for humans based on conventional studies of safety pharmacology, repeated dose toxicity, genotoxicity, toxicity to reproduction. Results from studies in rats, mice and dogs demonstrate that iomeprol has an acute intravenous or intra-arterial toxicity similar to that of the other non-ionic contrast media, as well as a good systemic tolerability after repeated intravenous administrations in rats and dogs. LD50 of iomeprol in g (Iodine)/kg and the relevant 95% confidence limits in animals are as follows: **Intravenous administration:** 19.9 (19.3-20.5) (mouse); 14.5 (13.2-16.0) (rat); > 12.5 (dog) **Intraperitoneal administration:** 26.1 (23.3-29,2) (mouse); 10 (8.9-11.3) (rat); **Intracerebroventricular administration:** 1.4 (1.3-1.6) (mouse); **Intracisternal administration:** >1.2 (rat) **Intracarotid administration:** 5.8 (4.64-7.25) (rat)

6. PHARMACEUTICAL PARTICULARS

6.1 List of excipients Trometamol, hydrochloric acid (d=1.18), water for injection

6.2 Incompatibilities Contrast media must not be mixed with other medicinal products, to avoid eventual incompatibilities.

6.3 Shelf life 5 years

6.4 Special precautions for storage Expiry date refers to the product stored correctly in intact packaging. Protect from light. Although the sensitivity of iomeprol to X-rays is low, it is advisable to store the product out of reach of ionizing radiation. Parenteral products should be inspected visually for particulate matter and discoloration prior to administration, whenever solution and container permit. Do not use the solution if it is discolored or particulate matter is present.

6.5 Nature and contents of container Type I or Type II glass vials or bottles with halobutyl stoppers and an aluminium crimp seal.

6.6 Instruction for use/handling Vial or bottles containing contrast media solution are not intended for the withdrawal of multiple doses. The rubber stopper should never be pierced more than once. The use of proper withdrawal cannulae for piercing the stopper and drawing up the contrast medium is recommended. The contrast medium should not be drawn into the syringe until immediately before use and should not be diluted. Solutions not used in one examination session or waste material, such as the connecting tubes, should be disposed. Any residue of contrast medium in the syringe must be discarded. Bottles of 500 ml should be used in conjunction with an injector system. After each patient examination, the connecting tubes (to the patient) and relevant disposable parts should be disposed because could be contaminated with blood. At the end of the sessions, the left over solution in the bottle and in the connecting tubes as well as any disposable parts of the injector system should be discarded. Any additional instructions from the respective equipment manufacturer must also be adhered to.

7. MARKETING AUTHORISATION INFORMATION

The Marketing Authorisation Holder, Number, and Date of Approval may be different in different Countries. Volumes, presentations, and indications may also differ.Refer to Local Summary of Product Characteristics. Please contact Bracco Imaging SpA – Via Egidio Folli, 50 20134 Milano- Italy for further information.

8. DATE OF PREPARATION OF THIS DOCUMENT May 2006

PREVIEW CENTRE

Only data projection will be provided for presentations. Speakers are requested to hand in their presentations to the preview-centre staff not later than 90 minutes before the beginning of their session. For sessions taking place in the early morning please hand in your presentation on the previous day.

Presentations have to be handed in using the following format: PowerPoint for PC version MS Office 2003 or older. (Macintosh presentations cannot be accommodated; only if saved to a PC-formatted disk Macintosh presentations are acceptable.) The presentation has to be saved on a CD-ROM, DVD-ROM or USB stick (no ZIP disks). The size of one presentation should not exceed 700 MB. If there are video sequences included, please make sure to save the video files on your CD-ROM in addition. To avoid missing links please save your Power- Point presentation as "pack&go" (".pps").

The Preview Centre is located next to the main lecture hall at the Hotel Le Méridien and open during the following hours:

Thursday, May 29	16:00 – 19:00
Friday, May 30	07:30 – 18:00
Saturday, May 31	07:30 – 18:00
Sunday, June 1	07:30 – 10:30

REGISTRATION

OPENING HOURS

Thursday, May 29	16:00 – 19:00
Friday, May 30	07:30 – 18:00
Saturday, May 31	07:30 – 18:00
Sunday, June 1	07:30 – 10:30

ONSITE FEES

Non Member	EUR 380
ESTI Member	EUR 300
One-day registration	EUR 200
Radiologist in training	EUR 150
Accompanying person	EUR 120

SPONSORS | EXHIBITORS | LUNCH SYMPOSIA | WORKSHOPS

ESTI wishes to gratefully acknowledge the following companies for supporting the meeting:

PLATINUM SPONSORSHIP

PHILIPS

Guerbet
Contrast for Life

SILVER SPONSORSHIP

MEDIAN

VITAL
The image of understanding

BRACCO
LIFE FROM INSIDE

OTHER SPONSORSHIP

GE Healthcare

TOSHIBA
Leading Innovation

AGFA HealthCare

TERUMO
We keep life flowing

FRIDAY, MAY 30, 2008

WS 01	08:30 - 14:00	**PHILIPS HEALTHCARE** Hands-on Workshop
WS 02	08:30 - 14:00	**MEDIAN** Hands-on Workshop
SY 01	12:30 - 13:30	**GE HEALTHCARE** Symposium "New processing in thorax imaging"

SATURDAY, MAY 31, 2008

WS 03	08:30 - 14:00	**PHILIPS HEALTHCARE** Hands-on Workshop
SY 02	12:30 - 13:30	**MEDIAN** Symposium "Managing pulmonary nodules in CT oncology"
SY 03	12:30 - 13:30	**TOSHIBA** Symposium "Challenges and Innovations for Thoracic CT"

Exhibitors

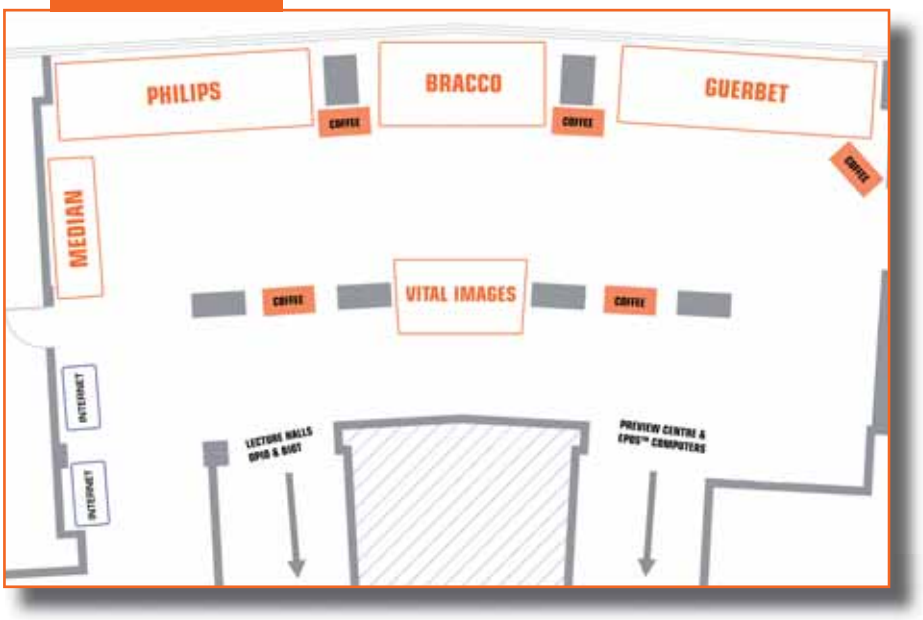
PHILIPS
BRACCO
GUERBET
COFFEE
COFFEE
COFFEE
MEDIAN
COFFEE
VITAL IMAGES
COFFEE
INTERNET
INTERNET
LECTURE HALLS OPIOS & BIOT
PREVIEW CENTRE & EPOS™ COMPUTERS

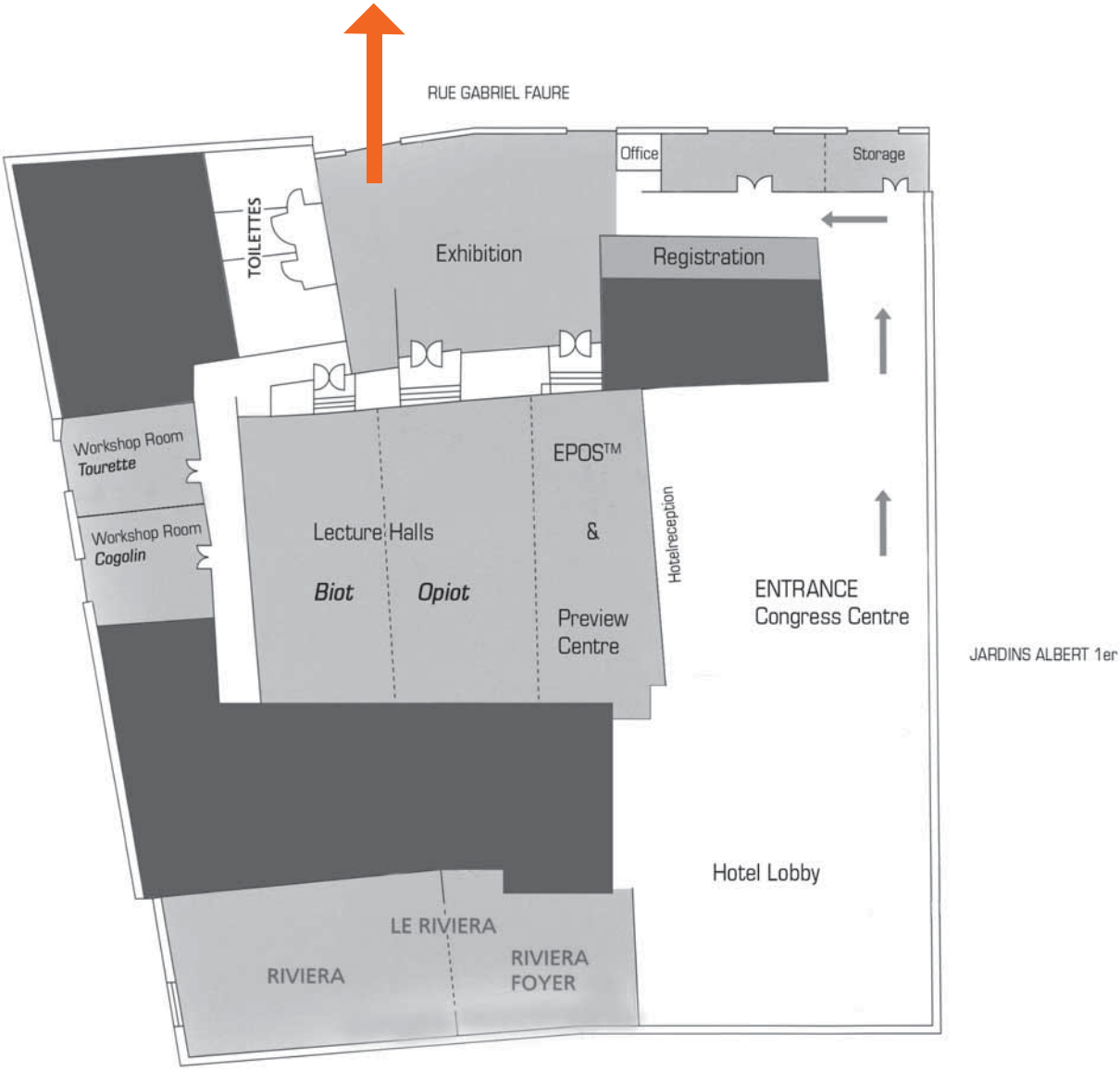
RUE GABRIEL FAURE
Office
Storage
TOILETTES
Exhibition
Registration
Workshop Room Tourette
Workshop Room Cogolin
Lecture Halls
Biot
Opiot
EPOS™
&
Preview Centre
Hotelreception
ENTRANCE Congress Centre
JARDINS ALBERT 1er
Hotel Lobby
LE RIVIERA
RIVIERA
RIVIERA FOYER
PROMENADE DES ANGLAIS

PROGRAMME OVERVIEW

	FRIDAY MAY 30	SATURDAY MAY 31		SUNDAY JUNE 1	
08:30 - 08:45	**Scientific Sessions 1 & 2** **Workshops PHILIPS & MEDIAN**	**Scientific Sessions 3 & 4** **Workshop PHILIPS**		**Film Panel Interpretation**	08:30 - 08:45
08:45 - 09:00					08:45 - 09:00
09:00 - 09:15					09:00 - 09:15
09:15 - 09:30					09:15 - 09:30
09:30 - 09:45					09:30 - 09:45
09:45 - 10:00					09:45 - 10:00
10:00 - 10:15	**Coffee Break**	**Coffee Break**		**Coffee Break**	10:00 - 10:15
10:15 - 10:30					10:15 - 10:30
10:30 - 10:45	**Opening Ceremony**				10:30 - 10:45
10:45 - 11:00	**Educational Session 1**	**Educational Session 4**		**Educational Session 7**	10:45 - 11:00
11:00 - 11:15	Thoracic infections	Computed aided diagnosis, digital radiography & radiation		Oncology imaging	11:00 - 11:15
11:15 - 11:30					11:15 - 11:30
11:30 - 11:45					11:30 - 11:45
11:45 - 12:00					11:45 - 12:00
12:00 - 12:15	**Lunch Break**	**Lunch Break**		**Concluding Remarks**	12:00 - 12:15
12:15 - 12:30					12:15 - 12:30
12:30 - 12:45	**GE Symposium**	**MEDIAN Symposium**	**TOSHIBA Symposium**	**General Assembly**	12:30 - 12:45
12:45 - 13:00	New processing in thorax imaging	Managing pulmonary nodules in CT oncology	Challenges and innovations for thoracic CT		12:45 - 13:00
13:00 - 13:15					13:00 - 13:15
13:15 - 13:30					13:15 - 13:30
13:30 - 13:45	**Lunch Break**	**Lunch Break**			13:30 - 13:45
13:45 - 14:00					13:45 - 14:00
14:00 - 14:15	**Educational Session 2**	**Educational Session 5**			14:00 - 14:15
14:15 - 14:30	Cardiac and aortic imaging (CT & MR) including CTA of the coronary arteries	Pulmonary embolism, pulmonary hypertension & aorta			14:15 - 14:30
14:30 - 14:45					14:30 - 14:45
14:45 - 15:00					14:45 - 15:00
15:00 - 15:15					15:00 - 15:15
15:15 - 15:30					15:15 - 15:30
15:30 - 15:45	**Coffee Break**	**Coffee Break**			15:30 - 15:45
15:45 - 16:00					15:45 - 16:00
16:00 - 16:15	**Educational Session 3**	**Educational Session 6**			16:00 - 16:15
16:15 - 16:30	Diffuse lung diseases	Airway diseases & functional lung imaging			16:15 - 16:30
16:30 - 16:45					16:30 - 16:45
16:45 - 17:00					16:45 - 17:00
17:00 - 17:15					17:00 - 17:15
17:15 - 17:30					17:15 - 17:30
17:30 - 17:45	**Cases of the day 1 & 2**	**Cases of the day 3 & 4**			17:30 - 17:45
17:45 - 18:00					17:45 - 18:00
18:00 - 18:15					18:00 - 18:15
18:15 - 18:30					18:15 - 18:30
Evening	**Welcome Reception**	**Faculty Dinner**		**Free**	Evening

SS 01 08:30 - 10:00 SCIENTIFIC SESSION: DIFFUSE LUNG DISEASE

ROOM: OPIO

Moderator: T. Franquet, Barcelona/ES
P. Armstrong, London/UK

The respective abstracts can be found on pages 33-35.

SS 01.1 08:30

Autoantibodies and the morphology of fibrosing lung disease in patients with idiopathic pulmonary fibrosis, rheumatoid arthritis and poly/dermatomyositis.
M. Quigley[1], N. Sverzellati[2], A. Devaraj[1], A.U. Wells[1], D.M. Hansell[1]; [1]London/UK, [2]Parma/IT

SS 01.2 08:38

Comparative study of CT based score with pulmonary function test and clinical status in adult patients with cystic fibrosis (CF)
I. Tsangaridou, E. Sotiropoulou, A. Bouga, S. Velitsista, C. Kampolis, E. Pouliou, A. Georgiadi, L. Thanos; Athens/GR

SS 01.3 08:46

Axial vs coronal HRCT images in the follow-up of patients with idiopathic pulmonary fibrosis
M. Mereu, P. D'Ambrosio, V. Di Mizio, P. Santodirocco, R.L. Patea, M.L. Storto; Chieti/IT

SS 01.4 08:54

Drug-induced respiratory diseases: a prospective comparison between high-resolution CT and bronchoscopy in 42 patients.
S. Piciucchi[1], M. Romagnoli[2], V. Poletti[2], M. Chilosi[3], C. Bigliazzi[2], A. Dubini[2], G. Gavelli[4], A. Carloni[5]; [1]Meldola-forlì/IT, [2]Forlì/IT, [3]Verona/IT, [4]Bologna/IT, [5]Terni/IT

SS 01.5 09:02

Micronodular lesions in patients with pulmonary sarcoidosis: is this a sign of chronicity?
I. Tsangaridou, M. Seferos, A. Tzanetaki, E. Sotiropoulou, S. Velitsista, F. Laspas, M. Dimadi, L. Thanos; Athens/GR

SS 01.6 09:10

Correlation of mean pulmonary artery diameter (MPAD) on the CT scan with 2D ECHO PAP (Pulmonary Arterial Pressure) results in patients having DILD (Diffuse Interstitial Lung Disease).
I. Tsangaridou, M. Dimadi, P. Tsagouli, F. Laspas, P. Kokkinis, R. Triggidou, A. Manataki, L. Thanos; Athens/GR

SS 01.7 09:18

Depiction of malignancy in patients with diffuse interstitial lung disease (DILD) presenting with nodular opacities.
R. Triggidou, I. Tsangaridou, M. Dimadi, K. Malagari, P. Kokkinis, E. Sotiropoulou, P. Tsagouli, L. Thanos; Athens/GR

SS 01.8

Withdrawn by authors

SS 01.9 09:26

Role of MDCT chest in evaluating febrile neutropenic patients
C.J. Das[1], A. Seith[2], G.S. Pangtey[2], K. Medhi[2]; [1]New Delhi/IN, [2]Delhi/IN

SS 02 08:30 - 10:00 SCIENTIFIC SESSION: ONCOLOGIC IMAGING – INTERVENTIONAL RADIOLOGY

ROOM: BIOT

Moderator: J. Neuwirth, Prague/CZ
M. Carette, Paris/FR

The respective abstracts can be found on pages 35-38.

SS 02.1 08:30 **Correlation of radiological findings suggestive of inactive tuberculosis with new M. tuberculosis-specific assays of T-cell immune response in patients with hematological cancers.**
P. Torricelli, F. Fiocchi, A. Ferrari, M. Luppi, R. D'Amico, M. Losi, L. Richeldi; Modena/IT

SS 02.2 08:38 **Radiofrequency ablation (RFA) of intrathoracic malignancies.**
A. Bouga, E. Sotiropoulou, P. Filippousis, P. Tsagouli, F. Laspas, L. Thanos; Athens/GR

SS 02.3 08:46 **Percutaneous CT-guided lung biopsy: complications and their direct management in high risk patients.**
F. Laspas, P. Filippousis, E. Sotiropoulou, R. Triggidou, A. Bouga, M. Seferos, L. Thanos; Athens/GR

SS 02.4 08:54 **"Bronchial artery embolization" - treating massive hemoptysis in patients of pulmonary tuberculosis**
B.K. Saha, K.B. Taori; Nagpur/IN

SS 02.5 09:02 **Treatment with radiofrequency ablation (RFA) of metastases in patients with surgically resected lung cancer**
E. Sotiropoulou, P. Filippousis, A. Bouga, M. Seferos, F. Laspas, L. Thanos; Athens/GR

SS 02.6 09:10 **CT analysis of mass-like consolidations: differential points between benign and malignant lesions.**
E.S. Lee[1], S. Paik[2], J.G. Yi[1], J.I. Jung[1]; [1]Seoul/KR, [2]Kyeongki-do/KR

SS 02.7 09:18 **Pulmonary nodules discovered by CT-differential diagnosis classification-guidelines for management**
I. Pantou, M. Kampanarou, K. Bouhra, D.K. Filippiadis, G. Oikonomou, S. Tanteles, A. Pomoni, E. Chatzimichael, M. Pomoni, D. Kelekis; Athens/GR

SS 02.8 09:26 **Frequency and significance of solitary pulmonary nodules on CT in patients with extra pulmonary malignancy**
S. Ganeshalingam, L.J. Menezes; London/UK

SS 02.9 09:34 **Computerized tomography of tuberculosis in patients with different lung neoplasms: the analysis of 8499 lung CT scans**
A. Ivkovic[1], T. Spasic[2], S. Ristic[2]; [1]Nis/RS, [2]Vranje/RS

WS 01 08:30 - 14:00 PHILIPS HEALTHCARE HANDS-ON WORKSHOP

ROOM: COGOLIN

08:30 - 10:30 **Chest CT: Interactive hands-on Interpretation Session**
E. Coche, Brussels/BE
C. Beigelman-Aubry, Paris/FR

10:30 - 14:00 **Individual hands-on training.**
Feel free to walk inside and experience our clinical applications.

WS 02 08:30 - 14:00 MEDIAN WORKSHOP

ROOM: TOURETTE

08:30 - 10:30 **Presentation and hands-on LMS-Lung application.**

LMS-Lung is a software application designed to assist the radiologists to detect, evaluate, follow and report lesions identified in CT images covering the chest. It is composed of two modules: LMS-Lung/CAD offers Computer Aided Detection techno logy for easy identification of lung lesions, and LMS-Lung/Track facilitates the follow-up over time of lesions identified inside or outside the lungs, automatically calculates their growth and generates reports according to RECIST criteria.

Participants to the workshop will listen to a general presentation of the software followed by a live demonstration on clinical cases. They will then be able to try the software with the full support of an application specialist.

10:30 - 14:00 Individual hands-on training.

10:30 - 10:50 OPENING CEREMONY

ROOM: OPIO-BIOT

10:30 **Welcome Address**
P.A. Grenier, Paris/FR

10:35 **ESTI Honorary Membership Award**
P. Schnyder, Lausanne/CH

10:40 **Introduction of ESTI 2008 guest lecturers**
A. de Roos, Leiden/NL
D. Naidich, New York, NY/US

FRIDAY, MAY 30, 2008

ES 01 10:50 - 12:00 THORACIC INFECTIONS

ROOM: OPIO-BIOT

Moderator: C.J. Herold, Vienna/AT

10:50 **Infections of the airways**
J.A. Verschakelen, Leuven/BE

11:20 **Pulmonary infections in the immunocompromised host: a radiologist´s perspective**
J. Cáceres, Barcelona/ES

11:40 **New directions in the diagnosis and management of pleural infection. The radiologist and pleural sepsis.**
F. Gleeson, Oxford/UK

SY 01 12:30 - 13:30 GE SYMPOSIUM - NEW PROCESSING IN THORAX IMAGING

ROOM: OPIO-BIOT

Moderator: L. Katz, Buc/FR

12:30 **Introduction**

12:35 **VolumeRad using volumetric radiography for pulmonary disease in daily practice**
J. Vikgren, Göteborg/SE

12:55 **CT Dose and image quality solutions**
D. Dessalles-Martin, Buc/FR

13:10 **New developments in lung disease CT management**
M.-P. Revel, Paris/FR

13:25 **Conclusions & questions**

ES 02 14:00 - 15:30 CARDIAC AND AORTIC IMAGING (CT & MR) INCLUDING CTA OF THE CORONARY ARTERIES

ROOM: OPIO-BIOT

Moderator: L. Bonomo, Rome/IT

14:00 **Invited Lecture: the heart between the lungs**
A. de Roos, Leiden/NL

14:30 **Coronary artery CTA: understanding the artifacts and pitfalls**
E.J.R. van Beek, IowaCity, IA/US

14:50 **MDCT of the coronary arteries: normal anatomy and variants**
S.P.G. Padley, London/UK

15:10 **Chest pain in the emergency room: evaluation and triage with CTA**
M.L. Storto, Chieti/IT

ES 03 16:00 - 17:40 DIFFUSE LUNG DISEASES

ROOM: OPIO-BIOT

Moderator: M. Maffessanti, Trieste/IT

16:00 **Organizing pneumonia revisited**
D.M Hansell, London/UK

16:20 **Pulmonary sarcoidosis: one disease, many faces**
C. Schaefer-Prokop, Amsterdam/NL

16:40 **The ageing lung and other normal HRCT variants**
S.J. Copley, London/UK

17:00 **Exposure related lung diseases**
A. Oikonomou, Alexandropoulis/GR

17:20 **Diffuse granulomatous lung diseases: HRCT-pathologic correlation**
T. Franquet, Barcelona/ES

CD 01&02 17:40 - 18:00 CASES OF THE DAY

ROOM: OPIO-BIOT

Moderator: T. Franquet, Barcelona/ES

17:40 **Case of the day 1**
C. Engelke, Würzburg/DE

17:50 **Case of the day 2**
A.R. Larici, Rome/IT

SS 03 08:30 - 10:00 AIRWAY DISEASE – PULMONARY EMBOLISM

ROOM: OPIO

Moderators: A. Mester, Budapest/HU
L.R. Goodman, Milwaukee, WI/US

The respective abstracts can be found on pages 38-41.

SS 03.1 08:30

A method for optimizing observer agreement for HRCT signs of airways disease
N. Sverzellati[1], A.U. Wells[2], S.R. Desai[2], A. Devaraj[2], M. Quigley[2], D.M. Hansell[2]; [1]Parma/IT, [2]London/UK

SS 03.2 08:38

Primary ciliary dyskinesia and idiopathic bronchiectasis: a comparative CT study.
M. Quigley[1], S.R. Desai[1], N. Sverzellati[2], R. Wilson[1], A.U. Wells[1], D.M. Hansell[1]; [1]London/UK, [2]Parma/IT

SS 03.3 08:46

CT findings of the chest in adults with aspirated foreign bodies: report of 23 cases
A. Osadchy, J. Smorjik, R. Zissin; Kfar Saba/IL

SS 03.4 08:54

CT indicators of pulmonary hypertension: accuracy in mild versus severe disease
A. Devaraj, A.U. Wells, M. Meister, D.M. Hansell; London/UK

SS 03.5 09:02

Pulmonary artery/ascending aorta ratio as a sign of pulmonary hypertension: validity in fibrotic versus non-fibrotic lung disease.
A. Devaraj, A.U. Wells, M. Meister, D.M. Hansell; London/UK

SS 03.6 09:10

Patient exposure and image quality at 80 kV in pulmonary CT angiography
Z. Szucs-Farkas, L. Kurmann, M.A. Patak, T. Strautz, P. Vock, S.T. Schindera; Berne/CH

SS 03.7 09:18

Pulmonary artery hypertension: correlations between cardiac morphologic and functional parameters assessed by MRI and invasive measurements.
V. Chabbert, J.-.P. Alunni, B. Degano, N. Blot-Souletie, C. Arnaud, H. Rousseau, P. Otal; Toulouse/FR

SS 03.8 09:26

To evaluate the correspondence between coronary artery vascularization and 17-segment heart model.
F. Fiocchi, G. Ligabue, A. Barbieri, L. Verganti, M.G. Modena, P. Torricelli; Modena/IT

SS 03.9 09:34

Graft versus host disease of the lungs in bone marrow transplant (BMT) patients: HRCT findings at presentation and correlation with pulmonary function tests
N.R. Bogot[1], E.A. Kazerooni[2], S. Patel[2], K.R. Cooke[2], G.A. Yanik[2]; [1]Jerusalem/IL, [2]Ann Arbor, MI/US

SS 04 08:30 - 10:00 CAD FOR THE CHEST – IMAGE QUALITY

ROOM: BIOT

Moderators: P. Schnyder, Lausanne/CH
J. Biederer, Kiel/DE

The respective abstracts can be found on pages 41-44.

SS 04.1 08:30 **Increasing the detection sensitivity of lung nodules on digital chest radiographs by the use of CAD**,
N.R. Bogot[1], D. Shaham[1], R. Eliahou[1], A. Manevitch[1], J. Stoeckel[1], N. Hiller[1], S.S. Mansur[2], M.S. Dinesh[2], M. Acharyya[2], I. Leichter[1]; [1]Jerusalem/IL, [2]Bangalore/IN

SS 04.2 08:38 **Evaluation of a Computer Aided Detection (CAD) system for non solid pulmonary nodules.**
X. Boulanger, A.L. Brun, C. Hill, D. Leclercq, P.A. Grenier, C. Beigelman-Aubry; Paris/FR

SS 04.3 08:46 **Computer-aided detection of pulmonary embolism (CAD): can a junior radiologist benefit from consensus with CAD in detecting of segmental and subsegmental pulmonary embolism?**
J. Baxa, J. Ferda, A. Bednarova, R. Vondrakova, H. Mirka, B. Kreuzberg; Plzen/CZ

SS 04.4 08:54 **3D texture analysis of thorax CTs allows for the differentiation of mixtures of pathological patterns in the lung**
R. Huttary[1], W. Recheis[1], A. Ruiu[1], M. Zompatori[2]; [1]Innsbruck/AT, [2]Parma/IT

SS 04.5 09:02 **Gender differences in emphysema phenotypes in non-COPD smokers**
N. Sverzellati[1], E. Calabrò[2], G. Randi[2], C. La Vecchia[2], A. Marchianò[2], J.M. Kuhnigk[3], P. Spagnolo[4], M. Zompatori[1], U. Pastorino[2]; [1]Parma/IT, [2]Milano/IT, [3]Bremen/DE, [4]Modena/IT

SS 04.6 09:10 **Oxygen-enhanced magnetic resonance imaging: influence of different gas delivery methods on the T1-changes of the lungs.**
F. Molinari[1], M. Puderbach[2], M. Eichinger[2], S. Ley[2], M. Bock[2], L. Bonomo[1], H.U. Kauczor[2]; [1]Rome/IT, [2]Heidelberg/DE

SS 04.7 09:18 **Quantitative analysis of volumetric paired thin section multi detector computed tomography scans and pulmonary function tests in patients with severe emphysema**
A. Grgic[1], H. Wilkens[1], R. Kubale[2], J.M. Kuhnigk[3], G.W. Sybrecht[1], A. Buecker[1]; [1]Homburg/DE, [2]Pirmasens/DE, [3]Bremen/DE

SS 04.8 09:26 **Comparison of thin axial and coronal images versus maximum intensity projections sensitivity concerning the detection of pulmonary nodules on MDCT images**
D.K. Filippiadis, G. Oikonomou, I. Pantou, M. Kampanarou, K. Bouhra, E. Chatzimichael, S. Tanteles, A. Pomoni, M. Pomoni, D. Kelekis; Athens/GR

SS 04.9 09:34 **Comparison of image quality in AP chest radiography vs. AP whole-body linear slit scanning radiography by EU quality criteria**
P. Vock, Z. Szücs; Berne/CH

SATURDAY, MAY 31, 2008

WS 03 08:30 - 14:00 PHILIPS HEALTHCARE HANDS-ON WORKSHOP

ROOM: COGOLIN

08:30 – 10:30 **Chest CT: Interactive hands-on Interpretation Session**
E. Coche, Brussels/BE, C. Beigelman-Aubry, Paris/FR

10:30 - 14:00 **Individual hands-on training.**
Feel free to walk inside and experience our clinical applications

ES 04 10:30 - 12:00 COMPUTED AIDED DIAGNOSIS, DIGITAL RADIOGRAPHY & RADIATION

ROOM: OPIO-BIOT

Moderator: P. Vock, Berne/CH

10:30 **Invited Lecture: CAD in the Chest**
D. Naidich, New York, NY/US

11:00 **CAD for Pulmonary Embolism**
E. Coche, Brussels/BE

11:20 **New trends in digital radiography**
M. Prokop, Utrecht/NL

11:40 **Dose reduction challenge**
D. Tack, Brussels/BE

SY 02 12:30 - 13:30 MEDIAN SYMPOSIUM MANAGING PULMONARY NODULES IN CT ONCOLOGY

ROOM: OPIO

Moderator: P.A. Grenier, Paris/FR

12:30 **Introduction**
P.A. Grenier, Paris/FR

12:35 **Benefits of a software application for the management of non-solid nodules**
C. Beigelman-Aubry, Paris/FR

12:49 **Lung nodule follow-up: evaluation of an automated solution**
A.R. Larici, Rome/IT

13:03 **New ways to communicate radiological findings to oncologists**
D. Wormanns, Berlin/DE

13:17 **Initial experience with the implementation of LMS-Lung in a General Hospital**
J. Vilar, Valencia/ES

SY 03 12:30 - 13:30 TOSHIBA SYMPOSIUM CHALLENGES AND INNOVATIONS FOR THORACIC CT

ROOM: OPIO

Moderation: H.U. Kauczor, Heidelberg/DE

12:30 **Thoracic CT of the heart and great vessels**
L.J.M. Kroft, Leiden/NL

12:45 **Computer assisted analysis of pulmonary CT**
J. Ley-Zaporozhan, Heidelberg/DE

13:00 **Functional CT diagnostics of the lung**
P. Rogalla, Berlin/DE

13:15 **First clinical experience with dynamic volume CT (Aquilion ONE)**
Y. Ohno, Kobe/JP

ES 05 14:00 - 15:40 PULMONARY EMBOLISM, PULMONARY HYPERTENSION & AORTA

ROOM: OPIO-BIOT

Moderator: D. Hahn, Würzburg/DE

14:00 **MDCT of pulmonary thromboembolism: where are we now?**
M.-P. Revel, Paris/FR

14:20 **Imaging of pulmonary arteries and veins (embolism excluded)**
B. Ghaye, Liège/BE

14:40 **Non-thrombotic pulmonary embolism**
K. Malagari, Athens/GR

15:00 **MR imaging methods of pulmonary hypertension**
S. Ley, Heidelberg/DE

15:20 **MDCT imaging of the aorta**
F. Laurent, Bordeaux/FR

SATURDAY, MAY 31, 2008

ES 06 16:00 - 17:40 AIRWAY DISEASES & FUNCTIONAL LUNG IMAGING

ROOM: OPIO-BIOT

Moderator: E. Pallisa, Barcelona/ES

16:00 **New frontiers in CT imaging of airway disease**
C. Beigelman-Aubry, Paris/FR

16:20 **Air-trapping: not just small airways disease**
E.J. Stern, Seattle, WA/US

16:40 **Functional-morphologic relationships in emphysema**
P.-A. Gevenois, Brussels/BE

17:00 **Investigation of airways using MDCT for visual and quantitative assessment**
P.-Y. Brillet, Bobigny/FR

17:20 **MRI in COPD: current status and perspectives**
H.U. Kauczor, Heidelberg/DE

CD 03&04 17:40 - 18:00 CASES OF THE DAY

ROOM: OPIO-BIOT

Moderator: T. Franquet, Barcelona/ES

17:40 **Case of the day 3**
A. Giménez, Barcelona/ES

17:50 **Case of the day 4**
D. Wormanns, Düsseldorf/DE

FP 01 08:30 - 10:00 FILM PANEL INTERPRETATION

ROOM: OPIO-BIOT

Moderator: P. Armstrong, London/UK

K. Malagari, Athens/GR
G. Ferretti, Grenoble/FR
W. de Wever, Leuven/BE
S. Ellis, London/UK
J. Ley-Zaporozhan, Heidelberg/DE
M. Maffessanti, Trieste/IT

ES 07 10:30 - 12:10 ONCOLOGY IMAGING

ROOM: OPIO-BIOT

Moderator: J. Vilar, Valencia/ES

10:30 **Management of the incidental pulmonary nodule in patients with and without known malignancy**
S. Diederich, Düsseldorf/DE

10:50 **Role of PET-CT in lung cancer: limitations and pitfalls**
N. Howarth, Chêne-Bougeries/CH

11:10 **Lung metastases: imaging overview**
I.E. Tyurin, Moscow/RU

11:30 **CT volumetry of pulmonary metastases**
K. Marten, Munich/DE

11:50 **Diagnosis and staging of malignant pleural mesothelioma: a role for imaging?**
S.R. Desai, London/UK

12:10 – 12:30 CONCLUDING REMARKS

ROOM: OPIO-BIOT

12:30 – 13:30 GENERAL ASSEMBLY

ROOM: OPIO-BIOT

EPOS

Electronic Presentation Online System

PRESENTATIONS

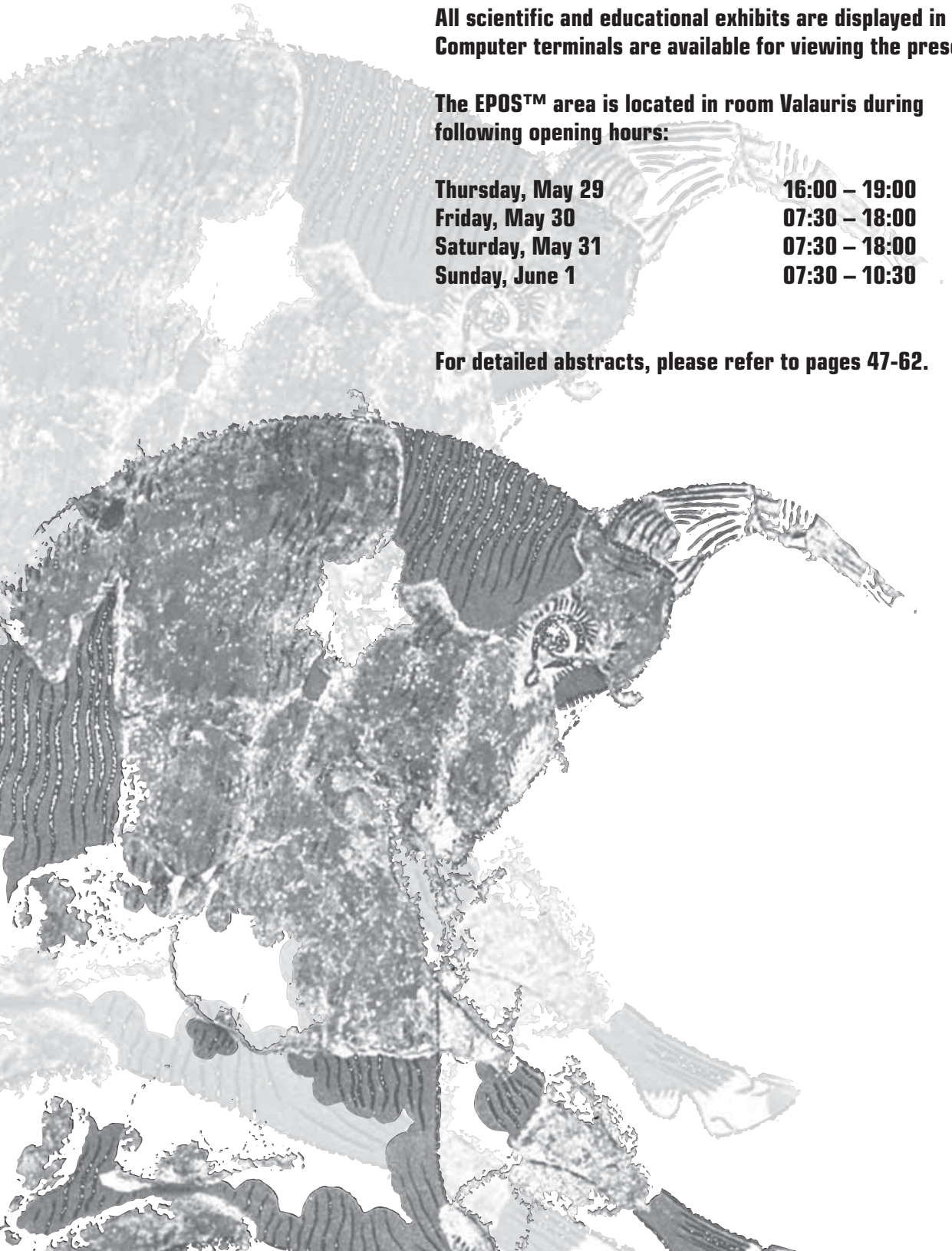

All scientific and educational exhibits are displayed in EPOS™ format. Computer terminals are available for viewing the presentations.

The EPOS™ area is located in room Valauris during following opening hours:

Thursday, May 29	**16:00 – 19:00**
Friday, May 30	**07:30 – 18:00**
Saturday, May 31	**07:30 – 18:00**
Sunday, June 1	**07:30 – 10:30**

For detailed abstracts, please refer to pages 47-62.

AIRWAY DISEASE

P 01 **Impact of increased noise in low dose CT for evaluation of emphysema (iLEAD Study)**
J. Ley-Zaporozhan[1], S. Ley[1], D. Takenaka[2], T. Kubo[3], Y. Ohno[2], H. Hatabu[4], H.U. Kauczor[1]; [1]Heidelberg/DE, [2]Kobe/JP, [3]Kyoto/JP, [4]Boston/US

P 02 **Various causes of tracheobronchial polypoid lesions: CT-bronchoscopic and radiologic-pathologic correlations**
K. Lee, K. Kim, C.H. Sohn, D.K. Yang, S.G. Lee, P.J. Choi, M.S. Noh; Busan/KR

CAD FOR THE CHEST

P 03 **Pulmonary emphysema in patients with chronic anorexia nervosa: preliminary findings**
N. Sverzellati[1], M. Pescarolo[1], W. Recheis[2], A. Ruiu[2], M. Amore[1], A. Chetta[1], M. Zompatori[1]; [1]Parma/IT, [2]Innsbruck/AT

P 04 **Quantitative assessment of airway dimension for pulmonary disease: development of dedicated software for multi-detector CT**
Y.H. Kim, S. Choi, H.J. Sun, J.K. Kim, J.G. Park, H.K. Kang; Kwangju/KR

INTERSTITIAL LUNG DISEASES

P 05 **Comparison of pulmonary CT findings and serum KL-6 level in patients with cryptogenic organizing pneumonia**
K. Honda, Y. Ando, F. Okada, H. Mori; Yufu/JP

P 06 **Uncommon occupational lung diseases: high-resolution computed tomography findings**
L. Flors, M.L. Domingo, G. Figueres Muñoz, C. Leiva-Salinas, E. López-Pérez, R. Medina, J. Vilar; Valencia/ES

P 07 **Cystic lung disease in Birt-Hogg-Dubè syndrome**
N. Sverzellati[1], S. Tommasetti[2], A. Carloni[3], S. Piciucchi[2], M. Chilosi[4], M. Zompatori[1], V. Poletti[2]; [1]Parma/IT, [2]Forlì/IT, [3]Terni/IT, [4]Verona/IT

P 08 **Study for prognostic indicators in patients with usual interstitial pneumonia and nonspecific interstitial pneumonia: correlation of imaging findings with cellular patterns in bronchoalveolar lavage fluid**
J.S. Park[1], S.H. Paik[1], J. Hwang[2], D.H. Kim[1], D.L. Choi[2]; [1]Bucheon/KR, [2]Seoul/KR

P 09 **Pulmonary sarcoidosis - a chameleon among interstitial lung diseases**
A. Grgic[1], R. Bohle[1], R. Kubale[2], H. Wilkens[1], A. Buecker[1]; [1]Homburg/DE, [2]Pirmasens/DE

P 10 **Quantitative computed tomography in the interstitial lung diseases: correlation with bronchoalveolar lavage flow cytometry**
J. Moczova[1], V. Belan[1], J. Plutinsky[2]; [1]Bratislava/SK, [2]Nitra/SK

P 11 **HRCT imaging of the lung in rheumatology patients: spectrum of findings and grading according to severity**
A. Kazantzi, P. Zambakis, P. Korfiatis, D. Daoussis, S. Liossis, T. Petsas, C. Kalogeropoulou; Patras/GR

P 12 **Lung cysts in non-smokers with neurofibromatosis: CT findings**
A. Oikonomou, G. Daskalogiannakis, P. Prassopoulos; Alexandroupolis/GR

P 13 **Metastatic pulmonary calcifications in hyperparathyroidism: report of two cases**
S. Piciucchi[1], V. Poletti[2], N. Sverzellati[3], S. Ascani[4], G. Gavelli[5], A. Carloni[4]; [1]Meldola-forlì/IT, [2]Forlì/IT, [3]Parma/IT, [4]Terni/IT, [5]Bologna/IT

LUNG INFECTIONS

P 14 **Assessment of pneumonia severity: multi-detector row CT in comparison to clinical score CRB-65**
S. Pauls[1], S. Krüger[2], R. Muche[1], D. Klemen[1], C. Billich[1], S.A. Schmidt[1], V. Hombach[1], H. Brambs[1]; [1]Ulm/DE, [2]Aachen/DE

P 15 **Comparison of HRCT findings in mycobacterium avium and mycobacterium intracellulare**
Y. Ando[1], F. Okada[2], H. Mori[2], K. Sugisaki[1], S. Takikawa[1], Y. Zaizen[1], H. Kawano[1], K. Tenda[1], T. Otsu[1]; [1]Beppu/JP, [2]Yufu/JP

P 16 **Clinical and pulmonary HRCT findings in acute klebsiella pneumoniae pneumonia**
F. Okada, Y. Ando, K. Honda, T. Nakayama, S. Tanoue, H. Mori; Yufu/JP

P 17 **Miliary tuberculosis: comparison of CT findings in HIV-seropositive and HIV-seronegative patients**
Y.J. Jeong, K. Kim, J.Y. Kim, S.H. Lee; Busan/KR

P 18 **Withdrawn by authors**

P 19 **Chest CT findings of pulmonary actinomycosis**
J.S. Kim, C.Y. Han; Seoul/KR

P 20 **Chronic granulomatous disease. A rare case report involving the lungs.**
I. Tsangaridou, A. Bouga, E. Sotiropoulou, P. Tsagouli, M. Seferos, F. Laspas, V. Sotiropoulou, L. Thanos; Athens/GR

P 21 **Successfully treated pulmonary mucormycosis in a diabetic renal transplant recipient**
Z.M. Lénárd, A. Németh, E. Hartmann, Z. Gerlei, K. Földes, A. Doros; Budapest/HU

MISCELLANEOUS

P 22 **The cisterna chyli - evaluation of prevalence, characteristics and predisposing factors**
S. Feuerlein, G. Kreuzer, H. Brambs, S. Pauls; Ulm/DE

P 23 **Multidetector CT angiography of aberrant subclavian arteries**
A. Türkvatan, F.G. Büyükbayraktar, T. Cumhur, T. Ölçer; Ankara/TR

P 24 **Sirolimus lung toxicity**
E. López-Pérez, M.L. Domingo, C. Barber Hueso, L. Flors, C. Leiva-Salinas, G.F. Muñoz, J. Vilar; Valencia/ES

P 25 **Left superior vena cava. CT-MRI findings and differential diagnosis.**
I. Vollmer, J.M. Maiques, A.M. Rodríguez, J. Sánchez, I.F. Enciso, A. Gayete; Barcelona/ES

P 26 **Withdrawn by authors**

P 27 **Withdrawn by authors**

P 28 **Amlyoidosis: overview using imaging findings**
W. Kwon; Wonju/KR

P 29 **Portable ICU chest x-ray: where calamities often lurk!**
A. Asrani, S. Digumarthy, R. Kaewlai, M. Gilman, J. Shepard; Boston/US

P 30 **Normal anatomy, variations, and disease spectrum of the diaphragm made easy with multi-detector spiral CT**
Y.W. Choi, S.C. Jeon; Seoul/KR

P 31 **Pectus excavatum: evaluation using multi-detector CT**
K.J. Park; Suwon/KR

P 32 **Ultrasound use in thoracic pathology: spectrum of applications and findings**
J. Pires, M. França, A. Ramos, M. Certo, J. Reis; Porto/PT

P 33 **Intrathoracic arteriovenous communications. Radiological features of different entities**
I. Vollmer, A. Gayete, A.M. Rodríguez, A. Solano, I. Fuertes, J.M. Maiques; Barcelona/ES

P 34 **Occult pneumothorax. Incidence and locations.**
G. Figueres Muñoz, M.L. Domingo Montañana, C. Leiva Salinas, L. Flors Blasco, E. López Pérez, J. Vilar; Valencia/ES

P 35 **Withdrawn by authors**

P 36 **Withdrawn by authors**

P 37 **Left cervical aortic arch with multiple saccular aneurysm associated with aortic narrowing, branch artery aneurysm and anomalous innominate vein**
A. Türkvatan, Ü. Kervan, T. Ölçer, T. Cumhur, A. Sarıtaş; Ankara/TR

P 38 **Semiology of thoracic ultrasonography**
I. Vollmer, A.M. Rodríguez, J.M. Maiques, A. Radosevic, E.A. Márquez, A. Gayete; Barcelona/ES

P 39 **About four cases of air in strange places**
R. Gosselin, L. Delrue, P. Smeets, P. Duyck; Gent/BE

P 40 **Bilious pleural effusion after percutaneous transhepatic biliary drainage**
J.S. Kim[1], C.S. Park[2]; [1]Seoul/KR, [2]Koyangsi/KR

P 41 **A case report: isolated hydatid cyst in axilla**
E.D. Cicek, G. Eker, I. Gulcan, B. Saydam; Istanbul/TR

ONCOLOGY IMAGING

P 42 **Mediastinal staging with diffusion- weighted MR Imaging in patients with non-small cell lung cancer**
I. Hasegawa[1], P.M. Boiselle[2], K. Kuwabara[1], M. Sawafuji[1], H. Sugiura[1]; [1]Kawasaki/JP, [2]Boston/US

P 43 **Withdrawn by authors**

P 44 **Incidental Solitary Pulmonary Nodules on CT: an audit of their management.**
S. Simkin, Z. Viney, M.K. Duncan, R. Dennett, L.J. Menezes; London/UK

P 45 **Early CT changes of radiation injury after tomotherapy for pulmonary malignancy**
H.J. Park[1], K. Kim[2], C.S. Kay[2], M.I. Ahn[3], M.H. Chung[4], S.H. Park[1]; [1]Seoul/KR, [2]Incheon/KR, [3]Suwon/KR, [4]Bucheon/KR

P 46 **Small cell lung cancer - a pictorial review of presentations and complications**
P. Pissay Gopala Rao, L.D. Wheeler, H. Adams; Cardiff/UK

P 47 **Lung perfusion CT: the differentiation of cavitary mass**
W. Kwon, Y.H. Lee; Wonju/KR

P 48 **RFA in patients with single lung**
J. Goyers, D. Brisbois, P. Magotteaux; Liege/BE

P 49 **Chest CT screening of asbestos-exposed workers: lung lesions and incidental findings**
T. Vierikko[1], R. Järvenpää[1], T. Autti[2], P. Oksa[1], M. Huuskonen[2], S. Kaleva[2], J. Laurikka[1], S. Kajander[3], K. Paakkola[3], S. Saarelainen[1], E. Salomaa[3], A. Tossavainen[2], P. Tukiainen[2], J. Uitti[1], T. Vehmas[2]; [1]Tampere/FI, [2]Helsinki/FI, [3]Turku/FI

P 50 **What is the significance of lung nodules in patients with testicular cancer?**
S. Ganeshalingam, M. Gilligan, G. Rottenberg; London/UK

P 51 **Review of the small pulmonary nodule management, after to have practiced some hook-wire guided videothoracoscopic resections.**
E. Mauri, V. Querol, S. Llaverias, A.M. Gallart, A.M. Martinez, C. Montull, M.J. Conde, E. Mundt, M.T. Maristany, L. Molins; Barcelona/ES

PULMONARY EMBOLISM AND HYPERTENSION

P 52 **In which patients in 6months after acute PE control sCT shoud be perform**
R. Pacho, A. Kaczy□ska, M. Kostrubiec, J. Kunikowska, P. Pruszczyk; Warsaw/PL

P 53 **Preductal aortic coarctation in an adult as a cause of arterial hypertension**
M. Vukelic Markovic, P. Marusic, I. Cikara, Z. Djurasevic, Z. Borkovic, B. Brkljacic; Zagreb/HR

THE HEART BETWEEN THE LUNGS

P 54 **Chest involvement in Erdheim-Chester disease: CT and MR findings.**
A. Brun, D. Touitou, J. Haroche, P. Grenier, D. Toledano, P. Cluzel, C. Beigelman-Aubry; Paris/FR

P 55 **Non-invasive evaluation of 102 patients after coronary artery bypass surgery with 16-slice computed tomographic angiography**
A. Türkvatan, S.F. Bıyıkoğlu, F.G. Büyükbayraktar, T. Ölçer, T. Cumhur, E. Duru; Ankara/TR

P 56 **The role of color identification for coronary plaque imaging in interpretation of gray scale coronary MDCT**
S. Choi, Y.H. Kim, H.J. Sun, J.K. Kim, J.G. Park, H.K. Kang; Kwangju/KR

P 57 **Clinical value of 16-slice multidetector computed tomography in symptomatic patients with suspected coronary artery disease**
A. Türkvatan, S.F. Bıyıkoğlu, F.G. Büyükbayraktar, T. Ölçer, T. Cumhur, E. Duru; Ankara/TR

P 58 **Anatomy of pericardial recesses on CT**
C. Leiva-Salinas, M.L. Domingo, L. Flors, G. Figueres Muñoz, E. López-Pérez, M. Mazon, J. Vilar; Valencia/ES

ABSTRACTS
SCIENTIFIC SESSIONS

SCIENTIFIC SESSION 01 – DIFFUSE LUNG DISEASE

SS 01.1

Autoantibodies and the morphology of fibrosing lung disease in patients with idiopathic pulmonary fibrosis, rheumatoid arthritis and poly/dermatomyositis.

M. Quigley[1], N. Sverzellati[2], A.U. Wells[1], D.M. Hansell[1], A. Devaraj[1]; [1]London/UK, [2]Parma/IT

Purpose: To examine the relationships between autoantibody profiles and the HRCT pattern of pulmonary fibrosis in patients with rheumatoid arthritis, poly/dermatomyositis and idiopathic pulmonary fibrosis. **Material and methods:** The CTs of 223 consecutive individuals diagnosed with idiopathic pulmonary fibrosis [IPF] (n=124) rheumatoid arthritis [RA] (n=60) poly/dermatomyositis [PM/DM] (n=39) were reviewed. Two pulmonary radiologists independently scored CTs for: the extent of interstitial fibrosis (and proportion of reticular pattern to ground glass opacity), organising pneumonia (OP) pattern, the bronchocentricity of disease, coarseness of reticular pattern, and traction bronchiectasis. These scores were correlated with contemporaneous autoantibody profiles. The group with idiopathic fibrosis contained patients with non-specific usual interstitial pneumonia (NSIP) and usual interstitial pneumonia (UIP). **Results:** In patients with idiopathic pulmonary fibrosis there was a significant relationship between the extent of lung disease and rheumatoid factor positivity (p=0.006) and anti-nuclear antigen antibody negativity (p=0.003). In rheumatoid arthritis patients, rheumatoid factor titre had a significant relationship with the following: extent of lung disease (p=0.03), proportion of reticular pattern (p=0.02), coarseness of reticular pattern (p=0.04) and severity of traction bronchiectasis (p=0.02). In PM/DM, no significant relationships were demonstrated between the serological profile (including Jo1 autoantibody) and disease morphology on HRCT. **Conclusion:** In idiopathic fibrosis and rheumatoid arthritis, rheumatoid factor positivity is associated with more extensive pulmonary fibrosis. In the patients with rheumatoid arthritis there is also a relationship with more extensive and coarser lung fibrosis and greater traction of the airways. By contrast, there were no correlations between serological and morphological variables in PM/DM.

SS 01.2

Comparative study of CT based score with pulmonary function tests and clinical status in adult patients with cystic fibrosis (CF)

I. Tsangaridou, E. Sotiropoulou, A. Bouga, S. Velitsista, C. Kampolis, E. Pouliou, A. Georgiadi, L. Thanos; Athens/GR

Purpose: To estimate the correlation of an overall score on specific CT findings in CF with pulmonary function tests and clinical status. **Material and methods:** HRCT findings were assessed in 22 adults patients with CF (age 22±4,8). Images were examined for specific abnormalities that were scored with respect to their severity and anatomic extent by using a modification of Bhalla system (the presence of centrilobular nodules additional to mucus plugging was included.) The global score for each patient was compared with their pulmonary function test results (FEV1 and FVC) and clinical status (according to Shwachman-Kulczycki score). **Results:** The overall CT score was 14,82±4,5. Overall CT scores were significantly correlated with FEV1 (r=0,89, p<0,001), FVC (r=0,83, p<0,001) and certain clinical parameters (finger clubbing, r= 0,63, p<0,002), but correlated poorly with BMI (r=0,35, P<0,11). **Conclusion:** Our initial results show that CT based scoring system in patients with CF provides a reliable method to monitor disease status

SS 01.3

Axial vs coronal HRCT images in the follow-up of patients with idiopathic pulmonary fibrosis

M. Mereu, P. D'Ambrosio, V. Di Mizio, P. Santodirocco, R.L. Patea, M.L. Storto; Chieti/IT

Purpose: To compare axial and coronal HRCT images in the follow-up of patients treated for idiopathic pulmonary fibrosis (IPF). **Material and methods:** We retrospectively evaluated 36 patients (28 M; 8F; mean age = 64 years) with a histological diagnosis of usual interstitial pneumonia (UIP) who had undergone HRCT scans of the chest at baseline and every four months during the first year of therapy. Pulmonary function tests and carbon monoxide diffusing capacity (DLCO) performed on the same day of HRCT were also available. Two chest radiologists, blinded to clinical and functional data, evaluated HRTC scans for the presence and extent of parenchymal abnormalities including honeycombing, intralobular interstitial thickening, septal lines, and ground-glass opacities.Two separate reading sessions were performed: axial images at four levels (aortic arch, carina, middle lobe bronchus, right inferior pulmonary vein) were assessed first; coronal reformatted images 1mm-thick and 10mm-interspaced were evaluated in the second session. The mean reading time of axial and coronal images was recorded. **Results:** Pulmonary function tests, clinical data, DLCO demonstrated a progression of disease in 14 patients (38%) whereas the remaining 22 (61%) remained stable. Axial images correctly identified all stable patients and 8/14 patients with progression. On the contrary, MPR coronal images allowed a correct definition of both progression and stability of disease. The mean reading time of axial and coronal images was 176 sec and 188 sec respectively (p>.05). **Conclusion:** Coronal HRCT images seem to be a reliable tool in assessing disease evolution in patients with IPF.

SS 01.4

Drug-induced respiratory diseases: a prospective comparison between high-resolution CT and bronchoscopy in 42 patients.

S. Piciucchi[1], M. Romagnoli[2], V. Poletti[2], M. Chilosi[3], C. Bigliazzi[2], D. Alessandra[2], G. Gavelli[4], A. Carloni[5]; [1]Meldola-forlì/IT, [2]Forlì/IT, [3]Verona/IT, [4]Bologna/IT, [5]Terni/IT

Purpose: To prospectively compare high resolution CT findings with histological and cytological findings, proven by fiber-optic bronchoscopy, in the assessment of patients with drug-induced respiratory diseases. **Material and methods:** Forty-two patients with a clinico-radiological diagnosis of drug-induced pulmonary disease were prospectively included into a five-year study protocol. All the patients underwent fiber-optic bronchoscopy, with a transbronchial biopsy or bronchoalveolar lavage and HRCT. Two radiologists blindly reported data regarding HRCT findings, distribution of parenchymal changes, and predominant pattern. Then in a second step, in cases of discrepancy, the diagnosis was obtained by consensus. Correlation between HRCT pattern, distribution, and extent were prospectively compared with pathological findings. These data were compared using Spearman Rank correlation coefficient and kappa index. **Results:** A good-to-excellent interobserver agreement was observed in the evaluation of each CT finding, relative distribution (K = 0.72 to 1.00). Histological and cytological findings showed DAD in 26%, OP in 17%, HP in 16%, AH in 37%, CIP in 19%, LP in 7%, and pseudo-sarcoid in 2% of patients. More frequent patterns of antineoplastic drugs has been CIP n = 6, DAD (n = 2), and OP (n = 2). Predominant pattern in non-antineoplastic drugs sample was DAD (n = 9) and OP (n = 5). Histological findings obtained with TBB showed a substantial concordance when compared with HRCT. K values showed good-to-excellent agreement for OP, DAD, HP; NSIP, and AH (K ranged from 0.69 to 0.89). A significant difference was observed between findings on CT scans in patients with antineoplastic agents and those scans obtained in patients with non-antineoplastic agents, particularly as regarded interlobular septal thickening (p = 0.003). **Conclusion:** HRCT showed excellent sensitivity in diagnosis of pattern as DAD, NSIP, and OP. In cases in which HRCT showed a lower sensitivity, it could be useful in the planning of a correct biopsy and in monitoring prognosis after drug suspension.

SS 01.5

Micronodular lesions in patients with pulmonary sarcoidosis: is this a sign of chronicity?

I. Tsangaridou, M. Seferos, A. Tzanetaki, E. Sotiropoulou, S. Velitsista, F. Laspas, M. Dimadi, L. Thanos; Athens/GR

Purpose: To assess the presence of diffuse micronodular opacities as a permanent, irreversible and treatment resistant finding in HRCT of patients with pulmonary sarcoidosis. **Material and methods:** A retrospective study of HRCT examinations (1-1,5 mm slice thickness) including 50 patients (22 men , 28 women) diagnosed with pulmonary sarcoidosis during a 3-year follow up period was performed in our department. Micronodular parenchymal lesions before, during and after therapy were comparatively studied. **Results:** 15 patients had micronodular opacities: 11 of them (7-8mm) [group A] with patchy distribution, mainly peribronchovascular, and 4 patients (3-4mm) [group B], with diffuse distribution. Imaging findings of micronodularity in group B, opposed to group A, revealed no changes during the above period. **Conclusion:** Diffuse micronodular opacities of pulmonary sarcoidosis remain invariable as disease progresses and do not regress after therapy, a finding that might be suggestive of chronic and fibrotic stage of disease.

SS 01.6

Correlation of mean pulmonary artery diameter (MPAD) on the CT scan with 2D ECHO PAP (Pulmonary Arterial Pressure) results in patients having DILD (Diffuse Interstitial Lung Disease).

I. Tsangaridou, M. Dimadi, P. Tsagouli, F. Laspas, P. Kokkinis, R. Triggidou, A. Manataki, L. Thanos; Athens/GR

Purpose: CT scans and ECHO cardiograms of 52 patients diagnosed with DILD, treated in our hospital during the recent 2 years, were retrospectively reviewed, for the evaluation of suspected pulmonary arterial hypertension (30 men and 22 women, middle age: 66,5 years). **Material and methods:** We measured the mean pulmonary artery diameter (MPAD) on the CT scan at the widest level. Patients with PAP <35mmHg were included in Group A (normal PAP), and those with PAP >35mmHg in Group B (consisted with Pulmonary Hypertension). **Results:** Patients of Group A had MPAD 2,97cm (31 patients) and those of Group B had MPAD 3,1cm. 22 patients of Group A had MPAD >2,7cm and 5 patients of Group B had normal MPAD. **Conclusion:** Statistically significant difference between the above groups was not established. Impressive observation was that a number of patients with normal PAP, measured by ECHO-cardiogram, had MPAD above the normal values.

SS 01.7

Depiction of malignancy in patients with diffuse interstitial lung disease (DILD) presenting with nodular opacities.

R. Triggidou, I. Tsangaridou, M. Dimadi, K. Malagari, P. Kokkinis, E. Sotiropoulou, P. Tsagouli, L. Thanos; Athens/GR

Purpose: To reveal an association of lung cancer with DILD **Material and methods:** We reviewed retrospectively 126 patients diagnosed with DILD and studied the CT scans of 22 of them (16 male, 6 female), mean age 66,15 years (range 47-81 years), who presented with solitary or multiple nodular opacities. 18 underwent CT guided FNA/FNCB and 4 open lung biopsy. **Results:** 13 patients (10,48%) with DILD developed lung cancer of which 8 cases were squamous carcinoma and 5 cases were adenocarcinoma. In the rest 9 patients a benign entity was diagnosed, of which 5 regarded BOOP/COP. **Conclusion:** Development of lung cancer in patients with DILD is a possibility not to be ignored. CT guided FNA/FNCB is a useful diagnostic modality contributing in early recognition and therapeutic management of the above patients

SS 01.8 - Withdrawn by authors

SS 01.9

Role of MDCT chest in evaluating febrile neutropenic patients

C.J. Das[1], A. Seith[2], G.S. Pangtey[2], K. Medhi[2]; [1]New Delhi/IN, [2]Delhi/IN

Purpose: MDCT evaluation to diagnose chest infections in a patient with febrile neutropenia. **Material and methods:** Total number of 100 patients (67 men; 33 women; mean age, 33.7 years; age range, 3-60 years) of febrile neutropenia ware evaluated with MDCT. All patients had neutropenia associated with various malignancies following chemotherapy [NHL (n=33), HD (n=27), AML (n=12), ALL (n=11), CML (n=10), multiple myeloma (n=7) and carcinoma breast (n=5)]. All the patients had fever with neutropenia at presentation. Chest radiography was performed in all cases before CT. CT was done in a 4-slice scanner (Volume Zoom, Siemens, Germany). All the images were evaluated by two radiologists who were blinded for the primary diagnosis. **Results:** Most common chest radiograph finding was bilateral diffuse infiltrates (n=20) and bilateral lower zone consolidations (n=17), pleural effusion (n=13). CT was abnormal in 68 patients and unremarkable in 32 patients. Most common CT finding was nodules with surrounding halo in 38 patients and parenchymal consolidation with or without surrounding halo in 16 patients and were diagnosed as invasive fungal infection. Of these 38 cases, 28 cases showed good response on antifungal treatment and 10 patients expired. Pneumonic consolidation with cavitary lesions suspicious for bacterial pneumonia was noted in 18 cases and of these two cases showed bilateral extensive changes. Pleural effusion was noted in 14 cases, mediastinal adenopathy in 3 patients and pericardial effusion in one patient. All these patients were treated with antibacterial therapy to whom they responded. In 9 patients, CT findings were indeterminate and hence treated with both systemic antifungal and antibacterial agents to whom 6 patients responded and 2 patients died eventually. Two patients had miliary tuberculosis and were treated with antitubercular therapy. . In 56% cases, CT could suggest a specific diagnosis of fungal vs. pyogenic infection. All 32 patients with unremarkable CT findings were treated symptomatically. **Conclusion:** MDCT can guide treatment by suggesting a specific diagnosis of fungal vs. pyogenic infection.

SCIENTIFIC SESSION 02 – ONCOLOGIC IMAGING – INTERVENTIONAL RADIOLOGY

SS 02.1

Correlation of radiological findings suggestive of inactive tuberculosis with new M. tuberculosis-specific assays of T-cell immune response in patients with hematological cancers.

P. Torricelli, F. Fiocchi, A. Ferrari, M. Luppi, R. D'Amico, M. Losi, L. Richeldi; Modena/IT

Purpose: To assess the correlation of the new blood T-cell interferon-gamma release assays (TIGRA) with the presence of radiological findings suggestive of inactive tuberculosis in a population of high-risk immuno-compromised patients. TIGRA: T-SPOT.TB (TS.TB) and QuantiFERON-TB Gold In-Tube (QFT-IT)) are now considered more specific than the tuberculin skin test (TST) for the diagnosis of latent tuberculosis infection (LTBI). **Material and methods:** Sixty-nine patients (mean age: 61.2 years, males: 53.6%) at their first diagnosis of hematologic cancer (53: Hodgkin lymphoma, 16: non-Hodgkin lymphoma) were enrolled in a prospective study; none of them was on anti-cancer chemotherapy at the time of testing. Fifty patients (72.4%) underwent chest CT as part of their clinical evaluation and 19 (17,6%) were evaluated by chest radiography. Two radiologists, independently and blinded to any demographic or clinical data, assessed all exams for the presence of abnormalities suggestive of inactive tuberculosis. TS.TB and QFT-IT were performed simultaneously in all patients and the kappa (k) statistic was used to assess the diagnostic agreement. **Results:** At CT or chest-radiography signs of inactive tuberculosis were find by at least one observer in 20 patients: inter-observers agreement was 87%, (k=0.56). At least one TIGRA was positive in 22 patients. However, agreement between TIGRA and the presence of radiologic abnormalities considered as due to inactive tuberculosis was extremely low: k value was close to zero, proving random concordance (k=0.05 for QFT-IT and k=0.21 for TS.TB). **Conclusion:** The radiologic findings interpreted as due to previous pulmonary tuberculosis infection were not correlated to the results of two highly specific T-cell based assays for the diagnosis of LTBI. Based upon our data radiologic diagnosis of inactive pulmonary tuberculosis might therefore be considered poorly specific.

SS 02.2

Radiofrequency ablation (RFA) of intrathoracic malignancies.

A. Bouga, E. Sotiropoulou, P. Filippousis, P. Tsagouli, F. Laspas, L. Thanos; Athens/GR

Purpose: To evaluate the safety and efficacy of CT-guided RFA as an alternative therapeutic method of lung malignancies.
Material and methods: In the last 22 months we performed 85 sessions of CT- guided RFA in 65 lung lesions (35 metastic and 30 primary, all inoperable) which measured 2 to 5.5 cm, in 47 patients. We used two types of electrodes (spiral and hooked type) and the procedure was performed under local anesthesia (lydocaine 2%). All patients had been administered 3mg per os Lexotanil or 0.5mg im Zinadol 30 minutes before starting the procedure. All patients were then placed in the appropriate position, based on the location of the lesion, and the electrode was inserted through a small skin incision under CT guidance. Mean RFA time was 16 minutes (time range 14-18 minutes). Follow-up consisted of a chest CT scan after contrast administration immediately after each session and then after 1, 3 and 6 months. **Results:** At the 6-month follow–up, CT scans reveal: - total tumor necrosis: 29/30 primary lesions (82.6%), 25/35 secondary lesions (77%), - partial tumor necrosis: 1/30 primary lesions (3.3%), 5/35 metastatic lesions (14%) Recurrence occurred in 10 cases, of which 4 were primary and 6 were secondary lesions. In all cases a second RFA session was performed. No major complications occurred, except 9 (10.6%) cases of pneumothorax (in 1 a pleurocath was inserted) and 2 (2.3%) cases of hemoptysis. **Conclusion:** CT-guided RFA is a safe and effective alternative therapeutic method of intrathoracic malignancies.

SS 02.3

Percutaneous CT-guided lung biopsy: complications and their direct management in high risk patients.

F. Laspas, P. Filippousis, E. Sotiropoulou, R. Triggidou, A. Bouga, M. Seferos, L. Thanos; Athens/GR

Purpose: To evaluate the risk for the development of pneumothorax and the need of chest tube placement in patients with emphysema who underwent fine needle aspiration of lung lesions. **Material and methods:** In a consecutive series of 1550 patients who underwent percutaneous CT-guided lung biopsy 120 present with emphysema. The variables that were examined included the size, the depth and the location of the lesion, the number of passes, the needle size, the experience of the interventional radiologist who performed the biopsy, and the presence of emphysema. The incidence of pneumothorax and its management were recorded. **Results:** Pneumothorax occurred in 27 (22,5%) of the 120 patients with emphysema and in 165 (11,5%) of the 1430 patients without emphysema. A chest tube was placed in 11 of the 27 emphysematous patients who developed pneumothorax (40,7%) and in 25 of the 165 without emphysema patients (15,2%). The criterion for chest tube placement was the aspiration with syringe of more than 450ml air. The higher incidence of pneumothorax was associated with the decreased size of the lesion. The number of passes, the needle size and the experience of the interventional radiologist were not related with the development of pneumothorax. Hemoptysis was observed in 6 patients **Conclusion:** The presence of emphysema is associated significantly with the development of pneumothorax and the need of thoracic drainage. However the risk of pneumothorax remains low and in the majority of the cases pneumothorax can be managed conservatively. Therefore emphysema is not an absolute contraindication to percutaneous lung biopsy for the diagnostic approach of pulmonary lesions.

SS 02.4

"Bronchial artery embolization" - treating massive hemoptysis in patients of pulmonary tuberculosis

B.K. Saha, K.B. Taori; Nagpur/IN

Purpose: Pulmonary tuberculosis is very common in developing countries in Asia including great prevalence in Indian subcontinent. One of the dreadful complications of pulmonary tuberculosis is massive hemoptysis. This study is about treating patients of massive hemoptysis by bronchial artery embolization. **Material and methods:** Bronchial artery embolization was done in 101 patients (85 male, 16 female) with massive hemoptysis between 14 to 73 years of age (mean age 46 years). Pre-procedure chest radiograph was done in each and every case. Bronchial artery embolization was performed on the side with the greater abnormality on the chest radiograph. Gel foam was used as embolising agent. These were introduced through a 4F visceral hook catheter. Pre and post-procedure angiographic films were obtained **Results:** Embolization was performed in 100 of 101 patients. Bronchial arteries (n=76); as well as nonbronchial arteries like intercostal arteries (n=98), internal mammary (n=36); lateral thoracic (n=25); costocervical trunk (n=3) and thyrocervical trunk (n=3) responsible for haemoptysis were selectively embolized. The average number of arteries embolized per patient was 2.7.Out of the 100 patients immediate control of hemoptysis was achieved in 98 patients within a period of 24-48 hours with a procedure success rate of 98%. 12 patients had rehaemoptysis within 30 days with re-bleed rate of 12%. Out of these 12 patients, 8 patients were re-embolized and remaining 4 patients were managed conservatively. **Conclusion:** Bronchial artery embolization is an effective procedure for treatment of massive hemoptysis in pulmonary tuberculosis.

SS 02.5

Treatment with radiofrequency ablation (RFA) of metastases in patients with surgically resected lung cancer

E. Sotiropoulou, P. Filippousis, A. Bouga, M. Seferos, F. Laspas, L. Thanos; Athens/GR

Purpose: To prove the efficacy and safety of RFA in patients with surgically resected lung cancer who presented with metastases. **Material and methods:** In our institution we performed 115 RFA sessions in 86 patients: 18 patients underwent 18 RFAs for painful bone metastasis. 22 patients with 35 liver metastases underwent 42 RFAs. 25 patients with adrenal metastases underwent 30 RFAs. 5 patients with intraperitoneal metastases underwent 7 RFAs. 16 patients with intrapulmonary metastases underwent 18 RFAs. Metastases with partial response and those with local recurrence post RFA underwent a second RFA. **Results:** Patients with liver metastases: 31/33 (88,6%) of the lesions showed complete necrosis and 4/33 metastases showed partial response (11,4%). 3/ 35 (8,6%) lesions showed local recurrence. Patients with adrenal metastases 22/25 (88%) of the lesions showed complete necrosis and 3/25 (12%) showed partial response. 2 lesions (8%) showed recurrence. Patients with intraperitoneal metastases 3/5 (60%) of the lesions showed complete necrosis and 2/5 (40%) showed partial response. Patients with intrapulmonary metastases 14/16 (87,5%) of the lesions showed complete necrosis and 2/16 (12,5%) showed partial response. No major complications occurred: A pneumothorax occurred in 3/18 cases RFA in intrapulmonary metastases and was treated conservatively. Symptoms of post ablation syndrome were present after 38/115 RFA sessions (33%). **Conclusion:** RFA of metastases in patients with surgically resected lung cancer seems to be efficient and safe treatment modality.

SS 02.6

CT analysis of mass-like consolidations: differential points between benign and malignant lesions.

E.S. Lee[1], S. Paik[2], J.G. Yi[1], J.I. Jung[1]; [1]Seoul/KR, [2]Kyeongki-do/KR

Purpose: To differentiate benign and malignant lesions of mass-like consolidations on chest CT. **Material and methods:** The patients consisted of the two groups. Ten patients of pathologically proven lung malignant group included adenocarcinoma in six cases, squamous cell carcinoma in two cases, nonmucinous bronchioloalveolar carcinoma in one case and lymphoma in one case. 13 patients of benign group proven by pathology or sputum culture included tuberculosis in five cases, staphylococcal pneumonia in three cases, klebsiella pneumonia in two cases, actinomycosis in one case, aspergillosis in one case and organizing pneumonia in one case. CT findings were compared in each group with respect to morphological appearances of the pulmonary lesions, adjacent pleural changes and mediastinal lymphadenopathies. **Results:** CT findings which favored the diagnosis of malignancy included enhancing high attenuation of the pulmonary lesions (50%), multiple mediastinal lymphadenopathies (50%). In contrast, CT findings of homogenous low attenuation (38%) and or peripheral high attenuation (23%) of the pulmonary lesions, pleural (61%) and extrapleural changes (54%) were commonly seen in benign group. Other findings including air-bronchogram, CT-angiogram and cavitation or necrosis in pulmonary lesions were not helpful in differential diagnosis of both groups. **Conclusion:** Although CT findings are nonspecific, frequent pleural or extrapleural changes may be helpful in diagnosis of benign lesions and multiple mediastinal lymphadenopathies favor malignancy.

SS 02.7

Pulmonary nodules discovered by CT-differential diagnosis-classification-guidelines for management

I. Pantou, M. Kampanarou, K. Bouhra, D.K. Filippiadis, G. Oikonomou, S. Tanteles, A. Pomoni, E. Chatzimichael, M. Pomoni, D. Kelekis; Athens/GR

Purpose: To review the diagnostic approach of pulmonary nodules using multislice CT. Application of multislice CT made possible the reconstruction of ≤1mm thickness images and the detection of nodules as small as 1-2 mm in diameter. **Material and methods:** During the last 6 months in our department, computed tomography of the thorax was performed on 868 patients with application of multislice CT (Philips Brilliance 64). Out of these, 356 cases involved inflammatory disease investigation (182/356 had smoking history) and 512 cases involved cancer follow up. **Results:** According to CT study the nodule may be classified into benign, indeterminate or highly suspicious for malignancy. Management of indeterminate nodule is of great importance and in 2005, Fleischner society suggested recommendations for their management. **Conclusion:** The introduction of multislice CT, has routined the incidental finding of pulmonary nodules and greatly contributed to their characterization upon which are classified and managed in accordance with international bibliography recommendations.

SS 02.8

Frequency and significance of solitary pulmonary nodules on CT in patients with extra pulmonary malignancy

S. Ganeshalingam, L.J. Menezes; London/UK

Purpose: To review the frequency and significance of solitary pulmonary nodules detected on CT in patients with extra pulmonary malignancy. **Material and methods:** We retrospectively evaluated all the CT scans performed on patients with an extra pulmonary malignancy and a solitary pulmonary nodule, in the calendar year 2006. The CTs were evaluated by two radiologists for the size and location of the solitary pulmonary nodule. Nodules were considered malignant based on their growth, PET scan results, or on biopsy results, and were considered benign either on histology or if their appearance remained stable 1 year after the initial examination. **Results:** 137 patients with an extra pulmonary primary had a solitary pulmonary nodule. Of these, 85 patients had nodules that met the criteria of a benign nodule (62%) and 52 (38%) met the criteria for malignant nodules. Nodules smaller than 8mm were more likely to be benign (n=78/85, 92% of cases), whereas 8 mm or greater nodules were more likely to be malignant (n=45/52, 87% of cases). Most nodules within 10mm of the pleura were benign, whereas approximately half of nodules 10mm away from the pleura were malignant. Patients with head and neck cancers, melanoma and testicular tumours were more likely to have malignant nodules. On analysis, nodule size and distance from the nearest pleural surface were predictive of malignancy. **Conclusion:** Nodule detection rate on CT in patients with extra pulmonary malignancy is high. Most of the nodules smaller than 8mm or within 10mm of pleura were benign.

SS 02.9

Computerized tomography of tuberculosis in patients with different lung neoplasms: the analysis of 8499 lung CT scans

A. Ivkovic[1], T. Spasic[2], S. Ristic[2]; [1]Nis/RS, [2]Vranje/RS

Purpose: The aim of the study was to correlate the frequency of different malignancies in patients with tuberculosis (TBC). **Material and methods:** The group of analyzed patients consisted of 7552 patients who underwent lung CT examination for suspicion of lung malignancies. There were 4480 males (59.33%) and 3072 females (40.67%). Also we examined 445 patients with laryngeal cancer, and 502 with thoracic trauma. **Results:** Out of 7552 examined patients there were 6947 (91.99%) with detected lung cancer. Among them different stages of TBC were identified and confirmed with additional diagnostic investigations in 2955 (39.25%) patients. It was confirmed that in 85% of patients with TBC there were tumours with slow progression, opposite to lower frequency of TBC in patients with metastatic disease and sarcomas. In the group of patients with laryngeal cancer, lung TBC was diagnosed in 21 (4.97%) patients. Out of 502 patients with thoracic trauma tuberculosis was identified in 21 patients, and confirmed in other 39. Additionally in patients with trauma 5 lung cancers were diagnosed. In all patients diagnosis of tuberculosis was confirmed with standard methods, in the group of surgically treated through pathologic examination. **Conclusion:** CT scan is powerful diagnostic tool in accidentally diagnosis of different stages of tuberculosis in patients examined for suspicion of lung neoplasm. Patients with cavernous TBC were more prone to lung neoplasm. In patients with laryngeal cancer it was observed fibro-caseous forms of TBC.

SCIENTIFIC SESSION 03 - AIRWAY DISEASE – PULMONARY EMBOLISM

SS 03.1

A method for optimizing observer agreement for HRCT signs of airways disease

N. Sverzellati[1], A.U. Wells[2], S.R. Desai[2], A. Devaraj[2], M. Quigley[2], D.M. Hansell[2]; [1]Parma/IT, [2]London/UK

Purpose:
This study was designed to assess a new method of observer scoring by quantifying the degree of interobserver variation in the evaluation of the high-resolution computed tomography (HRCT) signs of airways disease. **Material and methods:** HRCT scans of a mixed group of 143 patients with proven airways diseases were evaluated by two chest radiologists. Bronchial wall thickness (BWT) and the mosaic attenuation (MA) pattern were visually graded in each lobe according to a four-point scale and as a percentage of the lobar volume, respectively. The new method of agreement was tested by the same observers at one year following their original (standard system) scoring. The new system entailed “continuous learning” with the observers rescoring cases and reaching a joint opinion whenever their score differences were higher than predetermined thresholds (>1 for BWT and ≥20% for the MA). Weighted kappas (k_w) were calculated and compared between standard and new method systems. **Results:** Observer agreement for the standard and new systems showed substantially improved agreement for the new system: BWT k_w increased from 0.51 to 0.76 and for MA increased from 0.34 to 0.81. When analyzing k_w in succeeding groups of 20 observations with the new system we observed a straightforward improvement between the first group and the following ones (BWT 0.65-0.77; MA 0.66-0.79) suggesting an incremental training effect. **Conclusion:** This new system significantly increased agreement for the visual quantification of signs of airways disease and now needs to be tested in other CT signs that are scored for clinical studies.

SS 03.2

Primary ciliary dyskinesia and idiopathic bronchiectasis: a comparative CT study.

M. Quigley[1], N. Sverzellati[2], S.R. Desai[1], A.U. Wells[1], D.M. Hansell[1], R. Wilson[1]; [1]London/UK, [2]Parma/IT

Purpose: To identify morphological differences between primary ciliary dyskinesia (PCD) and idiopathic bronchiectasis on high resolution computed tomography (HRCT). To establish which variables affect airflow and to investigate whether the type of ciliary dysfunction reflects the HRCT pattern of disease. **Material and methods:** The CT scans of 151 individuals with idiopathic bronchiectasis (n=87) or PCD (n=64) were reviewed. Two observers scored abnormalities and disease distribution and the results were correlated with pulmonary function tests. Ciliary ultrastructure and motility data was documented in PCD patients.
Results: A tree-in-bud pattern was more frequent in PCD (p=0.001). Patients with PCD had more isolated middle lobe disease (p=0.03). On stepwise regression bronchial wall thickening was the strongest independent determinant of FEV_1 in both PCD (p=0.051) and idiopathic bronchiectasis (p=0.001). The mean FEV_1 in PCD was lower (63.6% predicted +/- 24.2) than in idiopathic bronchiectasis (72.6% predicted +/- 26) (p=0.04). In the sub-population of PCD with motile cilia, the link with between tree-in-bud pattern and FEV_1 was strong (p=0.0008).Other determinants of FEV_1 in this group were: mucus plugging (p=0.003), bronchial wall thickening (p=0.004), extent of bronchiectasis (p=0.01) and bronchial lumen dilatation (p=0.04). **Conclusion:** Patients with PCD are more likely to have disease concentrated in the middle lobes, and more extensive tree-in-bud pattern, than individuals with idiopathic bronchiectasis. Bronchial wall thickness is the most important CT abnormality that influences FEV_1 in both PCD and idiopathic bronchiectasis. In PCD the relationship between ciliary dysfunction and disease severity is complex.

SS 03.3

CT findings of the chest in adults with aspirated foreign bodies: report of 23 cases

A. Osadchy, J. Smorjik, R. Zissin; Kfar Saba/IL

Purpose: To assess the imaging findings in adult patients with tracheobronchial foreign body aspiration. **Material and methods:** 23 patients, 15 men and 8 women, aged 26-89 years, with foreign body aspiration were retrospectively reviewed. Nine were outpatients with non-specific symptoms and 14 were hospitalized with non-resolving pneumonia (n=9), after detection of a dental fragment on a chest radiograph following intubation or dental procedure (n=4) and one mentally retarded patient with empyema. **Results:** An aspirated dental fragment was seen on a chest radiograph in 4 patients and an endobronchial foreign body on CT in 19, appearing as an intraluminal structure within the bronchial lumen, most often hyperdense. The foreign body was right-sided in 17 cases and left-sided in 6. Five cases were missed at first interpretation. Associated findings on CT were volume loss, hyperlucency with air trapping and bronchiectasis in the affected lobe. Seventeen patients were managed with bronchoscopy, while 2 needed thoracotomy. In one patient bronchoscopy failed to detect a foreign body, indicating a false positive CT diagnosis. One patient expelled an aspirated tablet and 2 refused invasive procedure. The foreign bodies found mainly were bones and dental fragments. **Conclusion:** A high clinical suspicion is necessary to diagnose a foreign body. As CT is often used to evaluate various respiratory problems in adults it may be the first imaging modality to discover an unsuspected aspirated foreign body in the bronchial tree.

SS 03.4

CT indicators of pulmonary hypertension: accuracy in mild versus severe disease

A. Devaraj, A.U. Wells, M. Meister, D.M. Hansell; London/UK

Purpose: To compare the reliability of pulmonary artery signs on multi-detector CT (MDCT) in mild and severe pulmonary hypertension (PH). **Material and methods:** Eighty-two patients who had undergone thoracic MDCT and right heart catheterisation were included in the study (41 males, mean age 56 years; 33 with pulmonary fibrosis, 29 with pulmonary vascular diseases and 20 patients with a variety of other lung diseases). The population was divided into two groups: 1) normal or mild PH patients with mPAP ≤ 35 mmHg (n=45); and 2) severe PH patients with mPAP > 35 mmHg (n=37). Dimensions of the main pulmonary arteries, segmental, sub-segmental and sub-sub-segmental pulmonary arteries were recorded at predetermined levels. Measurements were correlated with mean pulmonary artery pressure (mPAP) in the two groups. **Results:** In contrast to a strong correlation between main pulmonary artery diameter and mPAP in patients with severe PH ($r=0.43$, $p<0.001$), no such correlation existed in the normal/mild PH group ($r=0.25$, $P=0.09$). However, significant correlations were demonstrated between mean segmental, sub-segmental and sub-sub-segmental artery size and mPAP in normal/mild PH patients ($r=0.43$, $p=0.02$; $r=0.47$, $p<0.005$, $r=0.44$, $p<0.01$ respectively). No correlations between mPAP and these smaller pulmonary arteries were found in severe PH. **Conclusion:** The diameter of the main PA on MDCT cannot be considered a reliable indicator of mPAP in patients with mild PH. However the segmental, sub-segmental and sub-sub-segmental arteries may reflect raised mPAP better in this group.

SS 03.5

Pulmonary artery/ascending aorta ratio as a sign of pulmonary hypertension: validity in fibrotic versus non-fibrotic lung disease.

A. Devaraj, A.U. Wells, M. Meister, D.M. Hansell; London/UK

Purpose: To evaluate the value of the pulmonary artery (PA)/ascending aorta (AA) ratio as a sign of PH in patients with fibrotic lung disease (FLD) compared to non-fibrotic lung disease (NFLD). **Material and methods:** Eight-two patients (41 males, mean age 56 years) were divided into two groups: 33 patients with FLD and 49 patients with NFLD. Patients were further categorised into those with a mean PA pressure (mPAP) > 30 mmHg, and those with a mPAP ≤ 30mmHg, as determined by right heart catheterisation. Dimensions of the main pulmonary artery and ascending aorta were measured in all patients at predetermined levels. Correlations between PA diameter and mPAP compared to PA/AA ratio and mPAP were analysed in the two groups. **Results:** The main PA diameter correlated with mPAP in patients with NFLD ($r=0.69$, $P<0.0001$) but not in patients with FLD ($r=0.23$, $p=0.18$). By contrast the PA/AA ratio correlated with mPAP in the FLD group ($r=0.57$, $p<0.001$), but did not significantly change the correlation in the NFLD group ($r=0.72$, $p<0.0001$). In patients with a mPAP ≤ 30mmHg, mean diameters of the PA and AA were larger in FLD than in NFLD (31.0 mm vs. 26.0 mm, $p<0.001$; and 34.1 mm vs. 30.9 mm, $p=0.12$ respectively). **Conclusion:** In patients with fibrotic lung disease, dilatation of the main PA and aorta occurs in the absence of PH. The PA/AA ratio is a better indicator of mPAP in patients with FLD than the absolute PA dimension.

SS 03.6

Patient exposure and image quality at 80 kV in pulmonary CT angiography

Z. Szucs-Farkas, L. Kurmann, M.A. Patak, T. Strautz, P. Vock, S.T. Schindera; Berne/CH

Purpose: To compare two pulmonary CT Angiography protocols using 80 and 100 kVp CT-tube energies in respect to patient exposure, vessel attenuation and subjective image quality. **Material and methods:** Our database was retrospectively searched for patients weighing less than 100 kg who underwent pulmonary CTA with suspected pulmonary embolism between September and December 2007. Twenty-five patients in group A were examined with a 100 kVp CTA protocol and 25 patients in group B at 80 kVp tube energy. Volume and flow rate of contrast medium were reduced in group B (75 mL at 3 mL/s) compared to group A (100 mL at 4 mL/s). Attenuation in the central and peripheral pulmonary arteries was measured and contrast-to-noise ratio (CNR) calculated. Quantitative image parameters and patient exposure characterized by dose length product (DLP) in both groups were compared by the t-test. Two blinded radiologists independently assessed subjective image quality on a five-grade-scale and the results were compared using non-parametric tests. **Results:** Except for the lung periphery, mean attenuation in the pulmonary arteries at all levels was significantly higher in group B compared to group A (CT number over all arteries: 410.9±96 vs. 340.4±88.3 HU, p= 0.0096). However, CNR showed no difference between the groups (group A, 19.9 ± 7.2 and group B, 19.9 ± 4.7, p= 0.98). Image quality did not differ significantly either (3.58 at 100 kVp and 3.69 at 80 kVp, p= 0.37). DLP with the 80 kVp-protocol (119.8 ± 16.7 mGy) was lower by more than 40% compared to 100 kVp (204.8 ± 63.1 mGy, p<0.0001). **Conclusion:** The use of 80 kVp tube energy for pulmonary CTA can reduce exposure by 40% and CM volume by 25% compared to 100 kVp protocols without deterioration in image quality in patients weighing less than 100 kg.

SS 03.7

Pulmonary artery hypertension: correlations between cardiac morphologic and functional parameters assessed by MRI and invasive measurements.

V. Chabbert, J.-.P. Alunni, B. Degano, N. Blot-Souletie, C. Arnaud, H. Rousseau, P. Otal; Toulouse/FR

Purpose: To compare cardiac MRI with right heart catheterism (RHC) in patients with pulmonary hypertension (PH) and evaluate the accuracy of MRI in estimating the severity of PH. **Material and methods:** Forty patients were included (24 women, mean age 58.8+/- 16.3 years). Idiopathic PH, chronic thromboembolic disease, HIV disease and systemic sclerosis represented the principal causes of PH (29 patients).The mean delay between MRI and RHC was 13.9 days +/- 22.3 days without significant clinical changes in the interval. MRI included cine and phase-contrast sequences and studied systolic and diastolic right and left functions, right and left cavities areas and ratios, the position of the interventricular septum (IVS) in systole and diastole, and flow parameters in the pulmonary artery trunk. **Results:** The values of systolic pulmonary pressure (sPAP) and vascular resistances (PVR) reflected high levels of PH (sPAP = 66.8mmHg +/- 21.8 and PVR = 7.89 WU +/-6.3). The position of IVS during diastole and systole was highly correlated to pulmonary artery pressures (PAP) and PVR. An abnormal position of IVS in diastole predicted a sPAP of more than 51 mmHg with Sen, Spe, positive and negative predictive values (VPP, VPN) of 97%, 60%, 88% and 86% respectively. An abnormal position in systole predicted a sPAP of more than 51mmHg with Sen, Spe, PPV and NPV of 83%, 90%, 96 % and 64% respectively. Correlation between diastolic ventricular area ratio and PVR was high (r = 0.67). A diastolic ventricular area ratio of more than 2 predicted a PVR of more than 10 WU with Sen, Spe, PPV and NPV of 89%, 93%, 80% and 96% respectively. **Conclusion:** Cardiac MRI can assist in the evaluation of the severity of PH by using simple morphologic parameters.

SS 03.8

To evaluate the correspondence between coronary artery vascularization and 17-segment heart model.

F. Fiocchi, G. Ligabue, A. Barbieri, L. Verganti, M.G. Modena, P. Torricelli; Modena/IT

Purpose: To evaluate the correspondence between coronary artery vascularization and 17-segment heart model in patients submitted to primary coronary angioplasty by means of Delayed Enhancement Magnetic Resonance Imaging (DE-MRI). **Material and methods:** 50 patients (18% female; 4% left dominancy) treated for first acute myocardial infarction with drug-eluting stents implantation where submitted within 2 weeks to DE-MRI. The distribution of risk area was evaluated on short and horizontal long axis, following the 17-segments model of American Heart Association. **Results:** In 30 patients, the culprit lesion was on left anterior descending artery (LAD), in 16 on right coronary artery (RCA) and in 4 on left circumflex artery (LCX). DE was found on 217/850 segments. DE presence in the basal anterior and antero-septal segment is specific for LAD occlusion (100%). DE presence in the medio-ventricular anterior, antero-septal, antero-lateral, apical anterior, apical septal segments and in the apex is highly indicative of LAD occlusion (84,7%). DE presence in the basal infero-septal and medio-ventricular inferior segments is not unquestionably indicative of RCA occlusion (78,1%); the concomitant presence of DE in the inferior segments increases specificity for RCA occlusion (100%). There is no certain correlation between LCX culprit lesion and myocardial risk territory. In case of DE on the basal infero-lateral, antero-lateral, medio-ventricular infero-lateral segments is not possible to categorize the ill vessel. **Conclusion:** The only anterior and antero-septal segments identify LAD occlusion; no other segment can be considered exclusively vascularized by a single coronary vessel. DE presence on RCA territory is highly related to RCA occlusion.

SS 03.9

Graft versus host disease of the lungs in bone marrow transplant (BMT) patients: HRCT findings at presentation and correlation with pulmonary function tests

N.R. Bogot[1], E.A. Kazerooni[2], S. Patel[2], K.R. Cooke[2], G.A. Yanik[2]; [1]Jerusalem/IL, [2]Ann Arbor/US

Purpose: To evaluate GVHD appearance on HRCT at initial clinical presentation & correlate with pulmonary function. **Material and methods:** 20 patients (mean age 47years;12 male, 8 female) with clinically suspected GVHD underwent inspiratory/expiratory HRCT & pulmonary function testing (PFT). BMT type: 10 matched-related peripheral blood stem cell transplant (PBSCT), 5 matched-unrelated BMT,3 unmatched-unrelated BMT, 1 5/6 unmatched-related PBSCT, 1 unspecified. GVHD diagnosed by: biopsy 7, clinically 13 (bronchiolitis obliterans syndrome criteria). Time from transplant to CT 0.2-9.5 years. Air-trapping extent & profusion of centrilobular nodules in each lobe on HRCT was graded for severity (0=normal;1=<33% of lobe;2=33-66%;3=>66%). Bronchiectasis in each lobe was graded (0=normal;1=bronchus diameter<1.5 times adjacent artery;2=1.5-2 times adjacent artery 3=>2 times). PFT results were graded (mild, moderate, severe). **Results:** Mean air trapping extent for each lobe: RUL 1.2, RML 1.3, RLL 1.5, LUL 1.1, LLL 1.3. Mean centrilobular nodule profusion: RUL 1.5, RML 0.5, RLL 1.2, LUL 1.4, LLL 0.8. Mean bronchiectasis diameter: RUL 0.9, RML 0.9, RLL 1.3, LUL 0.8, LLL 1.2. Nodule profusion was significantly greater in the upper lobes (mean 1.42) than the middle/lower lobes (mean 0.8) (t test p=0.0001). Air trapping scores (mean upper lobes 1.1, mean middle/lower lobes 1.36) (p=0.098) and bronchiectasis scores (mean UL 0.82, mean M/L lobes 1.08) (p=0.109) were not significantly different. There was significant relationship between greater extent of air trapping and centrilobular nodules profusion with severity of obstruction on PFTs (p=0.003 & 0.001 respectively; regression analysis); this was not found for bronchiectasis. Other findings included thick septal lines (4 patients), peribronchial air-space opacities (3 patients), patchy GGO (2 patients); subpleural nodules & pneumomediastinum (1 patient each). **Conclusion:** GVHD presents with mild air trapping, centrilobular nodules and bronchiectasis. Air-trapping and centrilobular nodules are more extensive in the upper lobes than middle/lower lobes, while bronchiectasis had a trend towards lower lobe predominance. Air trapping and centrilobular nodules extent correlate with obstruction severity.

SCIENTIFIC SESSION 04 - CAD FOR THE CHEST – IMAGE QUALITY

SS 04.1

Increasing the detection sensitivity of lung nodules on digital chest radiographs by the use of CAD

N.R. Bogot[1], D. Shaham[1], R. Eliahou[1], A. Manevitch[1], J. Stoeckel[1], N. Hiller[1], S.S. Mansur[2], M.S. Dinesh[2], M. Acharyya[2], I. Leichter[1]; [1]Jerusalem/IL, [2]Bangalore/IN

Purpose: To evaluate whether a prototype CAD algorithm improves detection of lung nodules on digital chest radiographs for readers with different levels of expertise. **aterial and methods:** Seventy-six digital chest radiographs (DR) were analyzed retrospectively by two independent expert readers, who correlated DR to chest CT, to establish the Ground Truth for the presence and location of masses and lung nodules 5-30mm in size. DR images were then read by two blinded readers, a radiology resident and a thoracic radiologist, who had no CT correlation. Each reader marked apparent lung masses and nodules without CAD assistance, and then reread with CAD marks displayed on the image, by a prototype detection algorithm (Siemens). Radiologist performance (sensitivity and false marks rates per case) without and with CAD assistance was compared. **Results:** A total of 39 nodules and seven masses were identified as the Ground Truth in 36 digital radiographs. The CAD algorithm improved detection of nodules but not of masses. The resident's detection rate for nodules increased with the CAD device from 17 nodules (43.6%) to 18 (46.2%). For the thoracic radiologist, nodule detection increased from 28 (71.8%) to 30 (76.9%).The resident's false marks rate per case increased from 0.25 without CAD to 0.54 with CAD. The thoracic radiologist's false marks rate increased from 0.57 to 0.95. **Conclusion:** The CAD algorithm improved nodule detection for both readers but particularly for the thoracic radiologist. The increase in sensitivity was associated with an increase in false marks.

SS 04.2

Evaluation of a Computer Aided Detection (CAD) system for non-solid pulmonary nodules.

X. Boulanger, A.L. Brun, C. Hill, D. Leclercq, P.A. Grenier, C. Beigelman-Aubry; Paris/FR

Purpose: The purpose of this study was to evaluate a CAD software for the detection of non-solid pulmonary nodules which have a higher prevalence of malignancy than solid nodules. **Material and methods:** 17 CT examinations from 17 patients were selected for having at least one non-solid nodule. There were 11 adenocarcinomas (3 bronchioloalveolar carcinoma and 8 mixed adenocarcinomas) and 1 benign lesion (desquamative interstitial pneumonitis). Acquisitions were performed using a 16 detector-row CT scanner (Lightspeed, GE Healthcare, Milwaukee, WI) and a 40 detector-row CT scanner (Brilliance 40, Philips Medical Systems, Best, Netherlands), reconstructed with a lung kernel and a slice thickness / interval of 1.25 mm / 0.6 mm (n=7), and of 0.8 mm / 0.4 mm (n=5) respectively. The ground truth was established by 2 experienced thoracic radiologists in consensus and consists in 24 solid nodules and 259 non-solid nodules. The examinations were read by 2 radiologists and analyzed by the CAD system (MEDIAN Technologies, France). As the CAD software was especially designed for lesions over 3 mm, the performances were evaluated for the sub-category of non-solid nodules greater than 3 mm (n=99). This category was composed of 69 pure ground glass opacities (GGO) and 30 mixed (part solid) nodules.**Results:** The sensitivities for non-solid nodules greater than 3 mm were respectively 55% for radiologist 1; 49% for radiologist 2; 61% for the CAD software. The overall predictive positive value of the CAD was 95%. When adding the findings found by the CAD and by each radiologist, the sensitivities were 83% for radiologist 1; 78% for radiologist 2. The combination CAD and radiologist was better than the results of both observers combined. **Conclusion:** The use of a CAD-system as a second observer can significantly improve the detection of non-solid nodules.

SS 04.3

Computer-aided detection of pulmonary embolism (CAD): can a junior radiologist benefit from consensus with CAD in detecting of segmental and subsegmental pulmonary embolism?

J. Baxa, J. Ferda, A. Bednarova, R. Vondrakova, H. Mirka, B. Kreuzberg; Plzen/CZ

Purpose: To evaluate the accuracy of a CAD tool for automated detection of segmental and subsegmental pulmonary embolism and the capability of software to help junior radiologist in evaluation of CT pulmonary angiography (CTPA). **Material and methods:** We selected 18 patients (9 women) from our set of CTPA´s with total of 78 emboli (41 segmental/37 subsegmental; 4.33 emboli per patient). As a control group we randomly picked 18 patients with negative CTPA. All 36 examinations were again analysed by CAD tool (PE-CAD, Siemens Medical Solutions, Germany), by junior radiologist (praxis length 2.5 years) alone and in consensus with the CAD tool and by senior radiologist (praxis length 14 years). **Results:** CAD correctly detected 44 emboli (30 segmental, 14 subsegmental) and 112 findings were false positive. As for the analysis of segments, the overall (segmental + subsegmental) sensitivity of the CAD was 56.4% (segmental = 73.2%; subsegmental = 37.8%) and the positive predictive value (PPV) was 42.3%. Junior radiologist profited by the consensus with the CAD, their overall sensitivity increased from 83.3% to 87.2% (segmental – 95.1% to 97.2%; subsegmental – 70.2 to 75.2%) and the PPV from 93.2% to 95.6%. Senior radiologist achieved the overall sensitivity of 92.3% (segmental = 100%; subsegmental = 94.1%) and PPV of 96.1%. As for the analyses of patients, the sensitivity of CAD was 83.3% and the negative predictive value (NPV) was 78.6%, the sensitivity of junior radiologist in consensus with the CAD was 94.5% and the NPV was 93.8%, the sensitivity and NPV of senior radiologist were 100%. **Conclusion:** Our results show the capability of the CAD to improve performance of a junior radiologist in detecting of segmental and subsegmental pulmonary embolism at CTPA. CAD is feasible as a “second reader” in the evaluation of CTPA, but low sensitivity in detecting subsegmental embolism and high false positive rate demand further improvement.

SS 04.4

3D texture analysis of thorax CTs allows for the differentiation of mixtures of pathological patterns in the lung

R. Huttary[1], W. Recheis[1], A. Ruiu[1], M. Zompatori[2]; [1]Innsbruck/AT, [2]Parma/IT

Purpose: Many lung pathologies are mixtures of different pathological patterns which are difficult to be differentiated in the radiological image. For example, the superimposition of ground glass and emphysema can fake honeycombing. The scope of this study is to show that the use of three-dimensional texture analysis can increase the quality of diagnostic findings in thorax CTs due to the better differentiation of various disease patterns. **Material and methods:** Retrospectively 15 thorax CTs (0.5 mm slice-thickness, low-dose protocol, native) from 12 patients with different lung diseases (COPD, emphysema, interstitial, granulomatous lung disease, smoke-induced lung disease) were independently analyzed by 2 radiologists with profound experience (5years, 25years). Further the same records were examined with the texture analysis algorithm 3D-AMFM (Adaptive Multiple Feature Method) contained in the software PASS (Pulmonary Analysis Software Suite, University of Iowa) concerning currently 5 disease-specific pathological parenchymal textures (normal, ground glass, honeycombing, emphysema, nodular, tree-in-bud). As training data base for the AMFM texture patterns in 100 patients were defined by the radiologists. The spirometric and clinical data were integrated into the evaluation **Results:** 92 percent of known lung pathologies were clearly identified by the software. Further in 11 out of 15 cases texture analysis delivered relevant additional information: Mixtures of pathologies could unequivocally be differentiated and confirmed by a second analysis. Mixtures of emphysema and ground glass could be detected in all cases (9 cases). In 2 cases mixtures of honeycombing and ground glass could unequivocally be detected. **Conclusion:** The disadvantage of the method presented is the absence of a ‚ground truth'. The definition of texture patterns is the key issue. Nevertheless the method seems to be capable to be employed in the separation and differentiation of several pathological patterns. For clinical routine application further studies will be necessary. 3D texture analysis can support the radiologist concerning the interpretation and differentiation of mixed pathological parenchymal patterns.

SS 04.5

Gender differences in emphysema phenotypes in non-COPD smokers

N. Sverzellati[1], E. Calabrò[2], G. Randi[2], C. La Vecchia[2], A. Marchianò[2], J.M. Kuhnigk[3], P. Spagnolo[4], M. Zompatori[1], U. Pastorino[2]; [1]Parma/IT, [2]Milano/IT, [3]Bremen/DE, [4]Modena/IT

Purpose: Data on gender differences in the emphysema features are available only in patients with chronic obstructive pulmonary disease (COPD). Thereby, the purpose of this study was to weight how gender influences emphysema phenotype, using multi-detector CT (MDCT) derived multiparametric objective measurements in non-COPD smokers. **Material and methods:** We retrospectively evaluated both clinical and low-dose MDCT data on 957 heavy smokers (343 women) without clinical evidence of significant airflow obstruction recruited by the Multicentric Italian Lung Detection trial (MILD trial). MDCT scans were analyzed with prototypical emphysema detection software (MeVis, Bremen) which provides a region-based assessment of the following measures: lung volumes, mean lung density, emphysema index and four classes of emphysema clusters with different volumes. For these measures, multiple regression models were applied to assess the effect of gender, after allowance for age, FEV_1, body mass index, pack-years, and pulmonary volume. **Results:** Compared to males, female smokers showed less severe mean MDCT emphysema measurements ($p<0.001$). However, fitting multivariate regression models, we observed that women, compared to men, exhibited an emphysema phenotype which was more extensive, more heterogeneous in distribution, and characterized by bigger hole sizes in the lower lobes. **Conclusion:** Men and women seem to respond differently in the type and location of lung damage due to tobacco exposure and this may provide an advance in understanding the pathophysiologic differences between genders.

SS 04.6

Oxygen-enhanced magnetic resonance imaging: influence of different gas delivery methods on the T1-changes of the lungs.

F. Molinari[1], M. Puderbach[2], M. Eichinger[2], S. Ley[2], M. Bock[2], L. Bonomo[1], H.U. Kauczor[2]; [1]Rome/IT, [2]Heidelberg/DE

Purpose: The clinical feasibility of oxygen-enhanced MRI of the lung may benefit from the use of a simple gas delivery method. In this study, the oxygen-induced T1-change of the lung obtained using a closed O_2-delivery system was compared with that obtained by a conventional nontight face mask. **Material and methods:** Twenty-three healthy subjects (15 men, 8 women, mean age=25 years, age range=20–35 years) underwent oxygen-enhanced MRI of the lung using a closed O_2-delivery system composed by a tightly fitting face mask and a 60–L reservoir bag (equipment A: n=13, 9 men, 4 women, mean age=24.4 years, range=20–32 years), or a clinically available nontight face mask (equipment B: n=10; 6 men, 4 women, mean age=25.8 years, age range=20–35 years). The effect of 100%-oxygen inhalation was assessed using a Snapshot FLASH T1-mapping technique (TR/TE=1.5–1.6/0.56ms; matrix=128×90; acquisition time=3.3–3.7 seconds; slice thickness=15–20 mm; number of images=40). By nonlinear curve fitting, the mean T1 values of the left and right lung at room-air and 100%-oxygen ventilation were calculated ($T1_{room\ air,right}$; $T1_{oxygen,right}$; $T1_{room\ air,left}$; $T1_{oxygen,left}$). The average T1 differences ($\Delta T1=T1_{room-air} - T1_{oxygen}$) of the two volunteer groups were compared. **Results:** Mean T1 values obtained using the two equipments at room-air or oxygen ventilation were not significantly different (A vs. B at room-air ventilation: p=0.85 for the right lung, p=0.27 for the left lung; A vs. B at oxygen ventilation: p=0.55 for the left lung, p=0.29 for the right lung). With both systems, the mean T1 values decreased significantly after oxygen inhalation (p=0.03–0.0002). For both lungs, the ΔT1 obtained using the equipment type A was statistically equivalent to that obtained using the equipment type B: $\Delta T1_{A,right}$=96±19 ms vs. $\Delta T1_{B,right}$=97±34 ms (p=0.82); $\Delta T1_{A,left}$=74±47 ms vs. $\Delta T1_{B,left}$=68±63 ms (p=0.85). **Conclusion:** Gas delivery in oxygen-enhanced MRI of the lung can be performed with a clinically available standard face mask, without the need for closed sophisticated equipments.

SS 04.7

Quantitative analysis of volumetric paired thin section multi detector computed tomography scans and pulmonary function tests in patients with severe emphysema

A. Grgic[1], H. Wilkens[1], R. Kubale[2], J.M. Kuhnigk[3], G.W. Sybrecht[1], A. Buecker[1]; [1]Homburg/DE, [2]Pirmasens/DE, [3]Bremen/DE

Purpose: To investigate relationship between volumetric three-dimensional CT-data sets obtained in inspiration and expiration and pulmonary function tests. **Material and methods:** Thirty-seven patients (19-w, 18-m, mean age [±SD] 62 ± 9 years) with severe emphysema due to COPD (GOLD IV) were included in this retrospective study. All scans were performed during inspiration and expiration in every patient on same standard 16-channel-multi-detector-CT (MDCT). MDCT-data were analyzed with MeVisPULMO^{3D} software to give following parameters: lung volume (LV), emphysema index (EI), emphysema volume (EV), and core to peel distribution for whole lung, each whole lung, each lung lobe separately. Four clusters with different emphysema volumes (>2, 8, 65, 120 mm³) were calculated. These results were correlated with body mass index (BMI), forced expiratory volume in 1 second (FEV_1), inspiratory vital capacity (VCin), residual volume (RV), total lung capacity (TLC), RV/TLC and 6-minute walk. **Results:** Inspiratory LV correlated well with TLC (r=0.92, p<0.001), expiratory LV with RV (r=0.93, p<0.001), RV/TLC with inspiratory/expiratory-LV (r=0.68, p<0.001). FEV_1 correlated with change of core volume (r=-0.48, p=0.002), VCin with change of peel volume (r=0.46, p=0.003). The mean inspiratory EI of 37 ± 9 decreased by 25 ± 9 % (p<0.001) during expiration resulting in a change of EV by 930ml ± 370ml (p<0.001). On the basis of the lobar distribution of emphysema we divided patients into predominantly upper-lobe (ULD) and lower-lobe disease (LLD). LLD-patients had lower RV (p=0.01) and greater VCin (p=0.002) in comparison with ULD-patients. The change of large emphysema clusters correlated with RV/TLC (r=-0.65, p<0.001) and inspiratory/expiratory-LV (r=-0.54, p<0.001). **Conclusion:** The results obtained from analysis of MDCT-scans reflect differently functional changes. While inspiratory data sets reflect better anatomic changes, expiratory scans are closer related to the pulmonary function test results. Volumetric core to peel and cluster analysis provide better insights into the regional hyperinflation areas.

SS 04.8

Comparison of thin axial and coronal images versus maximum intensity projections sensitivity concerning the detection of pulmonary nodules on MDCT images

D.K. Filippiadis, G. Oikonomou, I. Pantou, M. Kampanarou, K. Bouhra, E. Chatzimichael, S. Tanteles, A. Pomoni, M. Pomoni, D. Kelekis; Athens/GR

Purpose: To evaluate the sensitivity of thin axial and coronal images versus thin maximum intensity projections (thin MIP) upon pulmonary nodules detection on MDCT images.**Material and methods:** The chest CT scans of 50 selected patients (asymptomatic male or female smokers 50-65 years old with a history of cigarette smoking of at least 15 years) were evaluated by two blinded radiologists (a 10 years experienced radiologist and a 5th year resident) who independently studied both MIP and standard 0.9 mm axial and coronal images. Two experienced chest radiologists studied the CT scans of the 50 patients and decided that included 275 true positive pulmonary nodules with diameter ≥1mm and ≤5mm. **Results:** In our study we evaluated detection rates and reading times of both reviewers. Concerning the 10 years experienced radiologist, detection rate was 85±5.1% for standard 0.9mm axial and coronal images and 90±4.7% for thin MIP and the reading time was 40 min. for standard 0.9mm axial and coronal images and 35 min. for MIP. For the 5th year resident, detection rate was 61±3.9% for standard 0.9mm axial images and 74±4.7% for MIP and the reading time was 48 minutes for standard 0.9mm axial and coronal images and 40 minutes for MIP. **Conclusion:** Maximum intensity projections are more or equally sensitive to standard 0.9mm axial and coronal images in the detection of pulmonary nodules and since they are not time consuming these projections should be used, when available on the study of a chest CT scan.

SS 04.9

Comparison of image quality in AP chest radiography vs. AP whole-body linear slit scanning radiography by EU quality criteria

P. Vock, Z. Szücs; Berne/CH

Purpose: To compare image quality of AP chest radiographs by computed radiography (CR) versus whole-body linear slit scanning radiography (Statscan, Lodox Co., South Africa;LS), as used for the first evaluation of trauma patients. **Material and methods:** Scanning the whole trunk in 13 seconds, LS is mostly used for a fast early skeletal and chest overview in polytrauma patients. Radiographs of twenty consecutive patients undergoing both clinically indicated LS and CR were analysed according to the European guidelines on quality criteria for diagnostic radiographic images (EUR 16260). The criteria for erect chest radiographs were adapted to the supine position, using a score based on 10 criteria (maximum = 10). Scores of LS and CR were compared. **Results:** LS overall image quality was superior to CR in 85% (17/20), identical in 10% (2/20) and inferior in 5% (1/20). The mean score was 9.5 for LS and 8.4 for CR. Above all, the retrocardiac lung (LS 0.85, CR 0.53) and the mediastinum and spine (LS 0.95, CR 0.53) were more often poorly visualized by CR. **Conclusion:** Based on our experience with a relatively small number of patients, LS applied for a full-body scan can replace AP chest radiographs (CR) in the trauma setting. Further studies on a larger population will have to prove the diagnostic accuracy of this new technique that affords whole-body scans at fraction of the radiation exposure of equivalent CR radiographs.

ABSTRACTS
EPOS™ PRESENTATIONS
(Electronic Poster)

P 01

Impact of increased noise in low dose CT for evaluation of emphysema (iLEAD Study)

J. Ley-Zaporozhan[1], S. Ley[1], D. Takenaka[2], T. Kubo[3], Y. Ohno[2], H. Hatabu[4], H.U. Kauczor[1]; [1]Heidelberg/DE, [2]Kobe/JP, [3]Kyoto/JP, [4]Boston/US

Purpose: Detailed evaluation of the lung parenchyma might be impaired by use of low dose CT. Aim of the study was to analyze the image quality of different simulated dose settings to determine an adequate dose for chest CT of pulmonary emphysema in COPD patients. **Material and methods:** Twenty patients suffering from COPD, grade GOLD III and IV, underwent standard-dose (16-row detector, 120kV, 150mAs, 0.5s gantry rotation time, helical pitch 1.44) 3D-HRCT (1mm collimation). Original raw-data were used for simulation of ten different mAs settings from 10 to 100mAs in 10mAs increments. Randomized CT-images (high-resolution kernel, lung window, 1mm thickness) were analyzed on a PACS workstation by two blinded chest radiologists independently. Image quality was evaluated on a lobar level and additionally for lung apex and paravertebral regions above/below carina using a 5-point-score (1: non-diagnostic / 5: excellent). **Results:** For the lung the standard setting was rated 4.7±0.5 by reader-I and 4.1±0.8 by reader-II. Significant differences were found for upper lobes with ≤60mAs, left lower and middle lobes ≤40mAs and right lower lobe ≤50mAs by reader-I; ≤50mAs for all lobes by reader-II. For the apex the standard setting was rated 3.8 and 3.3, paravertebral regions above carina 4.6 and 3.8, below carina 4.6 and 4, by reader-I and II respectively. Significant differences were found with ≤90mAs and ≤60mAs for apex, ≤60mAs and ≤50mAs for paravertebral regions above/below carina by reader-I and II respectively. **Conclusion:** For the evaluation of pulmonary emphysema the dose can be lowered down to 60mAs (=41.7mAseff) without impairment of image quality due to increased noise. The apex is most severely affected by noise and might also benefit from denoising filters.

P 02

Various causes of tracheobronchial polypoid lesions: CT-bronchoscopic and radiologic-pathologic correlations

K. Lee, K. Kim, C.H. Sohn, D.K. Yang, S.G. Lee, P.J. Choi, M.S. Noh; Busan/KR

Learning objectives: To illustrate our experience with chest MDCT in the diagnosis of tracheobronchial polypoid lesions and to correlate CT and bronchoscopic findings with pathologic findings.**Background:** Endobronchial or endotracheal lesions are detected and diagnosed not only with bronchoscope but also with MDCT, because good quality of images are provided with advanced CT. The cause of endotracheobronchial lesions are various and some are characterisitc in CT findings which sometimes reveal their own typical histopathologic components.The comparison of CT findings to bronchoscopic and their correlation with patholigc findings in various endotracheal or endobronchial lesions are attributable to understand the different features of intraluminal polypoid lesions. **Imaging findings OR Procedure details:** MDCT scans in patients with endotracheobronchial polypoid lesions were correlated with fiberoptic bronchoscopic and pathologic findings; hamartoma, infection such as tuberculosis, aspergillosis in benign lesions, and adenoid cystic carcinoma, epidermoid carcinoma, carcinoid, paraganglioma, and extrathoracic metastases in malignant lesions. We also assessed about the various CT features including air-trapping or obstructive pneumonia with mucobronchograms. **Conclusion:** MDCT of tracheobronchial polypoid lesions showed good correlation with bronchoscopic and pathologic findings. There are the different features of tracheobronchial polypoid lesions of differential etiologies.

P 03

Pulmonary emphysema in patients with chronic anorexia nervosa: preliminary findings

N. Sverzellati[1], M. Pescarolo[1], W. Recheis[2], A. Ruiu[2], M. Amore[1], A. Chetta[1], M. Zompatori[1]; [1]Parma/IT, [2]Innsbruck/AT

Purpose: To re-examine the hypothesis that long-term anorexia nervosa results in emphysematous changes in the lung. **Material and methods:** Twelve women with chronic anorexia nervosa and three control subjects were prospectively evaluated. The institutional review board approved this protocol. Written informed consent was obtained from all subjects. All subjects were never-smokers. Three sets of 10 slices each were obtained from three regions of the lung respectively (at the level of the aortic arch, the carina and lung bases) using low-dose thin-section multi-detector CT (MDCT) scans. MDCT scans were evaluated both by visual score and by two automated analysis tools: a pure density-masking approach based program (Pulmo software, Siemens Medical Systems) and a “fractal dimensions”-based lung image analysis software (Pulmonary Analysis Software Suite, Iowa). Group means were calculated and Student’s t-tests were performed to determine significance. **Results:** Visual score did not detect any trace of emphysema in anorexic women although the presence of a subtle mosaic attenuation pattern was reported by the observers; in addition two anorexic women exhibited one pneumomediastinum and a few apical parenchymal bullae, respectively. Software packages reported in anorexic women a mean percentage of low attenuation areas below -950 HU of 15.44% +/-7.37% (mean +/- SD). Both softwares demonstrated that emphysema measurements (emphysema index, mean lung density) were greater in the group that was anorexic than in the control subjects ($p<0.001$). **Conclusion:** These data further demonstrate that emphysema-like changes are present in the lungs of women who are chronically malnourished.

P 04

Quantitative assessment of airway dimension for pulmonary disease: development of dedicated software for multi-detector CT

Y.H. Kim, S. Choi, H.J. Sun, J.K. Kim, J.G. Park, H.K. Kang; Kwangju/KR

Purpose: To design and prospectively validate the accuracy and reproducibility of dedicated software tool measuring airway dimensions on multi-detector row CT (MDCT) images in an in-vitro and animal model. **Material and methods:** With Delphi 7.0 software, we programmed a new dedicated software, AADM (Automated Airway Dimension Morphometry), for measuring of airway dimensions on MDCT images. AADM was validated in MDCT data set obtained with three silicon tubes and five rabbits. First, CT scans were performed in three silicon tubes with different diameters. CT data were analyzed on AADM for measuring tube dimensions such as wall area(WA), total area (TA) and percent wall area(WA/TA or %WA), and compared with actual dimensions measured with vernier calipers. Secondly, scanned CT data of five rabbits were analyzed on AADM for measuring airway dimensions (WA,TA, WA/TA or %WA). Immediately after CT scanning, all lungs including trachea were removed from freshly sacrificed rabbits and cut into 5mm-thickness transverse slices, in planes similar to those which were used in software, and their airway dimensions were evaluated with graphic analysis software. Airway dimensions obtained with AADM were compared with those obtained with excised lung samples by means of the Wilcoxon sign rank test. For analysis of airway dimensions on AADM, inner lumen of airway is segmented by "full-width-at-half-maximum" technique and outer lumen by "mirror-image Gaussian fit, MIGF" method. **Results:** Tube dimensions obtained with AADM were minimally overestimated, but not significantly different from actual dimensions measured ($p > 0.05$). Airway dimensions of rabbits obtained with AADM were also overestimated and there were statistically significant differences ($p < 0.01$). However, reproducibility of AADM was demonstrated by showing the regular pattern of airway dimensions. **Conclusion:** AADM to measure airway dimensions is able to perform segmentation of airway automatically and is accurate and reproducible tool to measure the CT dataset.

P 05

Comparison of pulmonary CT findings and serum KL-6 level in patients with cryptogenic organizing pneumonia

K. Honda, Y. Ando, F. Okada, H. Mori; Yufu/JP

Purpose: To retrospectively compare high-resolution CT findings between cryptogenic organizing pneumonia (COP) patients with normal and elevated serum KL-6 levels. **Material and methods:** Chest CT scans performed between April 1999 and April 2007 for 20 COP patients with a normal KL-6 level and 17 COP patients with an elevated KL-6 level were retrospectively evaluated by 2 chest radiologists. **Results:** The CT findings in the COP patients with a normal or an elevated KL-6 level mainly consisted of consolidation (n = 17 and 13, respectively), followed by ground-glass opacity (n = 11 and 13, respectively). Traction bronchiectasis and architectural distortion were significantly more frequent in patients with an elevated KL-6 level than those with a normal one (n = 7 and 1; 13 and 3, respectively) ($P = 0.0077$; $P = 0.00017$, respectively). In follow-up CT scans, a relapse within 1 year after initial treatment with steroids, performed in 16 patients with a normal KL-6 level and 16 with an elevated KL-6 level, occurred in 2 with a normal KL-6 level (12.5%) and 6 with an elevated KL-6 level (37.5%). The frequency of relapse in patients with an elevated KL-6 level was higher than in those with a normal KL-6 level; however, no significant difference between the 2 groups was observed ($p=0.103$). **Conclusion:** In COP patients, CT findings of traction bronchiectasis and architectural distortion are associated with increased serum KL-6 levels, which might be related to a relapse after treatment.

P 06

Uncommon occupational lung diseases: high-resolution computed tomography findings

L. Flors, M.L. Domingo, G. Figueres Muñoz, C. Leiva-Salinas, E. López-Pérez, R. Medina, J. Vilar; Valencia/ES

Learning objectives: To present the high-resolution CT findings of patients with uncommon occupational lung diseases. **Background:** Occupational lung diseases comprise a broad variety of disorders caused by the inhalation of dust particles or other noxious chemicals. High-resolution CT plays an increasing role in their radiologic evaluation. The CT features of silicosis, asbestosis and coal worker pneumoconiosis have been widely described. We present several cases of unusual occupational lung diseases and their high-resolution CT findings. **Imaging findings OR Procedure details:** The diseases studied were: siderosis (characterized by the presence of small ill-defined centrilobular nodules and patchy areas of ground-glass attenuation), silicosiderosis (with upper lobes masses and conglomerates), talcosis (small centrilobular nodules and heterogenous upper lobes conglomerate masses with internal foci of high attenuation), berylliosis (upper lobes nodules and conglomerate masses with intralobular septal thickening), calcicosis (small diffuse nodules, some calcified and subpleural compounding “pseudoplaques”), acute hypersensitivity pneumonitis (HP) due to wheat flour or miller´s lung (diffuse airspace consolidation and ground-glass opacities), subacute and chronic HP induced by isocyanates (small centrilobular nodules and fibrotic upper lobes changes respectively) and Ardystil syndrome due to Acramin-FWN (with features of chronic organizative pneumonia). **Conclusion:** In some occupational lung diseases certain diagnosis cannot be made on the basis of imaging features alone. Nevertheless characteristic described high-resolution CT findings together with clinical features and related occupational history can improve diagnostic accuracy.

P 07

Cystic lung disease in Birt-Hogg-Dubè syndrome

N. Sverzellati[1], S. Tommasetti[2], A. Carloni[3], S. Piciucchi[2], M. Chilosi[4], M. Zompatori[1], V. Poletti[2]; [1]Parma/IT, [2]Forlì/IT, [3]Terni/IT, [4]Verona/IT

Learning objectives: To describe the pulmonary thin-section CT features occurring in patients with Birt-Hogg-Dubè (BHD) syndrome to familiarize radiologists with this uncommon entity. **Background:** BHD syndrome is a rare clinicopathologic condition transmitted in an autosomal dominant fashion. This complex entity is characterized by cutaneous fibrofolliculomas, kidney tumors, pulmonary cysts, and spontaneous pneumothorax. **Imaging findings OR Procedure details:** We illustrate the thin-section CT features of eight patients who fulfill the diagnostic criteria for BHD syndrome. Correlations of radiologic, genetic, clinical and histopathologic aspects are also discussed. **Conclusion:** In BHD syndrome, cysts are round to oval in shape, ranged widely in size, and are randomly distributed throughout the lungs, except for a predilection to involve the lung bases more extensively. Radiologists, as well clinicians, must be able to recognize this syndrome and be aware of its associated findings and potential complications.

P 08

Study for prognostic indicators in patients with usual interstitial pneumonia and nonspecific interstitial pneumonia: correlation of imaging findings with cellular patterns in bronchoalveolar lavage fluid

J.S. Park[1], S.H. Paik[1], J. Hwang[2], D.H. Kim[1], D.L. Choi[2]; [1]Bucheon/KR, [2]Seoul/KR

Purpose: To evaluate prognostic indicators in patients with UIP and NSIP. To correlate HRCT findings with bronchoalveolar lavage fluid (BALF) patterns.**Material and methods:** We enrolled 27 patients with biopsy-proven UIP (n=17) and NSIP (n=10). BALF at initial diagnosis was classified into three patterns. The mean interval of HRCT follow-up was 3.3 years. HRCT scans were evaluated for the presence and extent of abnormalities such as ground glass attenuation (GGA), air-space consolidation, reticulation and honeycombing. We correlated HRCT findings with BALF patterns at initial and follow-up. **Results:** In UIP, BALF revealed COP pattern in 10 and UIP pattern in 7. Progression of reticulation (p=0.05) and honeycombing (p=0.01) was noted on follow-up in UIP patients with COP pattern while there was no significant change in patients with UIP pattern. In NSIP, COP pattern was noted in 6 and sarcoidosis pattern in 4. NSIP patients with COP pattern showed decreased air-space consolidation (p=0.04) and the patients with sarcoidosis pattern showed decreased extent of GGA (p=0.06). **Conclusion:** UIP patients with COP pattern showed progression of pulmonary fibrosis while no change was noted in patients with UIP pattern. NSIP patients showed decreased air-space consolidation and GGA on follow-up.

P 09

Pulmonary sarcoidosis – a chameleon among interstitial lung diseases

A. Grgic[1], R. Bohle[1], R. Kubale[2], H. Wilkens[1], A. Buecker[1]; [1]Homburg/DE, [2]Pirmasens/DE

Learning objectives: 1. To learn the typical and atypical radiographic appearances of pulmonary sarcoidosis.
2. To form a concise differential diagnosis for each typical and atypical radiographic appearance of pulmonary sarcoisosis. **Background:** The radiographic findings of pulmonary sarcoidosis are variable and can mimic a myriad of other lung diseases. A definitive diagnosis of sarcoidosis is made via biopsy, however, a combination of clinical, laboratory and radiographic findings can help to establish the diagnosis. **Imaging findings OR Procedure details:** Between 2005 and 2007 170 patients were identified with the diagnosis of sarcoidosis. In these patients several typical and atypical patterns of pulmonary sarcoidosis have been described like hilar adenopathy, perilymphatic distributed nodules, sarcoid galaxy sign, reticular opacities and fibrosis, ground glass opacities and multifocal consolidations. Each pattern has a different differential diagnosis. In this presentation we use plain film radiographs, high resolution CT images and slides of histologic specimens to address the multiple radiologic presentations of pulmonary sarcoidosis and review the differential diagnosis. **Conclusion:** Recongnition of radiological appearance of sarcoidosis enables appropriate diagnosis of this disease. Familiarity with differential diagnoses improve probability to establish a correct diagnosis based on imaging.

P 10

Quantitative computed tomography in the interstitial lung diseases: correlation with bronchoalveolar lavage flow cytometry

J. Moczova[1], V. Belan[1], J. Plutinsky[2]; [1]Bratislava/SK, [2]Nitra/SK

Purpose: Interstitial lung disease is a feared complication of sarcoidosis (SA), extrinsic allergic alveolitis (EAA) and collagen diseases (CD). Comparison of results of the quantitative HRCT (QCT) with those from the bronchoalveolar lavage flow cytometry (BAL/FC) in the interstitial lung diseases.**Material and methods:** A set of 113 patients with clinically suspected ILD of sarcoidosis, extrinsic allergic alveolitis and collagen diseases. Correlating results of QCT (mean lung density and automatic quantitative histogram analysis) derived from the HRCT scans and PULMO CT evaluation package (Siemens, Medical Systems) with BAL/FC. **Results:** A good linear correlation between QCT for C and D indices and BAL lymfocytosis CD4/CD8: r = 0,71 (SA), r = 0,72 (EAA), r = 0,43 (CD) for C index, and r = 0,53 (SA), r = 0,43 (EAA), r = 0,57 (CD) for D index. **Conclusion:** HRCT with QCT offers an accurate and save method of assessment of lung activity in patients with the interstitial lung diseases with impaired bronchoalveolar lavage flow cytometry. It is the best imaging modality for diagnosis and staging of alveolitis and fibrosis, and follow–up in the interstitial lung diseases.

P 11

HRCT imaging of the lung in rheumatology patients: spectrum of findings and grading according to severity

A. Kazantzi, P. Zambakis, P. Korfiatis, D. Daoussis, S. Liossis, T. Petsas, C. Kalogeropoulou; Patras/GR

Purpose: Interstitial lung disease affects a significant portion of patients with rheumatologic diseases. Although a direct correlation of early alveolar inflammation and progression to fibrosis has not been definitely established. The recognition of patterns and the extent of the disease is a useful prognostic factor as to the progression of the disease.The purpose of this study was to classify patients with rheumatologic diseases according to pulmonary HRCT findings and severity of disease. **Material and methods:** We examined 44 patients addressed from the Rheumatology Department: 21 pts with scleroderma, 11 pts with Rheumatoid Arthritis, 5 pts with Mixted Connective tissue disease, 4 pts with SLE.3 pts were not yet diagnosed. All patients underwent HRCT using a 16 multidetector GE CT Scan with slice thickness 0,625 mm and imaging findings were interpreted separately by two experienced radiologists. Severity of disease was graded according to semiquantitative Warrick scale (severity and extent of disease). **Results:** Imaging pulmonary findings involved at 18.8% ground glass pattern, at 9% reticular pattern, at 4.5% honeycomb pattern, at 25% reticular and ground glass pattern, at 9 % reticular and honeycomb, at 15.8 % other imaging findings (pleural effusion, atelectasis, consolidation, mosaic perfusion pattern). 11.3% of pts had no imaging findings at all. At 27%, patients had diameter of pulmonary artery over 2,5 cm (depicting pulmonary hypertension in these patients). **Conclusion:** Imaging findings in rheumatic lung varies from minor to major lesions. In scleroderma patients, pulmonary implication is severe, compared to other rheumatic diseases, as expressed by the results of grading according to Warrick scale. We present the spectra of imaging patterns in our group of study, as well as a review of the literature.

P 12

Lung cysts in non-smokers with neurofibromatosis: CT findings

A. Oikonomou, G. Daskalogiannakis, P. Prassopoulos; Alexandroupolis/GR

Purpose: To describe the chest CT findings in neurofibromatosis type I. **Material and methods:** One woman (case I: 64 year old) and two men (case II: 56 and case III: 22 year old) with history of neurofibromatosis type I, underwent CT / HRCT of the chest with indications not related to neurofibromatosis type I (spontaneous rupture of subclavian artery, trauma, atypical pneumonia). None of them was ever smoker. **Results:** The patients presented few (5-20), small (< 1,5 cm) lung cysts with extremely thin definable wall, which were both central and subpleural and had lower lung zone predominance in two cases and no zone predominance in one. There was no evidence of lung fibrosis, subpleural reticular pattern or honeycombing in the lung bases. Lower-lobe consolidation in case I was attributed to concomittant pneumonia. Lung cysts were attributed to neurofibromatosis associated lung disease. The other entities in the diferential diagnosis of cystic lung disease were excluded: emphysema and Langerhan's cell histiocytosis because of no history of smoking, lymphangiomyomatosis because of extreme age and lymphocytic interstitial pneumonia because of absence of history of immunodeficiency or Sjogren's disease. **Conclusion:** Lung disease in neurofibromatosis may manifest on CT as a minimal cystic pattern characterized by a small number of small thin-walled cysts not representing emphysema and not accompanied by radiologic evidence of lung fibrosis, honeycombing or bullous disease.

P 13

Metastatic pulmonary calcifications in hyperparathyroidism: report of two cases

S. Piciucchi[1], V. Poletti[2], N. Sverzellati[3], S. Ascani[4], G. Gavelli[5], A. Carloni[4]; [1]Meldola-forlì/IT, [2]Forlì/IT, [3]Parma/IT, [4]Terni/IT, [5]Bologna/IT

Purpose: Metastatic pulmonary calcification is the deposition of calcium in normal pulmonary parenchyma. Predisposing factors include chronic renal failure, hypercalcemia, and increased tissue alkalinity. Purpose of our repotr is to show pulmonary manifestations in hyperparathyroidism. **Material and methods:** The most common radiological manifestations od hyperparathyroisdism consists of poorly defined nodular opacities. These opacities reflect the deposition of calcium salts in the pulmonary interstitium. We describe two cases of secondary pulmonary metastatisc calcifications. **Results:** Case 1. A 53 years-old-man, factory-worker, mild smoker, with history of renal stones, diffuse arthralgias, hyperparathyroidism. He underwent chest X ray because of a recent cough and dyspnea. Chest X ray and HRCT were performed to evaluate his clinical presentation. HRCT showed bilateral scattered ground glass opacities in upper lobes, middle lobe and lingula, calcified lymph nodes and multiple calcified nodules. Case 2. A 55 years old-man, with chronic renal failure, history of renal transplantation rejection in 1998. In November 2007, he developed a rapid-onset head-ache, dizziness, he became lethargic. CT showed a red infarction. In the clinical examination the patient presented icterus and dyspnea. Laboratory exams showed a severe direct and indirect bilirubin values increase. Hepatic ultrasound didn't identify any pathological change of biliary ducts. HRCT showed spread pulmonary, tracheal, carotid and aortic calcifications. A vertebral fracture was observed, as well. The next days, patient died because of liquoral infection. In the autopsy specimens amyloidosis research resulted negative. **Conclusion:** The final diagnosis was in both cases: secondary metastatic pulmonary calcifications, in hyperparathiroidism. Radiological manifestations are diffuse calcifications and dense bilateral consolidations that may improve spontaneously. It may rarely present in patients with no apparent underlying disease or biochemical abnormality.

P 14

Assessment of pneumonia severity: multi-detector row CT in comparison to clinical score CRB-65

S. Pauls[1], S. Krüger[2], R. Muche[1], D. Klemen[1], C. Billich[1], S.A. Schmidt[1], V. Hombach[1], H. Brambs[1]; [1]Ulm/DE, [2]Aachen/DE

Purpose: Evaluation of the influence of diverse morphologic patterns of pulmonary infiltrates diagnosed with multi-detector row CT (MDCT) on severity of pneumonia. **Material and methods:** The retrospective study involved 92 patients with clinical diagnosed pneumonia and detectable infiltrates on chest MDCT. The extension and pattern of infiltrates as well as emphysema and pleural / cardiac effusion were documented. Differences in the frequency of these parameters were calculated for patients with mild pneumonia (CRB-65 0 and 1; group 1, n=80) as well as for patients with severe pneumonia (CRB-65 2,3, and 4; group 2, n=12) using the exact fisher-test, following explorative analyses using clinical interesting subgroup analysis as well as logistic regression including backward selection and ROC-analysis identifying the most influential factors on severity. **Results:** The frequency of singular morphologic changes did not differ significantly between the two patient groups. The combination of patchy infiltrates attended with a positive bronchogramm and the presence of atelectasis was associated with a significant higher severity score (p=0.002). Also the combination of patchy, multisegmental infiltrates and the presence of an atelectasis was associated with a higher CRB-65 (p=0.045). The most influential factors found by the regression analysis were empyema (p=0.055) and pleural effusion (p=0.111), giving a sensitivity of 75% and a specificity of 58% for prediction of CRB-65. All other factors had a p-value above 0.2. **Conclusion:** The presence of empyema and pleural effusion as well as an atelectasis in combination of patchy infiltrates and a positive bronchogramm / multisegmental infiltrates seems to have an influence on severity of pneumonia

P 15

Comparison of HRCT findings in mycobacterium avium and mycobacterium intracellulare

Y. Ando[1], F. Okada[2], H. Mori[2], K. Sugisaki[1], S. Takikawa[1], Y. Zaizen[1] , H. Kawano[1], K. Tenda[1], T. Otsu[1]; [1]Beppu/JP, [2]Yufu/JP

Purpose: To retrospectively evaluate and compare pulmonary high-resolution CT (HRCT) findings in patients with Mycobacterium intracellulare and Mycobacterium avium. **Material and methods:** We retrospectively reviewed and compared HRCT scans obtained between March 2004 and January 2008 of 77 patients (24 men, 53 women; aged, 29-93 years; mean, 76) with Mycobacterium intracellulare and of 59 patients (11 men, 48 women; aged, 22-94 years; mean, 70) with Mycobacterium avium. Patients with a concurrent infectious disease were not included in the study. Parenchymal abnormalities (centrilobular nodule, nodule, cavitary nodule, consolidation, ground-glass attenuation, bronchiectasis, and bronchial wall thickening) were evaluated, along with enlarged lymph nodes and pleural effusion. The distribution of parenchymal diseases was also evaluated. **Results:** In patents with Mycobacterium intracellulare or Mycobacterium avium, centrilobular nodules (96.1%, 91.5%, respectively) were observed most frequently, followed by bronchial wall thickening (96.1%, 89.8%), bronchiectasis (92.2%, 84.7%), nodules (83.1%, 74.6%), ground-glass attenuation (62.2%, 57.6%), and cavitary nodules (68.8%, 27.1%). In patients with Mycobacterium intracellulare, cavitary nodules were observed significantly more frequently than in patients with Mycobacterium avium (p<0.00001). In patients with Mycobacterium intracellulare, abnormal findings were mainly observed in the right segment 4 (S4) (86%), right S5 (82%), and right S2 (75%). On the other hand, in patients with Mycobacterium avium, the findings were mainly observed in right S2 (85.7%), right S5 (75%), and left S4 (73%). There were no significant differences in terms of the distributions of the abnormal findings. However, cavitary nodules in Mycobacterium intracellulare patients were significantly more common in S1 (36%), S2 (34%), and S6 (25%) of the right lung than in Mycobacterium avium patients. **Conclusion:** HRCT findings in patients with Mycobacterium intracellulare and Mycobacterium avium consisted mainly of centrilobular nodules and bronchial wall thickening. Cavitary nodules were significantly more common in Mycobacterium intracellulare than Mycobacterium avium patients.

P 16

Clinical and pulmonary HRCT findings in acute klebsiella pneumoniae pneumonia

F. Okada, Y. Ando, K. Honda, T. Nakayama, S. Tanoue, H. Mori; Yufu/JP

Purpose: To describe the patterns and frequency of pulmonary high-resolution CT (HRCT) findings in patients with acute Klebsiella pneumoniae pneumonia **Material and methods:** Chest HRCT scans obtained between January 1991 and December 2007 of 413 patients with acute Klebsiella pneumoniae pneumonia were retrospectively evaluated by two chest radiologists. Among the patients, 140 cases with Methicillin-resistant staphylococcus aureus (MRSA), 105 with Pseudomonas aeruginosa, 89 with Candida albicans, 65 with Enterobacter cloacae, 55 with Stenotrophomonas maltophilia, and 34 with Serratia marcescens were diagnosed with concurrent infectious diseases, and so were excluded. Thus, the study group we reviewed comprised 61 patients (44 men; 17 women; age range, 18-97 years; mean, 61.5). Underlying diseases were mainly postoperative status for malignant disease (n=19), pulmonary emphysema (n=16), diabetes mellitus (n=8), or collagen disease (n=5). Patients who were alcoholic or chronic smokers numbered 40 and 31, respectively. Parenchymal abnormalities (ground-glass attenuation, consolidation, centrilobular nodules, crazy-paving appearance, bronchial wall thickening, interlobular septal thickening, and bronchiectasis) were evaluated along with enlarged lymph nodes and pleural effusion. **Results:** Abnormal findings were seen on the HRCT scans of all patients; ground-glass attenuation (n=61), consolidation (n=56), crazy-paving appearance (n=33), bronchial wall thickening (n=19), interlobular septal thickening (n=5), centrilobular nodules (n=4), and bronchiectasis (n=4). Cavitary consolidation was seen just one case. These abnormalities were predominantly seen in the peripheral lung parenchyma (n=59) and the lower zone (n=46). Pleural effusions were found in 31 patients (unilateral effusions; 20, bilateral; 11). Mediastinal and/or hilar lymph node enlargement was observed in 3 patients. **Conclusion:** HRCT findings in patients with acute Klebsiella pneumoniae pneumonia consisted mainly of ground-glass attenuation, consolidation, and crazy-paving appearance, and were found in the peripheral and lower lung. In patients with underlying diseases, these HRCT findings can be considered as suggestive of acute Klebsiella pneumoniae pneumonia.

P 17

Miliary tuberculosis: comparison of CT findings in HIV-seropositive and HIV-seronegative patients

Y.J. Jeong, K. Kim, J.Y. Kim, S.H. Lee; Busan/KR

Purpose: To determine the differences in the CT appearance of miliary tuberculosis between patients with and without HIV infection. **Material and methods:** CT scans of 14 HIV-seropositive and 13 HIV-seronegative patients with miliary tuberculosis were reviewed. CD4 T-lymphocytes counts, measured in 14 seropositive patients, were at least 200 cells per microliter in one patient and were less than 200 cells per microliter in 13. **Results:** All of HIV-seropositive and HIV-seronegative patients had small nodules randomly distributed throughout both lungs on CT. The seropositive patients had a lower prevalence of cavitation (p=0.014) and large nodule (p=0.018) on CT. HIV-seropositive patients had a higher prevalence of interlobular septal thickening (p=0.036) on CT. **Conclusion:** HIV-seropositive patients had a lower prevalence of typical parenchymal changes of postprimary tuberculosis and a higher prevalence of disseminated changes throughout the interstitium on CT.

P 18 Withdrawn by authors

P 19

Chest CT findings of pulmonary actinomycosis

J.S. Kim, C.Y. Han; Seoul/KR

Purpose: To evaluate the CT findings of intrathoracic pulmonary actinomycosis in 5 patients **Material and methods:** We included 5 patients (2 men, 3 women, 44-78 years) proven pulmonary actinomycosis. All patients underwent enhanced chest CT scan and bronchofiberscopy. Histologic conformations were done with bronchoscopic biopsy in 3 patients and sonoguided transthoracic needle biopsy in 2. The CT findings were retrospectively reviewed by 2- radiologists with consensus. **Results:** Endobronchial actinomycosis were confirmed in 3 patients by bronchoscopic biopsy. Those patients all associated with calcified endobronchial calcified broncholiths, distal bronchiectasis and peribronchial consolidation in chest CT finding. One patient (52years old woman) demonstrated relatively well enhancing contour bulging consolidation in right middle lobe without bronchial obstruction. Sonoguided needle biopsy were proven lung parenchymal actinomycosis presenting sulfur granules. Optimal antibiotic therapy was done during 6months and slowly regressed. Another 81year old woman having moderately enhancing mass in right lower lobe on CT scan turned out to be lung cancer and coexisting actinomyces by sonoguided needle biopsy. She refused any treatment and lost follow up. **Conclusion:** Pulmonary actinomycosis can be manifested either endobronchial or parenchymal lesion. In cases of endobronchial actinomycosis, broncholiths or bronchiectasis are commonly associated. However parenchymal actinomycosis without bronchial obstruction would be difficult to differentiate with lung cancer in CT findings. Transthoracic needle aspiration and biopsy will be mandatory for diagnosis and optimal treatment in pulmonary parenchymal actinomycosis.

P 20

Chronic granulomatous disease. A rare case report involving the lungs.

I. Tsangaridou, A. Bouga, E. Sotiropoulou, P. Tsagouli, M. Seferos, F. Laspas, V. Sotiropoulou, L. Thanos; Athens/GR

Purpose: To report a case of a chronic granulomatous disease (GCD), an X-linked inherited disorder of phagocytic cells, which is a very rare entity (incidence 1 case in 220,000- 500,000 population). The underlying pathopysiologiacal mechanism is characterized by inability of phagocytes to produce bactericidal superoxide anions. **Material and methods:** A male patient, aged 22 years with a history of GCD with multisystemic involvement, presented with clinical findings suggestive of widespread pneumonia. CT scan images were suggestive of semi-necrotic form of Aspergillus f infection. The patient underwent a lung biopsy. **Results:** Lung biopsy revealed necrotic granulomas with vasculitis and BAL sample was positive for Aspergillus f. The patient had good response to intravenous antimicrobial therapy. **Conclusion:** In patients with early onset of GCD the systemic antimicrobial prophilaxis as well as early and aggressive treatment of infections is imperative, in order to avoid life threatening complications. In our case CT scan was valuable in early diagnosis and management of pulmonary infection by Aspergillus.

P 21

Successfully treated pulmonary mucormycosis in a diabetic renal transplant recipient

Z.M. Lénárd, A. Németh, E. Hartmann, Z. Gerlei, K. Földes, A. Doros; Budapest/HU

Purpose: Mucormycosis are seen with an increasing incidence in immunocompromised patients, and still has a 25-80% mortality rate even with aggressive surgical intervention. Most common presentations are rhinocerebral and pulmonary. **Material and methods:** This report describes the occurrence of a successfully treated renal tansplant recipient who had pulmonary mucormycosis following the development of post-transplant diabetes mellitus. **Results:** A 68-year old renal transplant recipient entered the emergency department with epigastrial pain. He had been diagnosed to have end-stage renal disease due to chronic glomerulonephritis ten years earlier, and he had recieved a cadaver renal transplant nine years earlier. Abdominal ultrasound did not show clinically positive finding, however, his routine chest x-ray showed right upper lobe consolidation with cavitation. We performed chest HRCT, which showed a cavitated right upper lobe mass without halo and air-crescent sign. Associated HRCT findings included mediastinal adenopathy and bilateral pleural effusion with right side-dominance. In the following days his signs and symptoms deteriorated including fever, cough and chest pain, but he had no hemoptysis. Diagnosis of Mucormycosis was established by microbiological culture of ultrasound-guided transthoracic biopsy. With this finding he was started on Amphotericin B, and his fever and complains were ceased quickly. At one-month control HRCT the cavitation became larger, pleural effusion decreased to minimal, but lymphadenopathy was found to be unchanged. At two-month control HRCT the pulmonary cavitated mass decreased in size by around 20%, pleural effusion was not seen and lymphadenopathy was unchanged. He was emissed to his home in a generally good condition.**Conclusion:** Optimal therapy begins with an early diagnosis and, and if mucormycosis is identified at early stage, aggressive treatment with Amphotericin B may help in increasing the survival rate in an otherwise fatal disease.

P 22

The cisterna chyli - evaluation of prevalence, characteristics and predisposing factors

S. Feuerlein, G. Kreuzer, H. Brambs, S. Pauls; Ulm/DE

Purpose: Apart from enlarged lymph nodes as a potential indicator for malignancy or infection the lymphatic system does not receive a lot of attention in cross sectional imaging. The prevalence of a cisterna chyli (CC) varies widely. The largest existing CT study reported only 7 cases of a CC. In addition no attempts have been made to link the presence or absence of a CC to clinical patient data. Consequently the subject of this study was to determine the prevalence and characteristics of the CC in a large patient cohort and to identify potential predisposing factors for the development of a CC. **Material and methods:** One thousand consecutive contrast-enhanced CT examinations of the chest and/or abdomen were included in this retrospective study. The following morphologic and clinical parameters were documented: size, location and CT attenuation of the cisterna chyli, presence or absence of malignancy including location and type of tumor, presence or absence of metastasis to the lung, liver, bones or lymph nodes. **Results:** A CC was found in 155 of 1000 patients (15.5%). There was a slight male predominance (17% vs. 13%). The average axial diameter was 7.4 x 6.4 mm with a length of 14 mm. The average density was 6.1 HU (range -21-32 HU). The most common location was on the TH12 level (63%). The prevalence of a CC in patients with malignancy was higher than in patients without malignant disease (18.3% vs. 10.3%) with a particularly high prevalence in the groups with hepatocellular carcinoma (57%), pancreatic carcinoma (35%) and melanoma (25%). The presence or absence of metastasis had no influence on the CC. **Conclusion:** The prevalence of a cisterna chyli in this large cohort is 15.5%. Malignant disease, especially hepatocellular and pancreatic carcinoma as well as melanoma could be identified as predisposing factors in subgroup analysis.

P 23

Multidetector CT angiography of aberrant subclavian arteries

A. Türkvatan, F.G. Büyükbayraktar, T. Cumhur, T. Ölçer; Ankara/TR

Purpose: To purpose of this study was to evaluate the utility of 16-slice multidetector computed tomographic (MDCT) angiography for identifying anatomic features of aberrant subclavian arteries. **Material and methods:** Seventeen patients with aberrant subclavian arteries were assessed by MDCT angiography. Aortic arch position, the presence of a Kommerell's diverticulum, aneurysm, vascular compression of trachea and oesophagus and associated cardiovascular abnormalities were evaluated. MDCT findings were confirmed by surgery in eight patients but in other nine patients no further evaluation or management was necessitated due to without significant clinical consequence of an aberrant subclavian artery. **Results:** Eleven patients had an aberrant right subclavian artery arising from left aortic arch and six patients had an aberrant left subclavian artery arising from right aortic arch. Kommerell's diverticulum was identified in three patients with aberrant right subclavian artery, and four patients with aberrant left subclavian artery. In four patients it was aneurysmatic. Oesophageal compression was detected in eight patients, and tracheal compression was identified only one pediatric patients. Aberrant subclavian arteries are associated with complex congenital heart disease in one patient, intracardiac defects in two patients, aortic coarctation in two patients, patent ductus arteriosus in two patients and aberrant vertebral artery in one patient. **Conclusion:** MDCT angiography is an excellent noninvasive alternative imaging modality to conventional angiography for the evaluation of thoracic vascular anomalies because it is able to exhibit the detailed anatomy of the vascular structures and their spatial relationships with adjacent organs within the same study.

P 24

Sirolimus lung toxicity

E. López-Pérez, M.L. Domingo, C. Barber Hueso, L. Flors, C. Leiva-Salinas, G.F. Muñoz, J. Vilar; Valencia/ES

Purpose: Sirolimus (or rapamycin) is a immunosupresive agent used in renal transplantation receptors. Laboratory disorders are common and well known side-effects. A rare and severe lung toxicity due to sirolimus has been described. The aim of our study was to describe the imaging findings of sirolimus pulmonary toxicity in kidney transplantation.**Material and methods:** We retrospectively reviewed 6 cases of sirolimus associated lung toxicity among kidney transplant recipients from March 2000 to December 2007. The diagnosis of pulmonary toxicity was established by: the onset of pulmonary symptoms after the exposure to sirolimus, exclusion of infection, alternative disease or other drug toxicity, resolution of symptoms after sirolimus interruption or dose reduction. The radiological findings of chest radiograph and computed tomography (CT) were recorded. Clinical symptoms and data related to sirolimus administration were also reviewed. **Results:** Five of the 6 patients were females. The median age was 58 (range 46-62). At presentation, the most frequent symptoms were: dyspnea, cough, fever and anemia. Radiological findings include: focal or multifocal parenchymal consolidations (n=4), perihiliar interstitial thickening (n=3) and pleural effusion (n=2) on chest radiographs. CT findings were: multifocal parenchymal consolidations or opacities (n=6) associated to interlobular septal thickening, (n=2), linear or bandlike opacities (n=1) and ground-glass opacities (n= 3) and pleural and pericardial effusion (n=2). Predominant distribution was subpleural and in the lower lobes. The lung abnormalities were persistent but changed in their location and appearance. **Conclusion:** Sirolimus pulmonary toxicity is frequently misdiagnosed as an infection. However, radiologists should suggest sirolimus toxicity when persistent lung abnormalities are found.

P 25
Left superior vena cava. CT-MRI findings and differential diagnosis.
I. Vollmer, J.M. Maiques, A.M. Rodríguez, J. Sánchez, I.F. Enciso, A. Gayete; Barcelona/ES

Purpose: To describe the embryology of persistent left superior vena cava, the CT and MRI findings and its clinical implications. **Material and methods:** We reviewed all thoracic examinations (CT and MRI) of patients with persistent left superior vena cava at our Institution. **Results:** The left superior vena cava disappears during the fetal development, persisting in a 3% of the adult population to be discovered during thoracic CT or MRIs, central vein catheterism or due to the production of an anomalous shunt. The development of embryological cardinal veins into the superior vena cava is reviewed. Different types of left superior vena cava are described: persistence of both SCV without the innominated vein, persistence of both SCV as well as the innominated vein, absence of the right SCV with persistence of the left SCV, and a left SCV with an anomalous drainage into the left atrium. The CT and MRI features of the persistence of the left SCV are reviewed as well as the different entities that may mimic this structure as the left superior intercostal vein, the partial anomalous return of the pulmonary vein or a bypass constructed with saphenous vein. **Conclusion:** The left SCV is seen as a thoracic vein that must be considered an anatomical variation usually with no clinical implications even though it can be the origin of anomalous right-to-left shunts. The diseases that produce the SVC syndrome can affect the left SVC when localized in the left hemithorax.

P 26 Withdrawn by authors

P 27 Withdrawn by authors

P 28
Amlyoidosis: overview using imaging findings
W. Kwon; Wonju/KR

Learning objectives: To illustrate the spectrum of amyloidosis. To overview the pathogenesis of multiorgan involved systemic amyloidosis. To promote awareness of careful evaluation of amyloidosis at radiologic findings. **Background:** Amyloidosis can involve any organ singly or in conjunction with other organs and can do so in the form of a focal, tumorlike lesion or an infiltrative process. To make a difference in diagnosis, the radiologist must be familiar with the diverse imaging findings of amyloidosis, which could raise the suspicion of amyloidosis. **Imaging findings OR Procedure details:** In this review, we describe CT and MR findings of variety of liver, GI tract, and lung involvements such as tracheobronchial, pulmonary nodular, and diffuse septal form. Ultrasonographic findings of renal and cardiac involvement are demonstraed. Nowadays developed MR imaging demonstrate cardiac, brain, and bone involvement. Plain radiography also be notified not to overlook this diagnosis. **Conclusion:** Imaging presentations of amyloidosis are usually varied and nonspecific, which may cause delay in diagnosis and appropriate treatment changes. In the proper suggestion, amyloidosis should be considered as a possible cause of worsening symptoms and landmark for treatment. The radiologist has the opportunity to minimize the prediagnostic delay and effect treatment change.

P 29
Portable ICU chest x-ray: where calamities often lurk!
A. Asrani, S. Digumarthy, R. Kaewlai, M. Gilman, J. Shepard; Boston/US

Learning objectives: Learning objectives of the exhibit Illustration of the urgent findings on portable chest radiographs and useful tips for easy recognition. Guidelines for communication of urgent findings. Guidelines for documentation of these findings. **Background:** Portable chest radiographs account for a majority of the inpatient radiographs especially from the intensive care units. Portable studies are usually performed on acutely ill patients who may have urgent findings, necessitating prompt detection and treatment. Urgent findings are defined as significant and unexpected findings requiring immediate intervention. Communication of such findings by phone or in person to the referring or treating physician is suggested. The purpose of this exhibit is to illustrate common examples of urgent findings on portable chest radiographs and to provide helpful hints for the radiologist. **Imaging findings OR Procedure details:** Portable chest radiographs are performed on acutely ill patients who cannot stand up for a standard two-view chest radiographic study. Although portable radiographs may be technically limited they still provide valuable information. Acutely ill patients often have multiple support devices and rapidly evolving findings. The examples in the exhibit are selected from various intensive care units including medical, cardiac, neurology, cardiothoracic surgery, general surgery, orthopedic and burn units. Knowledge of the clinical setting provides a clue to the urgent findings that might be expected. 1) Introduction 2) Indications and limitations of portable chest radiographs 3) The examples will be categorized into findings related to a) Lines and tubes b) Vessels c) Pleura d) Lung e) Mediastinum and f) Chest wall. 4) Suggested guidelines for communication and documentation of the urgent findings will be reviewed. **Conclusion:** Knowledge of the common urgent conditions that can be seen on a portable chest radiograph goes a long way in improving patient care for frequently severely ill inpatients.

P 30

Normal anatomy, variations, and disease spectrum of the diaphragm made easy with multi-detector spiral CT

Y.W. Choi, S.C. Jeon; Seoul/KR

Learning objectives: To display the normal anatomy, variations, and various diseases of the diaphragm and to illustrate the importance of multiplanar reformations of multi-detector spiral CT (MDCT) in evaluating the diaphragm. **Background:** The diaphragm is a thin dome-shaped structure interconnecting both thoracic and abdominal structures, only a small part of which is oriented in the axial plane. Although this anatomical feature make detection and characterization of diaphragmatic and peridiaphragmatic abnormalities on axial CT problematic, multiplanar reformations (MPRs) generated from the volume data of MDCT would solve much of the problems. **Imaging findings OR Procedure details:** There are wide spectrum of diaphragmatic diseases including various diaphragmatic configurations, congenital abnormality, congenital or acquired (including traumatic) hernia, and neoplasms. In addition, there are normal variations and aging processes involving the diaphragm. MPRs generated from the volume data of MDCT better illustrate three-dimensional relationship between these diaphragmatic diseases and the adjacent normal diaphragm rather than axial CT alone.**Conclusion:** There are wide spectrum of diaphragmatic diseases. MDCT with multiplanar reformation images allows accurate imaging of the diaphragm and peridiaphragmatic structures, displays the anatomy and disease entity, and serves as a useful tool in the evaluation of patients with diaphragmatic disease.

P 31

Pectus excavatum: evaluation using multi-detector CT

K.J. Park; Suwon/KR

Learning objectives: 1) To review classification of the dysmorphology of pectus excavatum, and its indication and methods of surgical correction. 2) To learn CT findings of pectus excavatum including a variety of CT morphologic index. 3) To learn how three-dimensional reconstruction of MDCT data can be used for pre- and postoperative evaluation. **Background:** CT is used as a major imaging tool to evaluate patients with pectus excavatum before and after surgical correction that has become more prevalent with the development of the less invasive procedures. Radiologists should be familar with the knowledge about CT findings of pectus excavatum including a variety of CT morphologic index at axial images, and how to use three-dimensional MDCT images that provide useful information for managing the patients with pectus excavatum. **Imaging findings OR Procedure details:** Pectus excavatum can be classified using the criteria including asymmetricity and length of sternal depression, localized or diffuse involvement, and the severity of sternal torsion. A variety of CT index including Haller index and vertebral index are used for the selection of candidates, planning and follow-up for surgical correction. Three-dimensional CT images demonstrates the orientation of the ribs and costal cartilages and their relationship to the sternum as well as the type, severity, or torsion of sternal depression that enables more precise evaluation for pectus excavatum. Lung volume changes can also be measured by MDCT data.**Conclusion:** MDCT examination provides information useful for pre- and postoperative evaluation of patients with pectus excavatum.

P 32

Ultrasound use in thoracic pathology: spectrum of applications and findings

J. Pires, M. França, A. Ramos, M. Certo, J. Reis; Porto/PT

Learning objectives: Become familiarized with the main applications of thoracic ultrasound examination and illustrate the main pathological findings. **Background:** Ultrasound is an easily available and non ionizing technique that may be used in thoracic pathology for much more than the work-up of pleural diseases. It's useful for the characterization of thoracic wall, lung and even in some cases mediastinal pathology. The guidance of interventional procedures is also of great interest. **Imaging findings OR Procedure details:** The assessment of thoracic wall pathology is sometimes very limited with plain film. Ultrasound may characterize masses, diagnose ribs fractures, evaluate lymph nodes and asses subcutaneous tissue pathology. Pleural pathology evaluation is the most widely spread application of thoracic ultrasound, not only for characterization of pleural effusions, but also for identification of pleural thickening, septation and masses. Ultrasound can even be more accurate than plain film in the diagnosis of pneumothorax. When an acoustic windows is present, evaluation of lung parenchyma (and sometimes mediastinum) is possible. Detection of lung nodules and cavities is achievable, occasionaly alerting the physician to the diagnosis. Pericardial evaluation is also of great interest. Diagnostic and therapeutic interventional procedures may also be guided by ultrasound, such as biopsies of masses, pleural effusions or abscesses drainage and central catheter placement. Pre-operative delineation of desired surgical field is sometimes very useful with ultrasound. **Conclusion:** Ultrasound is a widespread technique, with a broad spectrum of applications beyond pleural effusions characterization. It's essential for the radiologist to become familiarized with them.

P 33

Intrathoracic arteriovenous communications. Radiological features of different entities

I. Vollmer, A. Gayete, A.M. Rodríguez, A. Solano, I. Fuertes, J.M. Maiques; Barcelona/ES

Purpose: 1. To review the different entities that present with intrathoracic arteriovenous communications. 2. Description of radiological findings with roentgenographic, CT, MRI and radionuclide imaging. **Material and methods:** We reviewed all thoracic examinations (CT, MRI and radionuclide imaging) of patients with suspected intrathoracic arteriovenous communications during last five years. **Results:** We found different diseases that present with intrathoracic arteriovenous communications and we reviewed as follows: -Congenital arteriovenous fistulas: special focus in the hereditary hemorrhagic telangiectasia (Rendu-Osler-Weber syndrome). -Postoperative arteriovenous fistulas: uncommon presentation as a complication of atypical pulmonary resections. -Hepatopulmonary syndrome: rare disease in liver illness that presents with hypoxemia. -Abnormal pulmonary vein drainage: total or partial. Communication of one or more pulmonary veins with the systemic venous circulatory system. -Left superior cava vein with anomalous drainage to the left atrium: congenital disease with right-to-left shunt. -Cardiac communications: most commonly presenting as atrial septal defects and patent foramen ovale. -Acute respiratory distress syndrome: radionuclide studies have demonstrated that hypoxia is secondary to intrapulmonary shunts. **Conclusion:** Intrathoracic arteriovenous communications are rare entities that can be asymptomatic or they can present with hypoxia, paradoxical embolism or pulmonary bleeding. Therefore radiologists must be able to perform a correct diagnosis in order to treat the patients adequately.

P 34

Occult pneumothorax. Incidence and locations.

G. Figueres Muñoz, M.L. Domingo Montañana, C. Leiva Salinas, L. Flors Blasco, E. López Pérez, J. Vilar; Valencia/ES

Purpose: Occult pneumothoraces (OPTX) are considered when, despite the high clinical suspicion, there is no evidence in the chest X-ray. CT will confirm the presence of pneumothorax. The findings of pneumothorax (PTX) in supine chest films have been widely reported, but how often air is located in some pleural recesses is less commonly known. Detecting small PTX in critically ill patients is important because tension PTX may develop when positive pressure ventilation (VPP) is used. Our objectives are: 1- Analyze the incidence and location of occult pneumothorax (OPTX) in our Hospital. 2- Describe some mimics of OPTX. **Material and methods:** Two radiologists retrospectively reviewed all cases of PTX in our institution during a 2 year period. We established the diagnosis of PTX by using CT images and progression of chest radiographs. The following data were recorded: location of air from PTX in the different recesses: anteromedial, apicolateral, subpulmonic, and posteromedial, and presence of tension PTX. OPTX was considered when there was no evidence of PTX in the chest X-ray, and was confirmed at CT or using data from the radiological progression. Missed PTX (MPTX) was considered when radiographic signs were found only retrospectively. **Results:** A total of 101 PTX were found in 98 patients. Fifteen of 195 pleural recesses (7´7%) were occult to plain films. Six recesses (3,1%) in three patients were considered MPTX. The most common locations were anteromedial (41´8%, n=18 recesses), apicolateral (23´2%, n=10), at CT examinations, and apicolateral (36´8%, n=56), subpulmonic (25´6%, n=39), and anteromedial (13´1%, n=20), in the supine chest X-ray. **Conclusion:** Occult pneumothorax occurs in 9% of the cases, and missed pneumotothrax in 3%. The missed cases are more frequently located in the anteromedial and apicolateral recesses, are quantitatively small, and, usually, will not need pleural drainage unless VPP is undertaken.

P 35 Withdrawn by authors

P 36 Withdrawn by authors

P 37

Left cervical aortic arch wiıth multiple saccular aneurysm associated with aortic narrowing, branch artery aneurysm and anomalous innominate vein

A. Türkvatan, Ü. Kervan, T. Ölçer, T. Cumhur, A. Sarıtaş; Ankara/TR

Purpose: Cervical aortic arch (CAA) is rare congenital aortic anomaly. Occasionally it is associated with other cardiac and aortic abnormalities. In this paper, we report a patient with left cervical aortic arch who had multiple saccular arch aneurysm, proximal aortic arch narrowing, a right subclavian artery aneurysm and subaortic left innominate vein diagnosed by multidetector computed tomographic (MDCT) angiography. **Material and methods:** 27 year-old woman was admitted with a pulsatile mass in the left neck. A chest radiography showed smooth left-sided superior mediastinal mass. MDCT angiography was performed using a 16-row MDCT (Light-speed Ultra, GE medical System, Wisc., USA). After determining the contrast agent transit time using the smart prep bolus technique, we acquired image data during an intravenous injection of 90 ml of iodinated contrast agent at a rate of 4 ml/sec. **Results:** MDCT angiography revealed left CAA with normal branching of the innominate and left carotid arteries but the origin of the left subclavian artery was merging distally with the arch aneurysms. It clearly demonstrated multiple small saccular aneurysms at the transverse arch and a long segment moderate narrowing at the proximal arch just distal to the origin of the left carotid artery. A fusiform aneurysm of the right subclavian artery at 15 mm diameter was detected. The descending thoracic aorta was situated on the left side and somewhat hypoplastic. The walls of the aortic arch and aneurysms showed a several spotty calcification. A left subaortic innominate vein was present. At surgery, proximal narrowed segment and arch aneurysms was resected, and a bypass graft replaced the aortic arch. Histologic examination of the aneurysms revealed mediocystic necrosis. **Conclusion:** To our knowledge, this is the first report of CAA associated with combination of all of these vascular abnormalities, previously mentioned. This case report underlines the usefulness of MDCT angiography for a noninvasive diagnosis of thoracic vascular abnormalities.

P 38

Semiology of thoracic ultrasonography

I. Vollmer, A.M. Rodríguez, J.M. Maiques, A. Radosevic, E.A. Márquez, A. Gayete; Barcelona/ES

Purpose: To show the ultrasonographic findings in the thoracic patology, and its utility in diagnosis and management of diferent patologies of the lung, pleura, thoracic wall and diaphragm.**Material and methods:** We reviewed all thoracic ultrasonographic examinations realized during last five years.**Results:** We review the differences in semiology aspects of a different kind of diseases. -Neumothorax: comet tail artefacts, reverberation artefacts, lung sliding. -Pleural effusion: presence or absence of internal echoes, thin or thick septas, pleural thickening, and pleural nodules. -Pleural masses. -Pulmonary lesions with pleural contact (consolidations, neoplasm). -Chest wall lesions: fractures, neoplasic infiltration. We also review the utility of US like a guide of interventional procedures on the chest (thoracocentesis, pleural biopsy, pleural cytology, pulmonary biopsy or cytology). **Conclusion:** The thoracic ultrasonography is a useful tool on the diagnosis and treatment of thoracic diseases, and is an aid in a kind of interventional procedures on the chest and is because of that the radiologist does know of the ultrasound thoracic semiology.

P 39

About four cases of air in strange places

R. Gosselin, L. Delrue, P. Smeets, P. Duyck; Gent/BE

Purpose: Illustration and understanding of the propagation and the pathways of extraluminal/extrapulmonary air in the thorax by means of 4 iconographically exceptional cases of pneumothorax/pneumomediastinum. **Material and methods:** 4 patients admitted at the emergency department, essentially for acute respiratory distress/chest pain/trauma etc., with pathological chest x-rays revealing air "in strange places" had a workout with chest MDCT. The imaging results were confronted to the clinical examination and tests. Similar cases were looked up in the literature to archieve a better comprehension of the imaging data, the pathological condition of the patients and the prognostic factors.**Results:** 4 case reports are considered: The first patient presented with a spontaneous pneumomediastinum after attending a disco, no other risk factors were objectivated, the Macklin effect was found at CT, no tracheo-esophageal injury was identified, we concluded to a barotrauma with pneumomediastinum. The second case concerns a psychiatric patient with pneumopericardium on chronic gastric ulceration with fistulisation confirmed by gastroscopy. The third case concerns an insufficiency of the chest wall and intercostal muscles in a patient with morbid obesity presenting a pneumothorax and intercostal pulmonary herniation. The fourth case illustrates an exceptional case of perforating high velocity chest trauma with transthoracic expulsion of pulmonary tissue. **Conclusion:** MDCT very adequately depicted the mechanisms and the key features in all of these relatively rare cases of pneumothorax/pneumomediastinum and can therefore undoubtably be presented as the imaging modality of choice.

P 40

Bilious pleural effusion after percutaneous transhepatic biliary drainage

J.S. Kim[1], C.S. Park[2]; [1]Seoul/KR, [2]Koyangsi/KR

Purpose: To evaluate massive pleural effusion with respiratory distress following percutaneous transhepatic biliary drainage in 3 patients. **Material and methods:** We included 3 patients (all men, 48-67 years) having biliary malignancy with obstructive jaundice. All patients underwent sonoguided percutaneous transhepatic biliary drainage (PTBD) for relief of obstructive jaundice. We checked chest radiograps when the patients complained respiratory distress after PTBD. Sonoguided pig tail insertion were performed in all patients for pleural effusion drainage. Pleural fluids were analysed. And follow up chest radiographs were obtained. **Results:** The cause of biliary obstruction were common bile duct cancer in 2 patients and GB cancer in one-patient. All patients were normal in chest radiographs before PTBD. However after PTBD 8-9 days, all patients have complained respiratory distress and pain. Large amount of right sided pleural effusion were demonstrated in chest radiographs obtained 8 days after in 2 patients and 9days in one following PTBD. Drained pleural fluid was bilious in nature with 1.5 L-2L in amount. Bilious pleural effusions were completely drained via pig tail catheter during 1-2 days. There were no recurred bilious pleural effusion during admission period. **Conclusion:** Bilious pleural effusion making respiratory distress can occured following PTBD especially in cases of biliary malignancy. We assumed bilious pleurisy via biliopleural fistuous tract could be happened in patients with congenital pleuroperitoneal fistula. However it woud be easily resolved with thoracentesis using pig tail.

P 41

A case report: isolated hydatid cyst in axilla

E.D. Cicek, G. Eker, I. Gulcan, B. Saydam; Istanbul/TR

Learning objectives: Key words: Hydatid cyst, axillar mass **Background:** A 26 year old female patient referred to our hospital complaining of a 9 year history of palpable mass in her left axilla. It had been obtained from her past medical history that she underwent percutaneous drainage three times under the emergency surgery conditions with the presumed diagnosis of abscess in that localization. **Imaging findings OR Procedure details:** As a first step sonography examination was performed. According to preliminary findings of the sonography, possibilities of LAP or abscess were considered. Mammography and thorax CT examinations were done for the etiology of LAP. No pathologic finding was found that presumes malignancy in the mammography examination.In the thorax CT examination there was no pathology in lungs or mediastinum. Left shoulder MRI examination was performed for more detailed information about the mass. In the MRI there was a thick walled mass lesion with solid and cystic components with no invasion of the surrounding soft tissue. The radiological findings let us to consider abscess formation, tuberculosis lymphadenitis, necrotic LAP and malignancies especially synovial sarcoma for differential diagnosis. The

possibility of malignancies was low due to nine years of history of mass. Although axilla is not the typical localization for hydatid cyst, which can exhibit different radiological appereances, it was considered as a differential diagnosis since it is endemic in our country. We proposed to the surgery clinic of our hospital an excisional biopsy from the axillar mass. **Conclusion:** The report of the excisional biopsy of the cystic lesion stated hydatid cyst. We accepted our case as an isolated axiller hydatid cyst because there was no other focus of hydatid disease in the other parts of the body. Herein, we are presenting our isolated axillar hydatid cyst case of which there were only ten of them reported in the literature.

P 42

Mediastinal staging with diffusion- weighted MR Imaging in patients with non-small cell lung cancer

I. Hasegawa[1], P.M. Boiselle[2], K. Kuwabara[1], M. Sawafuji[1], H. Sugiura[1]; [1]Kawasaki/JP, [2]Boston/US

Purpose: The aim of this study was to describe our preliminary experience of evaluating mediastinal lymph node metastases with diffusion- weighted MR imaging in patients with non-small cell lung cancer. **Material and methods:** Seventy-four consecutive patients with non-small cell lung cancer underwent preoperative diffusion- weighted MR imaging using a non-breath-hold short inversion time inversion recovery- echo planar imaging sequence with a high b value of 1,000 s/mm2but 16 patients were excluded because they did not undergo mediastinal lymph node dissection or sampling due to poor cardiac or pulmonary reserve. Our final study population included 58 patients (41 male, 17 female; mean age of 64 years). An experienced thoracic radiologist prospectively evaluated each study for mediastinal lymph node metastases. The MR results were correlated with histopathology. **Results:** Diffusion- weighted MR imaging accurately identified 48 (96%) of 50 patients without mediastinal lymph node metastasis and demonstrated mediastinal lymph node metastasis in 5 (63%) of 8 patients with pathologically proven metastasis. Thus, 53 (91%) of 58 patients were accurately diagnosed. The sensitivity, specificity, positive predictive value, negative predictive value of diffusion- weighted MR imaging for mediastinal lymph node metastasis were 63%, 96%, 71%, and 94%, respectively. **Conclusion:** Our preliminary results demonstrate that diffusion- weighted MR imaging has a high negative predictive value for excluding mediastinal lymph node metastases from non-small cell lung cancer and has the potential to be an alternative non-invasive method for assessing mediastinal lymph nodes in patients with non-small cell lung cancer.

P 43 Withdrawn by authors

P 44

Incidental Solitary Pulmonary Nodules on CT: an audit of their management.

S. Simkin, Z. Viney, M.K. Duncan, R. Dennett, L.J. Menezes; London/UK

Purpose: Lung nodules are detected very commonly on CT. Indiscriminate follow up with serial CT for at least 2 years, is expensive and has substantial radiation exposure attached. In 2005, the Fleischner Society proposed new guidelines for the follow up and management of small pulmonary nodules detected on CT. We audited to what extent these recommendations are being followed in our institution. **Material and methods:** The radiology information system was searched for cases of solitary pulmonary nodules during the year 2006. Patients with a known cancer were excluded. The reports were assessed for nodule size, comparisons with old scans where available, risk assessment, and what further action was suggested. The electronic patient record was searched for the results of follow up CT or further investigations, such as PET or biopsy. **Results:** 63 patients met the inclusion criteria. Nodule size was documented in 73% of cases, with old scans used for comparison where available for 61.1%. A risk assessment was made in 21%. The Fleischner recommendations were followed in 46%. However, 46% of patients received no follow up when it was indicated. 45.5% of those for whom PET or histology was indicated received it. 3 patients (4.8%) had lung cancer, which was diagnosed between 1 to 8 months after the nodule was first seen on CT. **Conclusion:** Current compliance with the Fleischner guidelines is poor. Increased awareness of the guidelines by both radiologists and physicians is needed. The prevalence of cancer detected is similar to the screening trials.

P 45

Early CT changes of radiation injury after tomotherapy for pulmonary malignancy

H.J. Park[1], K. Kim[2], C.S. Kay[2], M.I. Ahn[3], M.H. Chung[4], S.H. Park[1]; [1]Seoul/KR, [2]Incheon/KR, [3]Suwon/KR, [4]Bucheon/KR

Purpose: To evaluate the early CT appearance of radiation injury of the lung after tomotherapy **Material and methods:** Thirty five patients with pulmonary malignancies, who underwent tomotherapy, were enrolled in our study. Four patients with central lung cancer and peripheral atelectasis were excluded, because of difficulty in interpretation. Of 31 patients, 25 patients with total 77 target lesions underwent follow-up CT within the first 3 months from completion of tomotherapy and 21 patients with total 69 lesions underwent CT within the first one month. We analyzed grade of pulmonary toxicity by South-West Oncology Group (SWOG) criteria and its CT findings, focusing on morphology and location. **Results:** Radiation pneumonitis (RP) developed around 37 target lesions (37/59, 63%) in 16 patients (16/22, 73%) during 3 months after tomotherapy. In one-month follow-up CT, RP was seen around 19 target lesions (19/55, 37%) in 10 patients (10/19, 53%). All patients were asymptomatic or presented with minimal clinical expression. The most common parenchymal change by RP was a localized inhomogeneous ground glass attenuation area (18/37) with irregular shape (18/37). RP was eccentrically located to the target (20/37) and 17 cases (17/37) were separated from the targets. In many cases (28/37), distant area of RP from target was denser than nearby area from target. Half cases (11/22) showed mild reticulations and mild traction bronchiectasis. **Conclusion:** Asymptomatic RP after tomotherapy is common within 3 months. CT finding of RP is non-specific, a focal irregular ground glass opacity, as expected. However, its common location is beside the target off the area with target radiation volume against all expectations.

P 46

Small cell lung cancer - a pictorial review of presentations and complications

P. Pissay Gopala Rao, L.D. Wheeler, H. Adams; Cardiff/UK

Learning objectives: To illustrate common and unusual radiological presentations of small cell lung cancer (SCLC) and its response to treatment. **Background:** Overall, lung cancer is the second commonest cancer in men and women in the developed world and SCLC accounts for about 20-25% of cases. In comparison with non-small cell lung cancer (NSCLC), SCLC typically exhibits more aggressive behaviour with rapid growth, early metastatic spread and frequent association with paraneoplastic syndromes. SCLC shows marked sensitivity to chemo-radiotherapy in the majority of cases. **Imaging findings OR Procedure details:** Sixty-four patients presenting with histologically proven SCLC over a two year period were identified from the local Lung Cancer Multidisciplinary Team database. All relevant radiological studies, including plain radiographs and CT scans, were reviewed and the images were used to produce a pictorial essay demonstrating the range of presenting features. SCLC typically presents with massive central intrathoracic lymphadenopathy in the presence or absence of a peripheral lung tumour. Limited SCLC is defined as tumour confined to the ipsilateral hemithorax, accounting for the minority of cases. Extrinsic compression or invasion of central airways or vessels is common and this may result in pulmonary collapse or superior vena-caval obstruction. 60-75% of patients with SCLC have extensive disease at presentation. Contralateral mediastinal lymphadenopathy is common. Typical locations for distant metastatic spread include liver and adrenal glands but unusual metastatic sites are more common than in NSCLC. Rarely, SCLC occurs in extra-pulmonary locations in the absence of radiological evidence of primary intrathoracic disease. SCLC is usually highly chemo-sensitive, many patients achieve complete remission. Complications of chemotherapy including neutropenic sepsis are common. Aggressive relapse of tumour is frequent, either locally or distantly and unusual sites of relapse may occur.**Conclusion:** SCLC is an aggressive malignancy with a wide range of clinical and radiological manifestations. Recognition of the radiological patterns of disease should suggest the correct diagnosis.

P 47

Lung perfusion CT: the differentiation of cavitary mass

W. Kwon, Y.H. Lee; Wonju/KR

Purpose: To evaluate lung perfusion maps based on region of interest (ROI)-studies in the differentiation of cavitary mass. **Material and methods:** Fifty-three patients with cavitary lung masses were analyzed. All patients underwent biopsy. Dynamic chest CT was performed contrast injection. The volume map, washout map, peak map, and time-to-peak (TTP) map were reformatted using IDL (Interactive Data Language). The perfusion patterns were classified into three scoring groups, and these scorings was repeated after 2-week intervals. Diagnostic confidence levels were assigned by consensus. McNemar's chi-square test was used to determine interobserver agreement, and Fisher's exact test was used to analyze statistical differences in perfusion scores. Receiver operating characteristic (ROC) analysis was performed to evaluate the usefulness of the perfusion maps. **Results:** Perfusion maps were reformatted pixel-by-pixel from the time-to-density curve analyses, and these maps showed perfusion values at a glance. Pyogenic cavities showed weak washout and slow TTP (69.6%). Conversely, malignant cavities showed strong washout (73.3%). Tuberculous cavities showed low perfusions in the volume and peak maps (66.7%). Interobserver agreement was excellent for each parameter. The performance of the combination of CT and the perfusion map was always better than that of CT alone. **Conclusion:** Lung perfusion CT could be a promising and feasible method for differentiation of cavitary mass.

P 48

RFA in patients with single lung

J. Goyers, D. Brisbois, P. Magotteaux; Liege/BE

Purpose: The purpose is to presentate two cases of percutaneous radiofrequency ablation in two patients with previously pneumonectomy. **Material and methods:** the first procedure was realised in a patient with a colorectal metastase with 5 years pneumonectomythe second patient presented a primary adenocarcinoma in the remaininig lung 9 years after controlateral pneumonectomy we use cool tip needles placed under CT guidance.**Results:** the follow-up is 6 months in both cases and demonstrate no sign of local recurrence patients are alive at 6 and 8 months after RFA hospitalisation was very variable (from 2 days for the first case to 12 days for the second one due to pneumothorax drainage and surinfection) **Conclusion:** percutaneous radiofrequency is possible as alternative therapeutic option even when patients with previously pmeumonectomy

P 49

Chest CT screening of asbestos-exposed workers: lung lesions and incidental findings

T. Vierikko[1], R. Järvenpää[1], T. Autti[2], P. Oksa[1], M. Huuskonen[2], S. Kaleva[2], J. Laurikka[1], S. Kajander[3], K. Paakkola[3], S. Saarelainen[1], E. Salomaa[3], A. Tossavainen[2], P. Tukiainen[2], J. Uitti[1], T. Vehmas[2]; [1]Tampere/FI, [2]Helsinki/FI, [3]Turku/FI

Purpose: The aim of this study was to determine the feasibility of chest computed tomography (CT) in screening for lung cancer among asbestos-exposed workers. In addition to benign and malignant lung lesions, incidental findings and their relevance were noted. **Material and methods:** Our study consisted of 633 workers examined with chest radiography and high-resolution CT (HRCT). Of these 180 current and ex-smokers (cessation within the previous 10 yrs) were also screened with spiral CT. Noncalcified lung nodules were considered positive findings and examined further according to a modification of the protocol used in the Early Lung Cancer Action Project (ELCAP) study. All incidental findings were also registered and the clinicians decided whether additional examinations were needed. **Results:** Five histologically confirmed lung cancers were found. Only one of these was also detected by plain chest radiography and three were from the group of patients with a pre-estimated lower

cancer probability. Two lung cancers were stage Ia and were radically operated. In total, 277 individuals presented 343 incidental findings of which 46 required further examination. Four of these were regarded as clinically important. **Conclusion:** CT and HRCT proved to be superior to plain radiography in detecting lung cancer in asbestos-exposed workers with many confounding chest findings. The numerous incidental, yet non-important, findings are a major concern for future screenings, which should be considered for asbestos-exposed ex-smokers and current smokers.

P 50

What is the significance of lung nodules in patients with testicular cancer?

S. Ganeshalingam, M. Gilligan, G. Rottenberg; London/UK

Purpose: To evaluate the incidence and significance of lung nodules in patients with a new diagnosis of testicular cancer. **Material and methods:** A retrospective analysis of the chest CT (thin section) and using Maximum intensity projections (MIP) was performed on 25 randomly selected patients at initial diagnosis of testicular cancer at a urological centre over a 3-year period. The patients selected ranged from 27 – 70 years of age (mean age of data 35). The images were reviewed by 2 radiologists and assessed for the presence of lung nodules. Nodules were considered malignant based on the growth of nodules, PET scan results or depending on biopsy results, and were considered benign either on histology or if their appearance remained stable 1 year after the initial study. Comparison of the results was also made with the original radiological report for the purposes of an audit. **Results:** Lung nodules were identified on the CT scans of 6 of the 25 study sample (24%). Of these, 3 were determined to be small calcified granulomas (12%) and had an average size of 4mm and the remaining 3 were classified as lung metastases (12%) and had an average size of 9mm. **Conclusion:** Nearly a quarter of the patients in this study group had nodules identified in the lung at the time of diagnosis and 12% were confirmed as metastases. The benign nodules were all small and calcified at initial diagnosis. The malignant nodules were larger and not calcified.

P 51

Review of the small pulmonary nodule management, after to have practiced some hook-wire guided videothoracoscopic resections.

E. Mauri, V. Querol, S. Llaverias, A.M. Gallart, A.M. Martinez, C. Montull, M.J. Conde, E. Mundt, M.T. Maristany, L. Molins; Barcelona/ES

Purpose: the small (<= 1 cm) and especially the small solitary pulmonary nodules has been studied with different algorithm, evaluating the morphologic, functional (PET, enhancement contrast CT, etc) or radiological follow up criteria, and in our Hospital we have a long experience (112 cases) with the CT-guided biopsy. We want to show how the application of the technique of the hook-wire placement (to guide a videothoracoscopic resection) has changed our algorithm, because of the low morbidity and good diagnostic and therapeutic results. **Material and methods:** Eight patients (mean age 65 years old, range 51-84 y.) 6 females/2 males: 6 patients with small solitary nodules with oncologic history (renal carcinoma, pulmonary contra lateral, 2 pulmonary ipsilateral, melanoma, and bronchoalveolar carcinoma (ground glass nodular), of 5, 11,10, 9,7,10 mm), another with 3 nodules (3 to 7 mm, breast carcinoma previous) and another with 8 nodules (6 to 9 mm) with multiples leyomiomas. We placed a hook wire guided by Multidetector-CT, locating it with axial scans (4*4,5 mm collimation). Immediately we transferred the patient to the surgical room. **Results:** We have been able to locate and resects all the nodules with less than 24 hours of hospital ingress. We confirmed the suspected metastasis in 5 cases (breast, melanoma, contralateral carcinoma, and two ipsilateral metastases) and benign lesions in the rest (lymph node, fibrous nodule, and bone metaplasia). **Conclusion:** 1-the hook-wire placement is a new technique very efficient, which permits to locate and resects the small pulmonary nodules. 2- It means a substantial change that it must take to us to consider a new algorithm to their management.

P 52

In which patients in 6months after acute PE control sCT shoud be perform

R. Pacho, A. Kaczyńska, M. Kostrubiec, J. Kunikowska, P. Pruszczyk; Warsaw/PL

Purpose: The aim of this research was to evaluate the presence of thrombi in pulmonary arteries six months after acute pulmonary embolism (APE). Despite long-term anticoagulation in some patients after APE pulmonary thrombi are not completely resolved. We hypothesized that elevated D-dimer concentration reflecting increased endogenous fibrinolysis may indicate incomplete pulmonary thrombi resolution after the first episode of PE. **Material and methods:** 55 patients aged 54,7±18,6 years were anticoagulated for 6 months with acenocumarol (74,5% pts) or low molecular weight heparin (25,5% pts) when control spiral computed tomography (sCT), lung perfusion scintigraphy and D-dimer assessment were performed. **Results:** Incomplete recanalization of pulmonary circulation was found in 39 (70,9 %) patients - thrombi at sCT and/or ≥ 1 wedge-shaped perfusion defect at scintigraphy. Age, sex, rate of unprovoked APE, malignancies, thrombolysis in the acute phase and type of long term anticoagulation were similar in patients without and with complete recanalization. D-dimer at follow-up but not on admission was higher in patients with then without incomplete recanalization (median 340 (80-2280) vs 160 (60-390) ng/ml, p = 0,02). All 11 (20%) patients with D-dimer level > 500 ng/mL at follow-up did not resolve thromboemboli completely. ROC analysis showed that D-dimer at follow-up identified patients with incomplete recanalization (AUC 0,709, 95% CI (0,560-0,831), p = 0,007). Multivariable analysis confirmed that D-dimer >350 ng/mL at follow-up and right ventricle dysfunction at the diagnosis were independent predictors of incomplete recanalization (OR 18,58 (95% CI 1,97-175,19) and 7,03 (95% CI 1,43-34,6), respectively, p = 0,0006 **Conclusion:** sCT should be performed in patients with elevated D-dimer after 6-month anticoagulation and right ventricular dysfunction at the diagnosis, because often these patients present incomplete recanalization of pulmonary circulation after first episode of APE.

P 53

Preductal aortic coarctation in an adult as a cause of arterial hypertension

M. Vukelic Markovic, P. Marusic, I. Cikara, Z. Djurasevic, Z. Borkovic, B. Brkljacic; Zagreb/HR

Purpose: To prove the importance of multidetector computed tomography angiography (MDCTA) and 3D reconstruction in the case of preductal aortic coarctation in an adult age as a rare cause of arterial hypertension **Material and methods:** We present a 44-year female patient who had therapy resistant, long-standing arterial hypertension and headache. The arterial hypertension had been observed for the first time 20 years ago.Physical examination revealed a 40-mmHg difference in brachial pressure between the right and left arms (170/100 vs. 130/95 mmHg, respectively).Difference in blood pressure between right arm and legs was also found (systolic pressure on the right arm 160 mmHg, systolic pressure on the legs 140 mmHg Color duplex-Doppler ultrasound of the neck and arms arteries demonstrated the incomplete subclavian steal-syndrome of the left vertebral artery, and biphasic spectra and decreased systolic velocities of the left axilar and brachial arteries. Doppler findings of the right axilar and brachial arteries were normal Transoesophagal echocardiography (TEE) demonstrated prominent infolding and increased velocity of flow (2.7m/sec) in the area between the aortic arch and descending aorta. DSA using right transbrachial approach demonstrated the narrowing and kinking of the aortic arch with dilatation of the left subclavian artery from the origin, but anatomic nature of the aortic obstruction could not be clearly shown. **Results:** MDCT angiography using 3D reconstruction revealed preductal stenosis of the aortic arch with poststenotic dilatation of the left subclavian artery. The stenotic segment was accompanied by two saccular aneurysms. **Conclusion:** The presentation of preductal aortic coarctation for the first time in an adult is unusual. MDCTA is diagnostically superior to conventional angiography to reveal anatomic nature of the aortic obstruction, especially due to possibility to achieve high quality 3 D reconstructions which can be rendered in any projection.

P 54

Chest involvement in Erdheim-Chester disease: CT and MR findings.

A. Brun, D. Touitou, J. Haroche, P.A. Grenier, D. Toledano, P. Cluzel, C. Beigelman-Aubry; Paris/FR

Purpose: To retrospectively review the chest findings at computed tomography and magnetic resonance imaging in 33 patients with biopsy-proven Erdheim-Chester disease. **Material and methods:** Thirty-three patients with Erdheim-Chester disease (23 men and 10 women; mean age 53,8 years, range 19-75) underwent CT of the chest (n=32), cardiac CT (n=25) and/or cardiac MRI (n=18). Analyses were reviewed in consensus by two experienced chest radiologists. **Results:** Circumferential periaortic infiltration was observed in 25 patients (78%). Extension of periaortic infiltration affected supraaortic trunks in 20 patients (61%), coronary arteries in 17 patients (51,5%), intercostal arteries in 7 patients (22%). Perivascular coronary infiltration was always located around the right coronary artery, and extended less frequently to the left coronary artery in 8 patients (24%). Eight patients (24%) presented with abnormal infiltration of the right atrial wall and 4 patients (12%) with severe narrowing of the right atrial lumen and superior vena cava stenosis. Pericardial thickening and/or effusion was observed in 19 cases (58%). Infiltration of the posterior mediastinum was seen in 16 patients (50%) with contiguous thickening and/or effusion of the pleura in 14 patients with a right predominance. Parenchymal involvement was observed in 15 patients (47%). Main patterns included smooth septal lines with an anterior and superior predominance (n=14), centrilobular nodules (n=8) and cysts (n=2). All patients with septal lines had cardiac involvement. One patient presented with isolated and diffuse cystic lesions without cardiac involvement. Uni or bilateral osteosclerosis was noted on clavicula in 4 patients (12,5%) and ribs in 7 patients (22%). **Conclusion:** This series provides a wide spectrum of different chest abnormalities associated with Erdheim-Chester disease. The combination of these peculiar patterns should be known by radiologists as highly suggestive of the diagnosis.

P 55

Non-invasive evaluation of 102 patients after coronary artery bypass surgery with 16-slice computed tomographic angiography

A. Türkvatan, S.F. Bıyıkoğlu, F.G. Büyükbayraktar, T. Ölçer, T. Cumhur, E. Duru; Ankara/TR

Purpose: The purpose of this study was to investigate the diagnostic accuracy and limitations of 16-slice MDCT in detection of significantly (>50%) stenosis of coronary artery bypass grafts (CABG) and native coronary arteries, in a large patients population. **Material and methods:** MDCT angiography was performed in 153 patients with suspected CAD and scheduled for conventional coronary angiography (CCA). The image quality was assessed in terms of artifacts and segment visibility and the assessable segments were screened for the presence of significant stenoses. The diagnostic performance of MDCT for detection of significant stenosis was compared with the results of CCA. **Results:** On a segment basis model, the evaluability of MDCT was 90.4% for CABG, 71.2% for all of native coronary arteries and 86.1% for postanastomotic recipient arteries. The most frequent causes of nonevaluable segments were motion artifacts in venous grafts, metalic clips artifacts in arterial grafts, severe calcification in native coronary arteries and small arterial lumen combined with insufficient opacification in postanastomotic recipient arteries. MDCT correctly diagnosed all of the 46 occluded grafts (sensitivity of 100%). Considering only the segments judged evaluable, the sensitivity, specificity and the positive and negative predictive value of 16-slice MDCT for the detection of CABG stenoses were 91.4%, 98.5%, 84.2% and 99.2%, respectively. Including all segments in the analysis (evaulable and nonevaulable), overall sensitivity was 84.2%. In the evaluation of native coronary arteries, the sensitivity, specificity and the positive and negative predictive value of MDCT for the detection of significant stenoses were 82.1%, 75.3%, 63.1% and 88.9%, respectively. The overall sensitivity for significant stenosis detection in the native coronary arteries was 62.1%. **Conclusion:** MDCT angiography allows very accurate evaluation of CABG patency and has high diagnostic accuracy in detecting graft stenoses with high sensitivity and specificity. But, evaluation of the native coronary artery stenoses may be limited, mainly due to severe calcification.

P 56

The role of color identification for coronary plaque imaging in interpretation of gray scale coronary MDCT

S. Choi, Y.H. Kim, H.J. Sun, J.K. Kim, J.G. Park, H.K. Kang; Kwangju/KR

Purpose: To evaluate the role of color identification (CI) according to CT number for coronary plaque imaging in the interpretation of gray scale coronary CT image. **Material and methods:** 111 coronary segments of 60 patients (M:F=47:13, Age=37~83yrs, mean= 57.5yrs) with atypical chest pain, underwent coronary MDCT with CI were evaluated in this study. Source images obtained with 64-channel MDCT were transferred to workstation, and then curved multiplanar reformation (MPR) images of major coronary artery (LAD, LCX and RCA) were reconstructed. CI display according to CT number (0~60 H.U: blue, 61~150 H.U: yellow, 151~600 H.U: green, > 601 H.U: red) was performed with overlapping on gray scale curved MPR images. Image analysis was performed by two radiologists with consensus to plaque nature and degree of luminal narrowing on both CI and gray scale MPR image, respectively. Plaque nature was classified into 4 groups as none/soft/mixed/calcified nature. Luminal narrowing was graded into 3 groups as 0%, < 50% and > 50%. Wilcoxon signed ranks test was used for statistical analysis of agreement. **Results:** In the evaluation of plaque nature, the overall agreement between CI with gray scale curved MPR image was 44% ($p > 0.05$). We had 62 (66%) cases of disagreement between CI and gray scale MPR image. Soft plaque was underestimated at CI in 41 segments. In the assessment of luminal narrowing, the overall between CI with gray scale curved MPR image was 56.7% ($p < 0.05$). **Conclusion:** CI appears to be a supplementary display tool with gray scale curved MPR image in the evaluation of coronary plaque. But, insufficient power of expression for soft plaque should be overcome.

P 57

Clinical value of 16-slice multidetector computed tomography in symptomatic patients with suspected coronary artery disease

A. Türkvatan, S.F. Bıyıkoğlu, F.G. Büyükbayraktar, T. Ölçer, T. Cumhur, E. Duru; Ankara/TR

Purpose: The purpose of this study was to investigate the diagnostic accuracy and limitations of 16-slice multidetector computed tomography (MDCT) in the detection of significantly (>50%) obstructive coronary artery disease (CAD). **Material and methods:** MDCT angiography was performed in 153 patients with suspected CAD and scheduled for conventional coronary angiography (CCA). The image quality was assessed in terms of artifacts and segment visibility and the assessable segments were screened for the presence of significant stenoses. The diagnostic performance of MDCT for detection of significant stenosis was compared with the results of CCA. **Results:** A total of 1989 coronary artery segments were evaluated. After exclusion of 394 non-evaluable segments (19.8%), 1595 segments (80.2%) were included to the analysis. The most frequent cause of poorly assessable segments was motion artifact (36%), followed by severe calcification (23%). Considering only the segments judged evaluable, the sensitivity, specificity and the positive and negative predictive value of MDCT were 85%, 97%, 79% and 98%, respectively. Including all segments in the analysis (evaulable and nonevaulable), sensitivity was 74% and specificity was 96%. **Conclusion:** Sixteen-slice MDCT enables the detection of coronary artery stenoses with high accuracy if image quality is sufficient, but its clinical use may presently be limited due to degraded image quality in a substantial number of cases, mainly due to rapid coronary motion. When all coronary artery segments are included, 16-slice MDCT has moderate sensitivity and very high specificity and NPV in assessing coronary artery stenoses. High specificity and negative predictive value indicate that MDCT may be a useful tool to reliably rule out significant lesions in patients with a low pretest probability.

P 58

Anatomy of pericardial recesses on CT

C. Leiva-Salinas, M.L. Domingo, L. Flors, G. Figueres Muñoz, E. López-Pérez, M. Mazon, J. Vilar; Valencia/ES

Learning objectives: To review the appearance of pericardial sinuses and recesses at computed tomography (CT). **Background:** The pericardial space normally contains a small amount of fluid, and the fluid-filled recesses can be misinterpreted as adenopathy or abnormalitiy of an adjacent mediastinal structure. Mistaking pericardial recesses for adenopathy in oncologic patients may lead to inaccurate clinical staging and inappropriate management and therapy. **Imaging findings OR Procedure details:** The pericardial recesses can be categorized on the basis of whether they arise from the pericardial cavitiy proper, the transverse sinus, or the oblique sinus. CT of the chest was performed in all patients on a Somatom Volume Zoom (Siemens, Erlangen, Germany) with 5-mm collimation or 1.25-mm collimation. **Conclusion:** Pericardial sinuses and recesses are usually depicted on CT scans. The knowledge of the pericardium sectional anatomy is helpful for differentiation of fluid-filled recesses from mediastinal masses or enlarged lymph nodes.

One destination. Many paths.

We'll take you there

Your radiology department and your path to digital is unique. Yet, your goal to provide the highest level of care is shared worldwide. We know. Found in 1 of every 2 hospitals, Agfa HealthCare works alongside radiologists every day. Our systematic steps to integrated digital radiology allow you to advance at your own pace, without jeopardizing current systems or investments. This allows you to choose the solutions you want: advanced imaging systems, integrated RIS/PACS/Reporting, sophisticated data management, or integrated digital workflows for radiology, mammography, cardiology and the healthcare enterprise. So as you consider your chosen path, let our proven experience support your next step, and every step after that.
www.agfa.com/healthcare

AGFA HealthCare

Deeper understanding is the mark of Brilliance.

Brilliance CT from Philips gives you the clinical advantages to attract referrals — and the productivity benefits to keep them. Advanced applications help you diagnose with more confidence and accuracy. Guided Flow™ Workspace design makes large image sets easier to manage. And RapidView technologies improve throughput with industry-leading reconstruction performance. On top of that, you can upgrade easily as your needs evolve. Philips Brilliance CT. It just makes sense.

www.medical.philips.com/CT

PHILIPS

sense and simplicity